

Supporting Information

Porous Shape-Persistent Rylene Imine Cages with Tunable Opto-electronic Properties and Delayed Fluorescence

Hsin-Hua Huang^a, Kyung Seob Song^b, Alessandro Prescimone^a, Alexander Aster^c, Gabriel Cohen^c, Rajesh Mannancherry^a, Eric Vauthey^c, Ali Coskun^{*b},
Tomáš Šolomek^{*a}

^a Department of Chemistry, University of Basel, St. Johannis-Ring 19, 4056 Basel, Switzerland, ^b Department of Chemistry, University of Fribourg, Chemin du Musée 9, 1700 Fribourg, Switzerland, ^c Department of Physical Chemistry, University of Geneva, CH-1211 Geneva, Switzerland.

E-mail: tomas.solomek@unibas.ch; ali.coskun@unifr.ch

<i>Section A. Materials / General Methods / Instrumentation</i>	2
<i>Section B. The Calculated Stability of the Organic Cages</i>	7
<i>Section C. Synthesis and Characterizations</i>	8
<i>Section D. NMR Spectroscopy and HR-ESI MS Spectroscopy</i>	17
<i>Section E. UV-VIS Absorption and Fluorescence Spectroscopy</i>	55
<i>Section F. Circular Dichroism (CD) Spectroscopy</i>	58
<i>Section G. Cyclic Voltammetry</i>	60
<i>Section H. Single-crystal X-Ray Diffraction</i>	65
<i>Section I. Gas Adsorption</i>	73
<i>Section J. TCSPC and Quantum Yields</i>	84
<i>Section K. Transient Absorption Spectroscopy</i>	89
<i>Section L. Computed Imidic C–N Bond Rotational Barriers</i>	91
<i>Section M. Cartesian Coordinates</i>	92
<i>Section N. References</i>	106

Section A. Materials / General Methods / Instrumentation

Materials

All commercially available compounds were purchased from Sigma-Aldrich, Acros, Apollo Scientific, Alfa Aesar or Fluorochem and used without further purification. Anhydrous solvents were purchased from Sigma-Aldrich and stored over molecular sieves (4 Å). Solvents for electrochemical and photophysical measurements were HPLC grade. Column chromatography was performed on silica gel P60 (40-63 μm) from Silicycle™, and the solvents were technical grade. Thin layer chromatography (TLC) was performed with silica gel 60 F254 aluminum sheets with a thickness of 0.25 mm purchased from Merck. All reactions with reagents that are easily oxidized or hydrolyzed were performed under argon (Ar) using Schlenk techniques with anhydrous solvents in glassware, which was dried prior to use. High resolution mass spectra (HR-MS) measurements were performed on a maXis™ 4G instrument from Bruker. MALDI-ToF mass spectra were measured on a Bruker microflex™ mass spectrometer, calibrated with CsI₃. A solution of a matrix, anthracene in CH₂Cl₂, was drop-casted onto a sample plate, and a solution of an analyte drop-casted directly onto the matrix. UV-Vis absorption spectra were recorded on a Jasco V770 Spectrophotometer. Circular Dichroism Spectroscopy (CD) measurements were performed using a JASCO J-1500 CD Spectrometer at 25°C in 1 cm quartz glass cuvettes. Fluorescence spectroscopy was carried out with a Fluoromax-4 Spectrofluorometer instrument from Horiba Jobin-Yvon.

Time-Correlated Single-Photon Counting and Quantum Yield Measurements

Time-correlated single-photon counting (TCSPC) experiments to determine the emission lifetimes were performed on FLS 1000 spectrometer. The lifetime was determined upon irradiating the samples with a laser with $\lambda_{\text{ex}} = 473$ nm and recording the emission at $\lambda_{\text{em}} = (600 \pm 18)$ nm. Prior to each measurement, the

purity of all compounds was determined by NMR spectroscopy and HPLC analysis. Samples were prepared by dissolving the compounds in dichloromethane (CH_2Cl_2), toluene and benzonitrile and deoxygenated by purging with Ar for at least 3 minutes. Quantum yields were recorded using a Hamamatsu absolute photoluminescence quantum yield spectrometer C11347. The solutions were deoxygenated by purging the sample with Ar for 15 mins before the measurements. The fluorescence decay curves were fitted with one or two exponential decay functions convoluted with the instrument response function.

Nuclear Magnetic Resonance Measurements

NMR solvents were obtained from Cambridge Isotope Laboratories, Inc. (Andover, MA, USA). NMR experiments were performed on Bruker Avance III NMR spectrometers operating at 400, 500 or 600 MHz proton frequencies. The instruments were equipped with a direct-observe 5 mm BBFO smart probe (400 and 600 MHz), an indirect detection 5 mm BBI probe (500 MHz), or a five-channel cryogenic 5 mm QCI probe (600 MHz). All probes were equipped with actively shielded z-gradients (10 A). The chemical shifts (δ) are reported in ppm relative to residual solvent peak and the coupling constants (J) are given in Hz (± 0.1 Hz). Standard Bruker pulse sequences were used, and the data was processed on Topspin 3.2 (Bruker) using twofold zero-filling in the indirect dimension for all 2D experiments.

High Performance Liquid Chromatography

A Shimadzu LC-20AT HPLC was used equipped with a diode-array UV/Vis detector (SPD-M20A VP from Shimadzu, $\lambda = 200\text{-}600$ nm) and a column oven Shimadzu CTO-20AC at 25°C. Chiralpak IA, 5 μm , 4.6 \times 250 mm, Daicel Chemical Industries Ltd, column was used for purification.

Gas Sorption Measurements

The adsorption and desorption measurements were carried out with Micrometrics ASAP 2020 porosimetry analyzer using Ar and N₂ at 77 K. Before the measurement, the samples were activated under vacuum at 100°C for 24 hours. The BET model was used to calculate surface areas and the respective pressure ranges obtained from the Rouquerol plot (we determined the pressure range where the $V(1-p/p_0)$ term increases with p/p_0 for BET calculation, Figure S63). To analyze the pore properties from the obtained isotherms, Nonlocal Density Functional Theory (NLDFT) adopting carbon slit pore model was employed. The low-pressure CO₂, CH₄ and N₂ adsorption and desorption isotherms were collected at 273, 298 and 323 K up to 1 bar. The temperature was kept constant during the measurements by using a circulator.

Single-Crystal X-Ray Diffraction

A suitable crystal was selected and mounted on a mylar loop in perfluoroether oil on a STOE StadiVari diffractometer (STOE & Cie GmbH, Darmstadt, Germany) equipped with a Pilatus300K detector and a Metaljet D2 source (Ga K α radiation) or Bruker APEX-II CCD diffractometer (Cu K α radiation). The crystal was kept at a steady $T = 130$ K during data collection. The structures were solved with the ShelXT¹ structure solution program using the Intrinsic Phasing solution method and by using Olex2² as the graphical interface. The model was refined with version 2014/7 of ShelXL¹ using least squares minimization.

Cyclic Voltammetry

Cyclic Voltammetry (CV) was performed with dry, degassed 100 mM tetra-n-butylammonium hexafluorophosphate in CH₂Cl₂ solutions. Voltammograms were recorded with a Versastat 4-200 potentiostat from Princeton Applied Research employing a glassy carbon disk working electrode, an Ag-wire as a (pseudo) reference electrode in combination with ferrocene as an internal standard and a platinum wire counter electrode. The glassy carbon electrode and Ag wire were polished prior to measurement.

Quantum Chemical Calculations

All calculations were performed with Gaussian 09 (ver. D01) package of electronic structure programs.³ The gas phase geometries were optimized with B3LYP functional and 6-31G(d) basis set. The frequency analysis of the minimum energy geometries confirmed that they represent the potential energy surface minima. The electronic transitions to simulate absorption and circular dichroism spectra in the gas phase were computed within the time-dependent density functional theory (TD-DFT) formalism using CAM-B3LYP and M06-2X functionals. The 30 lowest-energy transitions were calculated with 6-31G(d) basis set. Single point energy calculations were performed with B3LYP, BMK, and M06-2X functionals and 6-31+G(2d,p) basis set. The solvation free energies were accounted for with a SMD⁴ model of Truhlar and co-workers with the default settings implemented in Gaussian. The isotropic NMR chemical shifts were calculated at the B3LYP/6-31+G(d)/GIAO/PCM(dichloromethane) level of theory on gas phase B3LYP/6-31G(d) geometries.

Time-Correlated Single-Photon Counting and Quantum Yield Measurements

The visible transient absorption (TA) data presented in this work were recorded with a fs-ps visible (fs-VIS) and a ps- μ s visible (ps-VIS) TA setups. A detailed description of the general principle of the fs-ps as well as ps- μ s TA applying referenced detection with two spectrographs is presented elsewhere.⁵ The designs of the fs-VIS and the ps-VIS probe beam path are identical. The experimental details concerning these two setups and the data analysis are discussed below. The absorbance of the samples at the excitation wavelength was 0.05-0.4 on 1 mm. The samples were measured in 1 mm quartz cuvettes (Starna, model 1GS/Q/1) and bubbled with nitrogen during the measurements giving a wavelength dependent instrument response function (IRF) of about 80-350 fs (FWHM of the

optical Kerr effect (OKE) for fs-Vis). The absorption spectra of all samples showed no sign of degradation after the experiments.

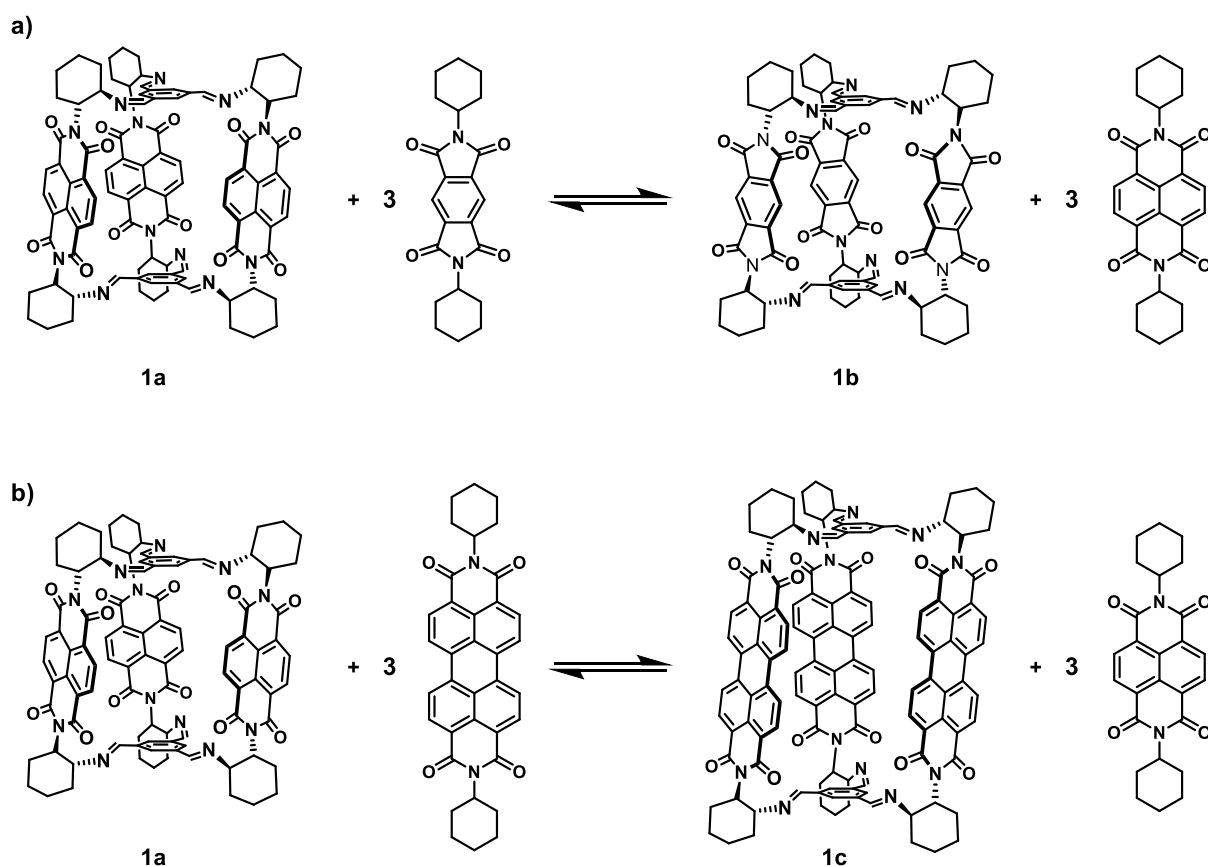
Visible Probe. Probing in both setups was achieved using white-light pulses generated by focusing the 800 nm pulses of the Ti:Sapphire amplified system in a CaF₂ plate. The experimental layout was the same as that described earlier,⁶ except that all lenses, after white light generation, were replaced by spherical mirrors to prevent chromatic aberration.

fs-ps Pump. Excitation was performed using 532 nm pulses generated by a TOPAS-Prime in combination with a NirUVis frequency mixer (both from Light Conversion), which were themselves seeded by the output of a 1 kHz Ti:Sapphire amplified system (Spectra Physics, Solstice Ace). The transient absorption signal was checked prior to the measurement to scale linearly with the pump intensity. The polarization of the pump pulses was set to magic angle relative to the white-light pulses.

ps- μ s Pump. The ps- μ s pumping was described in detail in ref. 7. Excitation was performed at 532 nm using a passively Q-switched, frequency doubled Nd:YAG laser (Teem Photonics, Powerchip NanoUV) producing pulses with a 500 Hz repetition rate, approximately 20 μ J energy, and 300 ps duration.

Data Treatment. The pixel to wavelength conversion was achieved using a standard containing rare earth metals (holmium oxide) which shows narrow bands from the UV to the visible spectral region. All transient absorption spectra were corrected for background signals showing up before time zero (e. g. spontaneous emission). The fs-ps spectra were corrected for the dispersion due to the optical chirp using the optical Kerr effect.⁸

Section B. The Calculated Stability of the Organic Cages



Scheme S1. Isodesmic reactions used to estimate the stability (ΔH of the reaction at 0K; see Table S1) of **1b** and **1c** using DFT calculations.

Table S1. DFT calculations of the stability^a, ΔH (0K), of **1b** and **1c** with respect to **1b** according to the isodesmic reactions in Scheme S1.

Compound	Energy ^a , ΔH (0K, in kcal mol ⁻¹)		
	B3LYP	BMK	M06-2X
Cage 1b	-0.2 (0.6)	0.2 (0.9)	0.5 (1.3)
Cage 1c	0.3 (0.2)	0.4 (0.3)	0.7 (0.6)

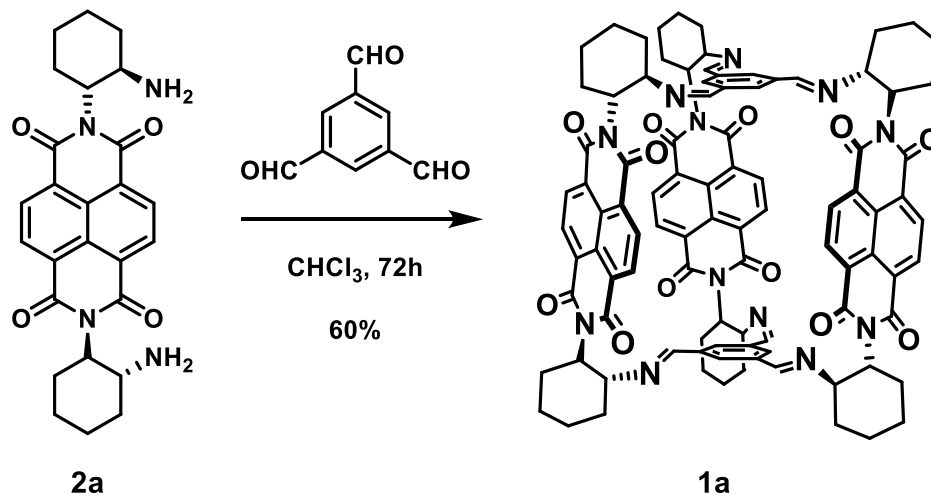
^aThe energy (in kcal mol⁻¹) calculated as the reaction (Scheme S1) energy at 0K with the respective functional and 6-31+G(2d,p) basis set on gas phase B3LYP/6-31G(d) optimized geometries with unscaled zero-point vibrational energy correction. The numbers in parentheses involve the SMD solvation (chloroform; B3LYP/6-31G(d)).

Section C. Synthesis and Characterizations

For the sake of simplicity, we abbreviate the configurations of the stereocenters in cyclohexylamines with a single stereochemical descriptor per redox-active PMDI, NDI, or PDI unit in all molecules. Therefore, we refer to the $(R,R,R,R,R,R,R,R,R,R,R,R,R,R)$ -enantiomer of the cages **1** and the (R,R,R,R) -enantiomer of **2**, **3** and **4** shortly as (RRR) -**1** and (R) -**2**, **3**, **4**, respectively, because the compounds were always synthesized from $(1R,2R)$ -cyclohexane-1,2-diamine. The corresponding (S) -enantiomers synthesized from $(1S,2S)$ -cyclohexane-1,2-diamine assume the same nomenclature principle.

Previously reported compounds: $(1R,2R)$ -cyclohexane-1,2-diamine,⁹ *tert*-butyl $((1R,2R)$ -2-aminocyclohexyl)carbamate,¹⁰ and (R) -**2a**⁷ were prepared following the reported procedures. The corresponding enantiomers were synthesized using $(1S,2S)$ -cyclohexane-1,2-diamine.⁹

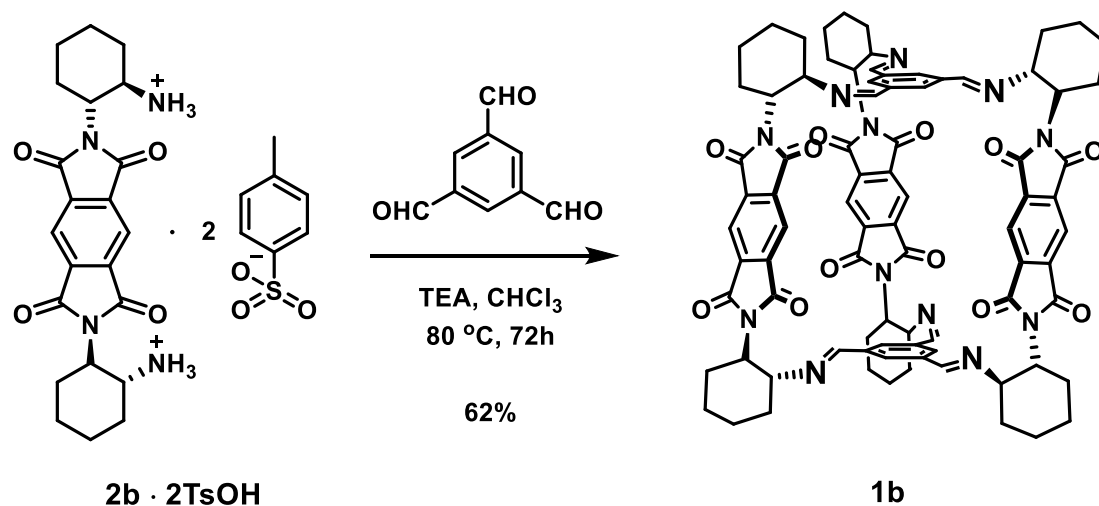
Cage 1a



Diamine (R) -**2a**¹¹ (230 mg, 0.5 mmol) was suspended in a solution of benzene-1,3,5-tricarbaldehyde (54 mg, 0.3 mmol) in dry chloroform (100 ml). The mixture was then stirred at room temperature for 72 hours after which the solvent was filtered through a disposable syringe filter. The filtrate was removed under reduced pressure to obtain a solid crude product. A small amount of methanol was added and the suspension was sonicated at room temperature for 30 minutes and filtered thereafter. The filter cake was washed with additional methanol followed

by a portion of diethyl ether and dried in air. The crude cage **1a** was purified by HPLC using CH₂Cl₂/*n*-Heptane (7:3) as eluent to yield a pure sample of **1a** as a white solid (166 mg) in 60%. The measured ¹H, ¹³C NMR spectra and the mass spectrum of **1a** matched those reported in the literature.¹²

Cage 1b



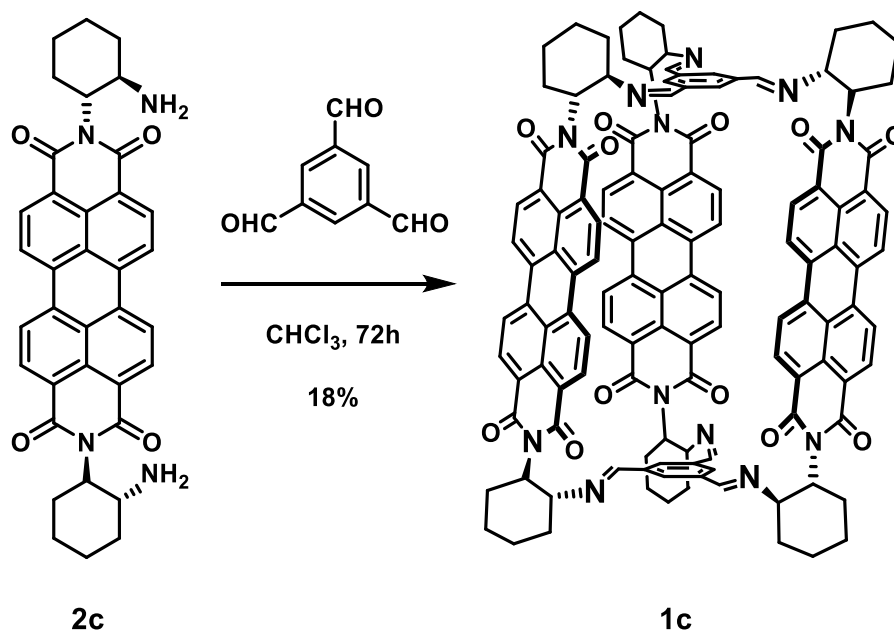
The ditosylate salt of **2b** (400 mg, 0.519 mmol) was suspended in a solution of benzene-1,3,5-tricarbaldehyde (56.1 mg, 0.346 mmol) in dry chloroform (52 ml) and TEA (0.486 ml, 3.46 mmol) was added quickly in one portion to the stirred mixture in a pressure flask at room temperature. The pressure flask was closed and heated to 80 °C. After 72 hours, the reaction mixture was cooled down to room temperature and filtered through a disposable syringe filter. The filtrate was concentrated under reduced pressure to obtain a white solid product. A small amount of methanol was added, and the solids were sonicated at room temperature for ~30 minutes and filtered. The filter cake was washed with additional methanol followed by a portion of diethyl ether and dried in air. The crude cage **1b** was purified by HPLC using *n*-heptane/CH₂Cl₂ (4:6) as eluent to afford a pure sample of **1b** as a white solid (160 mg) in 62%.

¹H NMR (500 MHz, CD₂Cl₂): δ 8.19 (s, 6H), 8.05 (s, 6H), 7.68 (s, 6H), 4.43 (ddd, *J* = 12.7, 10.4, 4.0 Hz, 6H), 3.96 (ddd, *J* = 10.4, 10.4, 4.6 Hz, 6H), 2.29 (tdd, *J* = 12.8, 12.6, 3.8 Hz, 6H), 1.88 (d, *J* = 13.0 Hz, 6H), 1.80–1.77 (m, 12H), 1.69–1.67 (m, 6H), 1.53–1.52 (m, 6H), 1.50–1.47 (m, 6H), 1.44–1.41 (m, 6H).

^{13}C NMR (126 MHz, CD_2Cl_2): δ 166.82, 166.47, 160.79, 137.46, 137.42, 136.95, 129.00, 117.92, 68.75, 56.98, 35.24, 28.53, 25.77, 24.56.

HR-ESI MS (m/z): calcd for $[\text{C}_{84}\text{H}_{79}\text{N}_{12}\text{O}_{12}]^+$ 1447.5935, found 1447.5925 ($[\text{M}+\text{H}]^+$); calcd for $[\text{C}_{84}\text{H}_{78}\text{N}_{12}\text{NaO}_{12}]^+$ 1469.5754, found 1469.5759 ($[\text{M}+\text{Na}]^+$); calcd for $[\text{C}_{85}\text{H}_{83}\text{N}_{12}\text{O}_{13}]^+$ 1479.6197, found 1479.6189 ($[\text{M}+\text{MeOH}+\text{H}]^+$).

Cage 1c



Diamine **2c** (67.6 mg, 0.116 mmol) was suspended in a solution of benzene-1,3,5-tricarbaldehyde (12.5 mg, 0.077 mmol) in dry chloroform (12 ml). The mixture was stirred at room temperature for 72 hours. The solvent was then filtered through a disposable syringe filter and the filtrate was concentrated under reduced pressure to obtain a red solid product. A small amount of methanol was added and the suspension was sonicated at room temperature for 30 minutes and filtered thereafter. The filter cake was washed with additional methanol followed by a portion of diethyl ether and dried in air. The crude cage **1c** was purified by HPLC using $\text{CH}_2\text{Cl}_2/i\text{-PrOH}$ (7:3) as eluent to afford a pure sample of **1c** as a red solid (14 mg) in 18%.

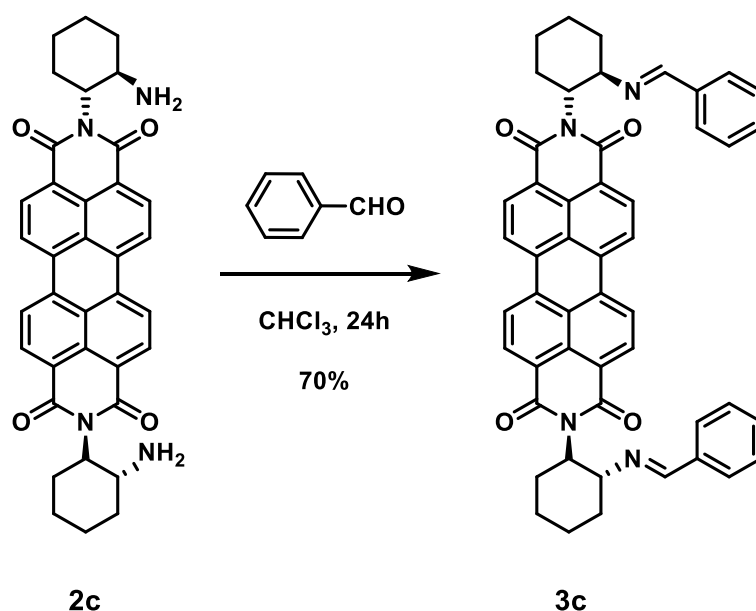
^1H NMR (500 MHz, CD_2Cl_2): δ 8.56 (d, $J = 8.0$ Hz, 6H), 8.48 (d, $J = 8.0$ Hz, 6H), 8.44 (d, $J = 8.0$ Hz, 6H), 8.43 (d, $J = 8.0$ Hz, 6H), 8.25 (s, 6H), 7.85 (s, 6H),

5.38 (ddd, $J = 10.3, 10.1, 3.9$ Hz, 6H), 4.51–4.46 (m, 6H), 2.46 (dddd, $J = 12.8, 12.6, 9.5, 3.8$ Hz, 6H), 1.89 (d, $J = 10.6$ Hz, 6H), 1.83 (d, $J = 11.5$ Hz, 6H), 1.75–1.72 (m, 6H), 1.68–1.64 (m, 12H), 1.58–1.50 (m, 12H).

^{13}C NMR (151 MHz, CD_2Cl_2): δ 164.25, 164.09, 160.24, 137.59, 134.67, 134.61, 132.04, 131.31, 129.79, 129.55, 126.54, 124.33, 123.66, 123.43, 123.36, 69.83, 58.64, 36.34, 28.33, 26.40, 24.95.

HR-ESI MS (m/z): calcd for $[\text{C}_{126}\text{H}_{98}\text{N}_{12}\text{O}_{12}]^{2+}$ 985.3708, found 985.3712 ($[\text{M}+2\text{H}]^{2+}$).

Compound 3c



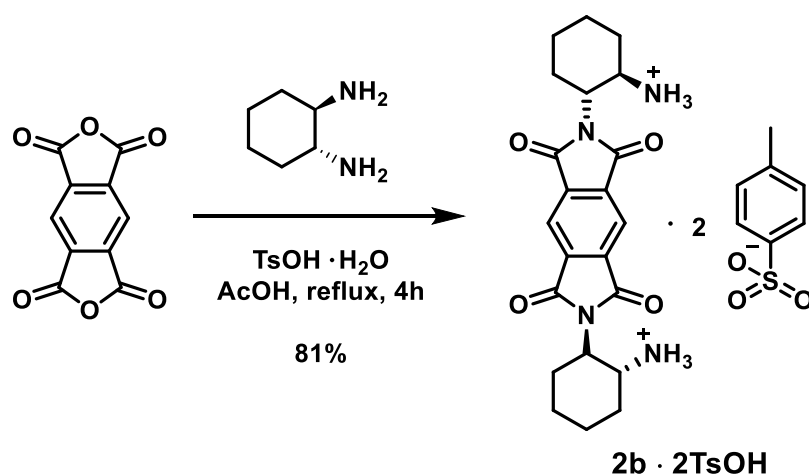
Diamine **2c** (100 mg, 0.171 mmol) was suspended in a solution of benzaldehyde (37.2 mg, 0.351 mmol) in dry chloroform (20 ml). The mixture was stirred for 24 hours at room temperature. The reaction mixture was then filtered by a disposable syringe filter and the filtrate was concentrated under reduced pressure to obtain a red solid product. A small amount of methanol was added and the suspension was sonicated at room temperature for 30 minutes and filtered thereafter. The filter cake was washed with additional methanol followed by a portion of diethyl ether and dried in air yielding **3c** as a red solid (91 mg) in 70%.

¹H NMR (600 MHz, CD₂Cl₂): δ 8.33–8.26 (m, 6H), 8.08–8.07 (m, 2H), 7.89–7.85 (m, 2H), 7.60–7.53 (m, 4H), 7.16–7.11 (m, 6H), 5.36–5.33 (m, 2H), 4.48–4.46 (br, 2H), 2.59–2.57 (br, 2H), 2.01–1.95 (m, 2H), 1.95–1.86 (m, 6H), 1.86–1.78 (m, 2H), 1.65–1.61 (m, 4H).

¹³C NMR (151 MHz, CD₂Cl₂): δ 164.25, 163.96, 160.88, 136.96, 134.44, 134.23, 131.68, 130.88, 129.47, 128.87, 128.41, 126.40, 126.24, 124.06, 123.37, 123.08, 122.96, 69.71, 58.88, 35.44, 28.61, 26.58, 25.07

HR-ESI MS (*m/z*): calcd for [C₅₀H₄₁N₄O₄]⁺ 761.3112, found 761.3118 ([M+H]⁺).

Compound 2b • 2TsOH



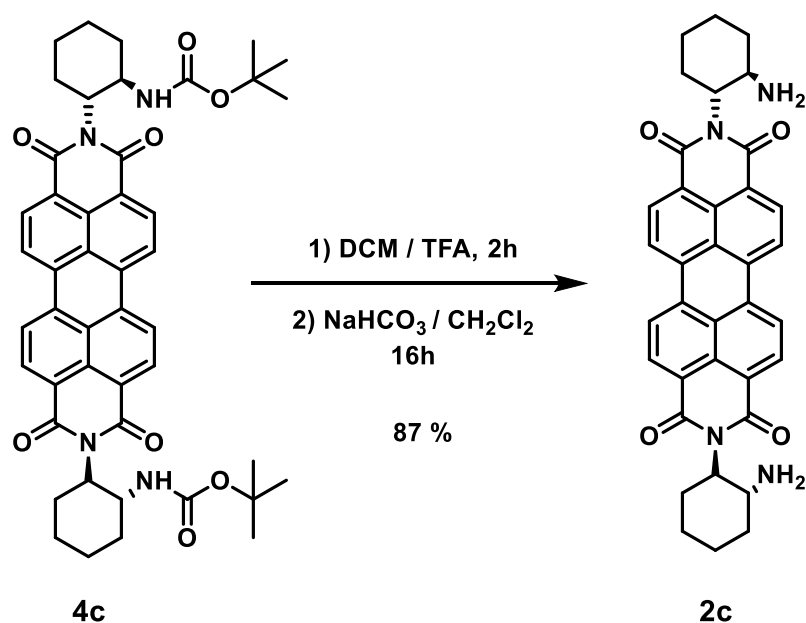
A slightly modified previously-reported strategy was followed.¹³ (1*R*,2*R*)-cyclohexane-1,2-diamine (288 mg, 2.5 mmol) was added quickly in one portion to a vigorously stirred suspension of pyromellitic dianhydride (273 mg, 1.25 mmol) and *p*-toluenesulfonic acid monohydrate (476 mg, 2.5 mmol) in glacial AcOH (10 mL) at room temperature. The reaction mixture was stirred at room temperature for 1 hour under Ar atmosphere. Later, the mixture was refluxed until a homogenous solution was obtained and the stirring was continued for additional 3 hours, after which the homogenous solution had transformed into a suspension. The reaction mixture was cooled down to room temperature and the solvent was removed under reduced pressure. The crude residue was purified by precipitation followed by filtration from MeOH/Et₂O to afford the ditosylate salt of **2b** as a white solid (797 mg) in 81%.

¹H NMR (500 MHz, TFA-*d*₁): δ 8.07 (s, 2H), 7.51 (d, *J* = 8.0 Hz, 4H), 7.20 (d, *J* = 8.0 Hz, 4H), 7.02 (br, 4H), 4.43–4.37 (ddd, *J* = 12.0, 11.0, 3.0 Hz, 2H), 4.31–4.28 (m, 2H), 2.40–2.25 (m, 6H), 2.34 (s, 6H), 1.94 (d, *J* = 12.0 Hz, 4H), 1.74–1.65 (m, 2H), 1.54–1.38 (m, 4H).

¹³C NMR (126 MHz, TFA-*d*₁): δ 169.57, 146.64, 138.97, 138.21, 131.38, 127.58, 127.02, 56.05, 54.49, 32.27, 30.57, 25.87, 24.93, 21.72.

HR-ESI MS (*m/z*): calcd for [C₂₂H₂₈N₄O₄]²⁺ 206.1050, found 206.1050 ([M]²⁺); calcd for [C₂₉H₃₅N₄O₇S]⁺ 583.2221, found 583.2221 ([M+TsOH-H]⁺).

Compound 2c



Compound **4c** (300 mg, 0.382 mmol) was dissolved in a mixture of CH₂Cl₂/TFA (50 ml, 1:1 v/v) and the resulting solution was stirred at room temperature for 2 hours. The solvent was removed under reduced pressure. The red solid was dissolved in CH₂Cl₂ (200 mL) and a saturated aq. NaHCO₃ solution (200 mL) was added. The resulting suspension was stirred for 16 hours at room temperature. The organic layer was separated, and the aqueous layer was extracted with CH₂Cl₂ (3 × 100 mL). The organic layers were combined, dried with Na₂SO₄ and concentrated under reduced pressure to get **2c** as pure red solid (194 mg) in 87%.

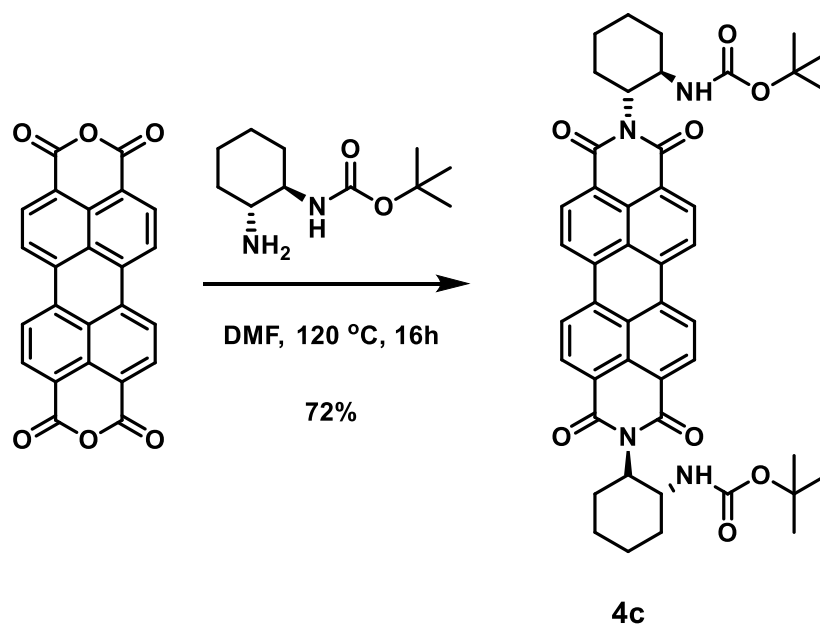
Note: Compound **2c** appears as a mixture (~1:1) of *syn* and *anti* diastereomers in a *d*-trifluoroacetic acid solution at room temperature in the NMR experiments. The rate of interconversion of the diastereomers commensurate to the NMR time scale therefore complicates the ^{13}C NMR spectra.

^1H NMR (400 MHz, TFA-*d*₁): δ 8.71–8.63 (m, 8H), 6.97 (br, 2H), 5.31–5.24 (m, 2H), 4.80–4.65 (m, 2H), 2.65–2.59 (m, 2H), 2.37 (d, $J = 12.0$ Hz, 2H), 2.04–1.94 (m, 6H), 1.70 (dd, $J = 11.8$ Hz, $J = 11.3$ Hz, 2H), 1.60–1.46 (m, 4H).

^{13}C NMR (101 MHz, TFA-*d*₁): δ 169.37, 169.25, 168.94, 168.88, 138.66, 138.47, 135.81, 135.57, 135.38, 135.24, 131.94, 131.87, 128.79, 126.98, 126.88, 126.77, 125.26, 125.20, 124.37, 59.47, 59.38, 55.33, 33.56, 30.50, 27.12, 25.86.

HR-ESI MS (m/z): calcd for $[\text{C}_{36}\text{H}_{31}\text{N}_4\text{O}_4]^+$ 583.2360, found 583.2332 ($[\text{M}-\text{H}]^+$).

Compound 4c



tert-Butyl ((1*R*,2*R*)-2-aminocyclohexyl)carbamate (1.17 g, 5.46 mmol) was dissolved in dry DMF (100 ml), perylene-3,4,9,10-tetracarboxylic dianhydride (1.02 g, 2.6 mmol) was added and the resulting mixture was stirred at room temperature for 1 hour. The reaction mixture was then further stirred at 120 °C for 16 hours under an Ar atmosphere. The solvent was removed under reduced pressure and the residue was purified by column chromatography (SiO_2 ,

cyclohexane/EtOAc 3:1) to afford the pure product **4c** as a red solid (1.45 g) in 72%.

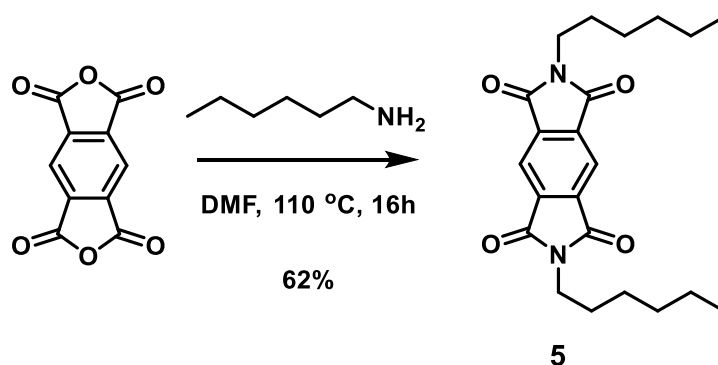
Note: Compound **4c** appears as a mixture (~1:1) of *syn* and *anti* diastereomers in a CDCl₃ solution at room temperature in the NMR experiments. The rate of interconversion of the diastereomers commensurate to the NMR time scale therefore complicates the ¹³C NMR spectra.

¹H NMR (600 MHz, CDCl₃): δ 8.71 (d, *J* = 6.4, 2H), 8.68–8.62 (m, 2H), 8.61–8.51 (m, 4H), 4.91–4.86 (ddd, *J* = 11.8, 11.8, 3.6 Hz, 2H), 4.60–4.59 (m, 2H), 4.48–4.46 (d, *J* = 12.0, 2H), 2.83 (ddd, *J* = 10.0, *J* = 10.0, *J* = 9.0, 2H), 2.19 (d, *J* = 11.3 Hz, 2H), 1.93–1.80 (m, 6H), 1.58–1.48 (m, 2H), 1.46–1.36 (m, 2H), 1.34–1.25 (m, 2H), 0.93 (s, 18H).

¹³C NMR (151 MHz, CDCl₃): δ 165.07, 163.94, 155.50, 134.79, 134.72, 134.26, 131.63, 131.57, 129.67, 126.47, 124.55, 123.43, 122.98, 78.90, 58.30, 49.54, 33.96, 28.66, 27.98, 26.04, 25.17.

HR-ESI MS (*m/z*): calcd for [C₄₆H₄₈N₄NaO₈]⁺ 807.3364, found 807.3374 ([M+Na]⁺).

Compound 5



Hexylamine (1.86 g, 18.3 mmol) was added quickly in one portion to a vigorously stirred suspension of pyromellitic dianhydride (2.00 g, 9.17 mmol) in DMF (40 mL) and the mixture was stirred at 110 °C overnight. After cooling to room temperature, the mixture was filtered and washed with methanol to obtain **5** as a white solid (2.23 g) in 62%.

¹H NMR (500 MHz, CDCl₃): δ 8.26 (s, 2H), 3.73 (t, $J = 7.5$ Hz, 4H), 1.70 (tt, $J = 7.3, 7.3$ Hz, 4H), 1.32 (m, 12H), 0.88 (t, $J = 10.0$ Hz, 6H).

¹³C NMR (126 MHz, CDCl₃): δ 166.48, 137.41, 118.26, 38.91, 31.43, 28.55, 26.64, 22.63, 14.13.

Section D. NMR Spectroscopy and HR-ESI MS Spectroscopy

Figure S1. ^1H NMR spectrum of **1b** (500 MHz, CD_2Cl_2 , 298K).

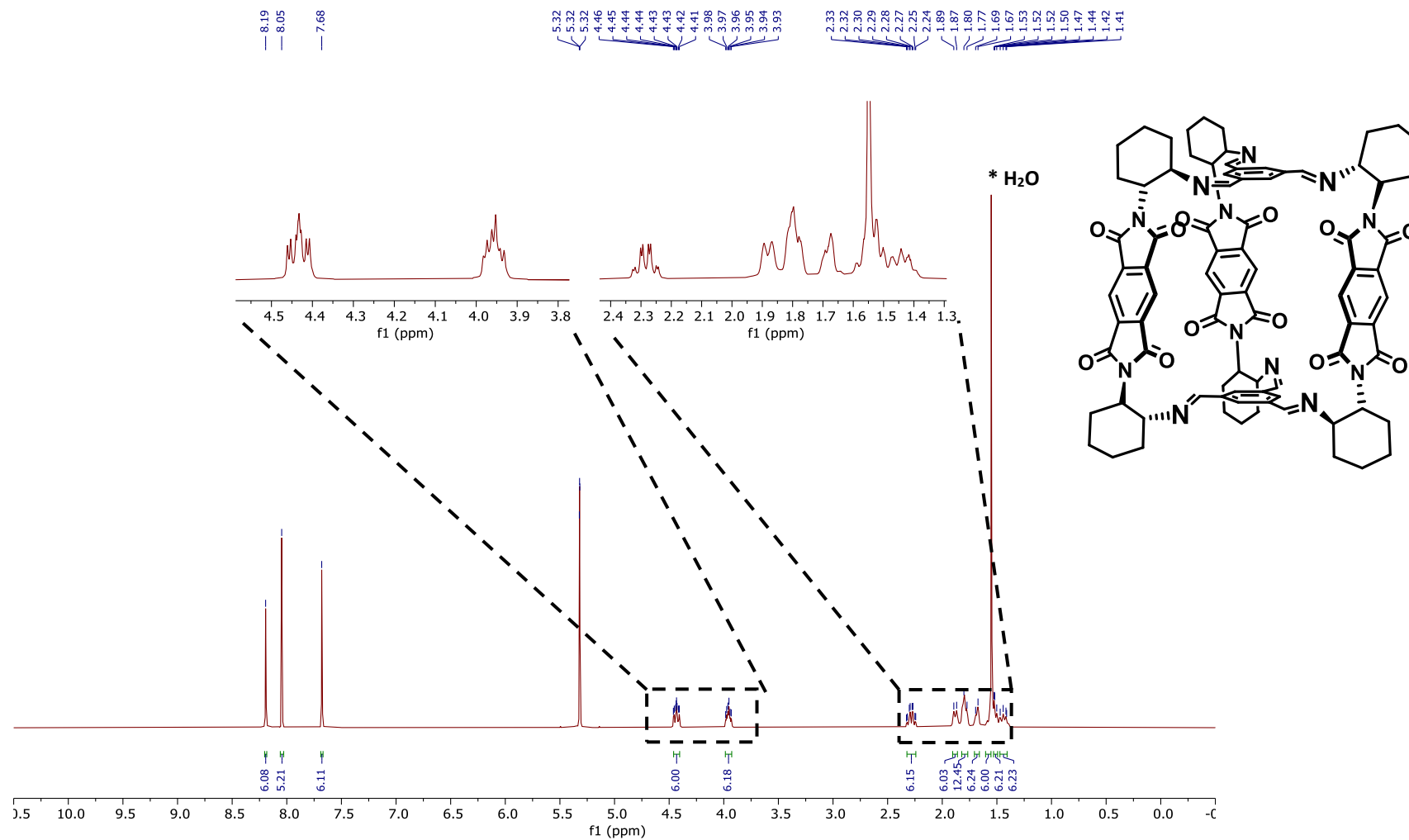


Figure S2. ^{13}C NMR spectrum of **1b** (126 MHz, CD_2Cl_2 , 298K).

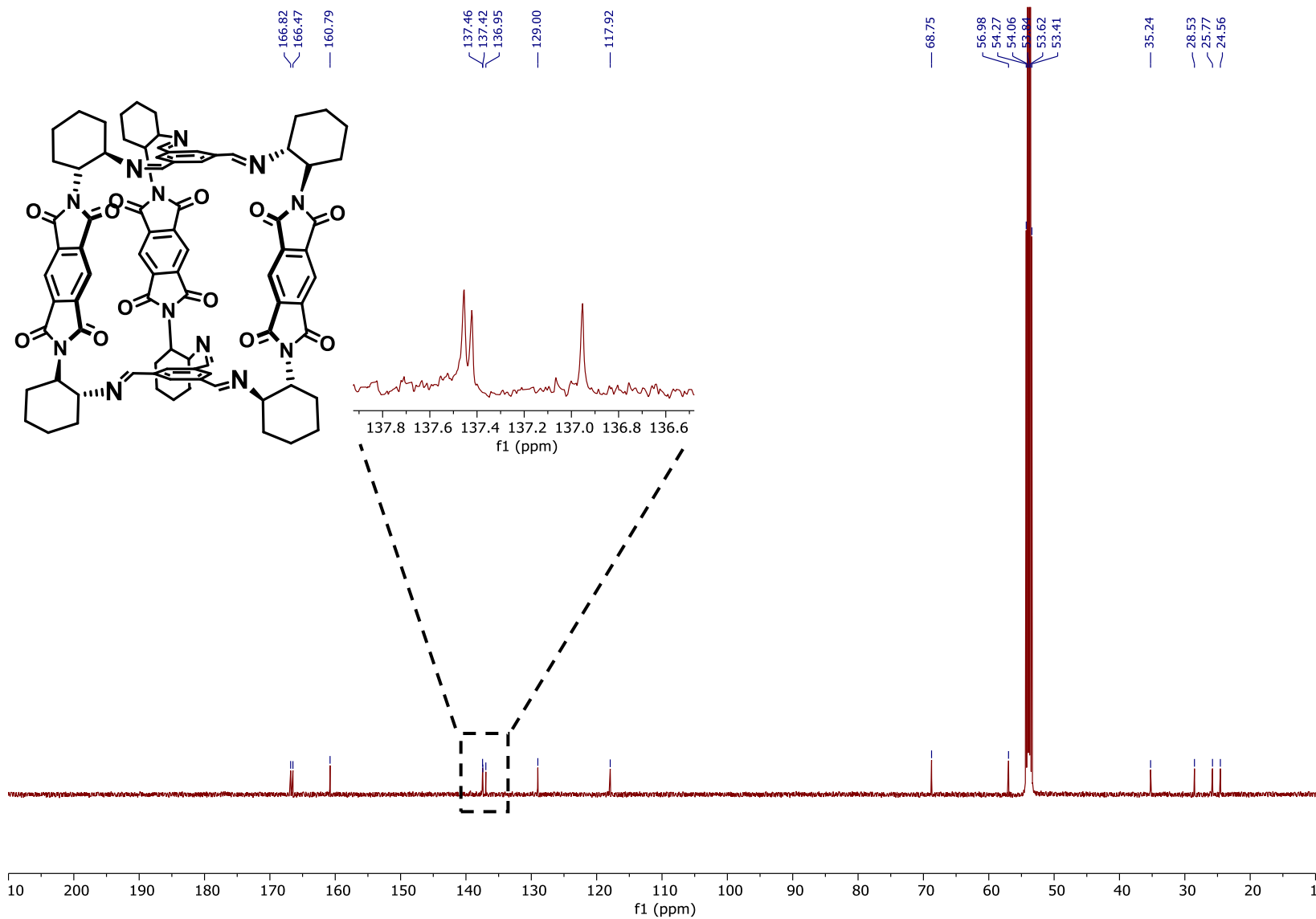


Figure S3. 2D ^1H - ^1H COSY NMR spectrum of **1b** (126 MHz, CD_2Cl_2 , 298K).

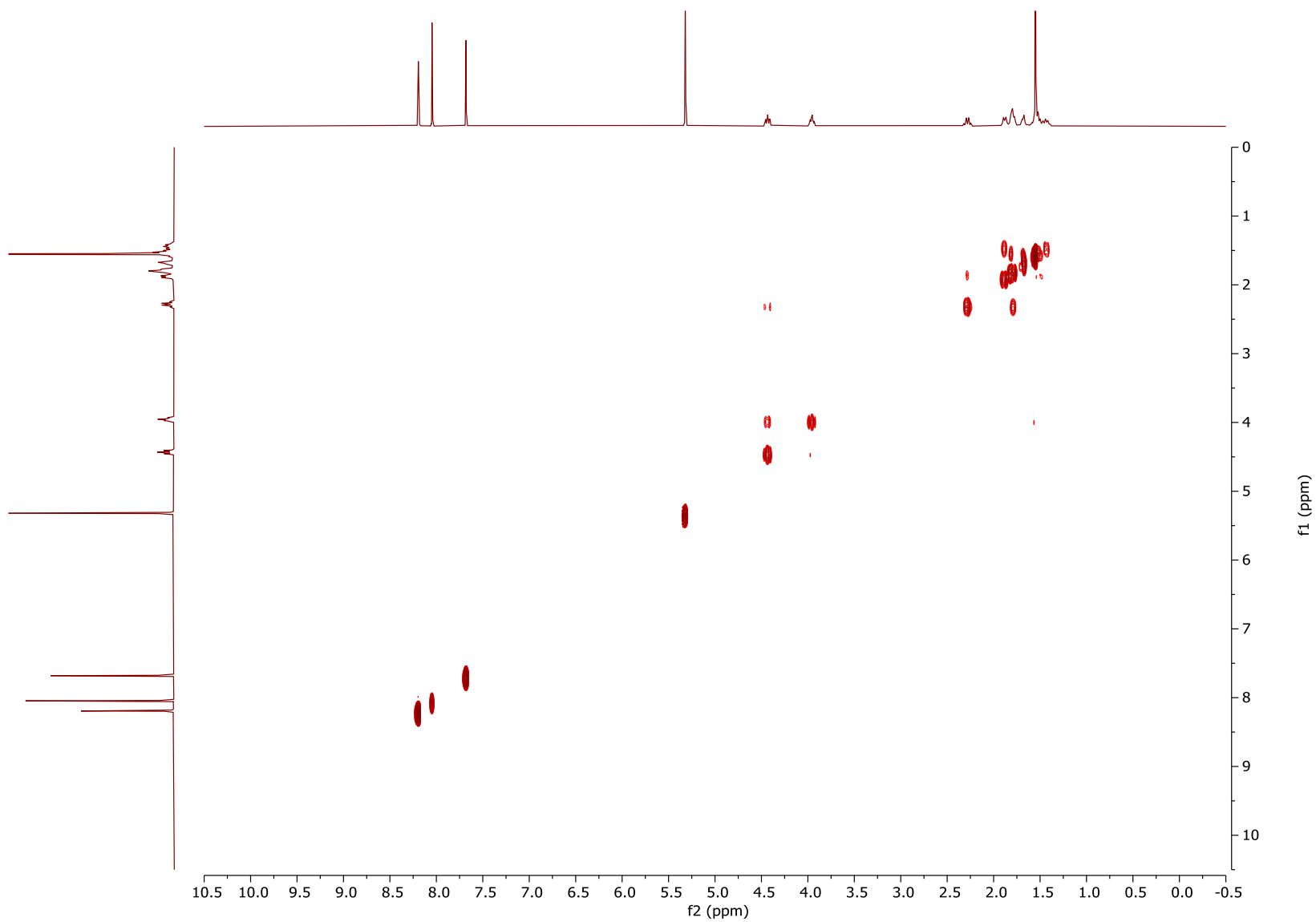


Figure S4. 2D ^1H - ^{13}C HMBC NMR spectrum of **1b** (500 MHz, CD_2Cl_2 , 298K), full spectrum.

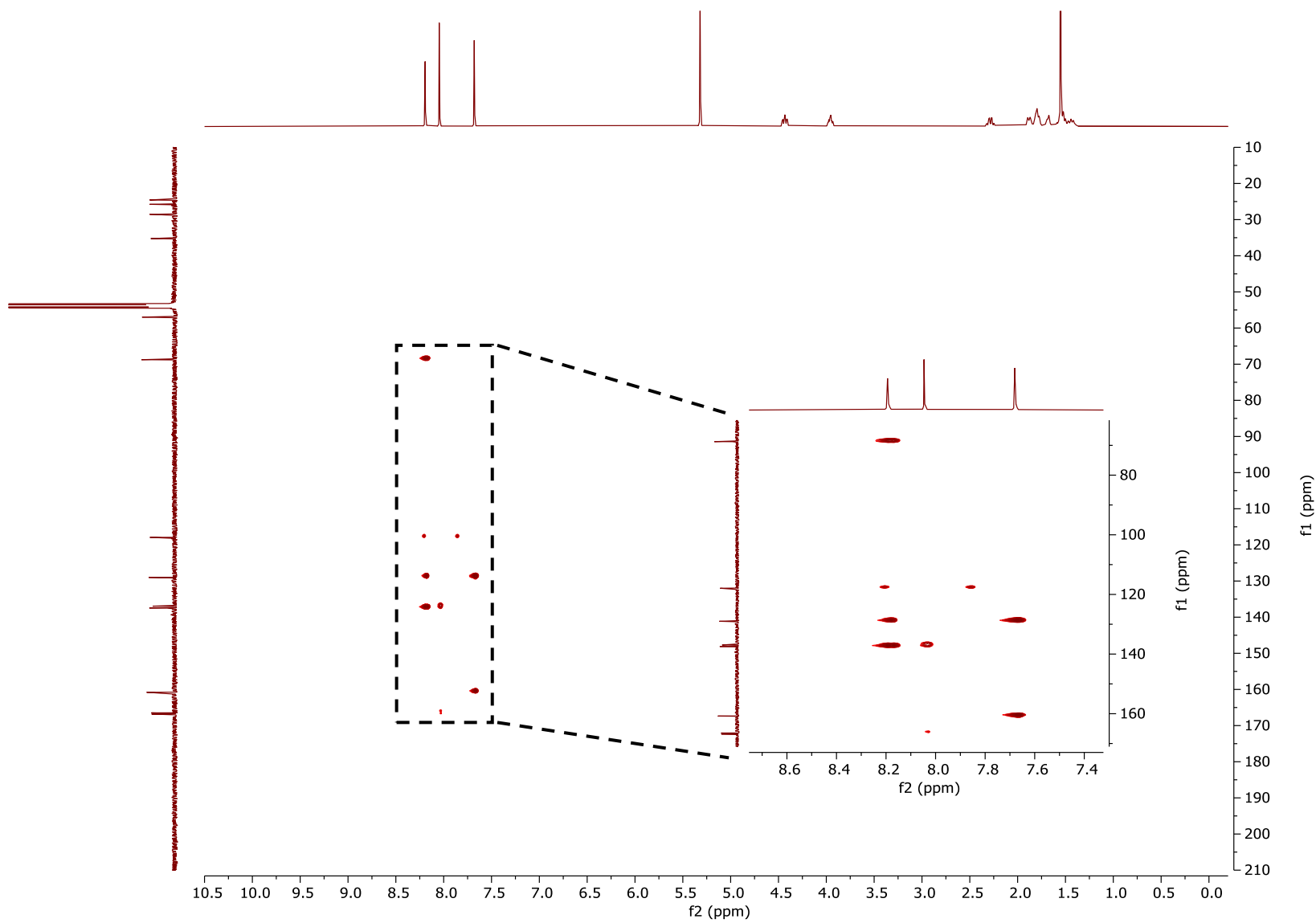


Figure S5. 2D ^1H - ^{13}C HMQC NMR spectrum of **1b** (500 MHz, CD_2Cl_2 , 298K), full spectrum.

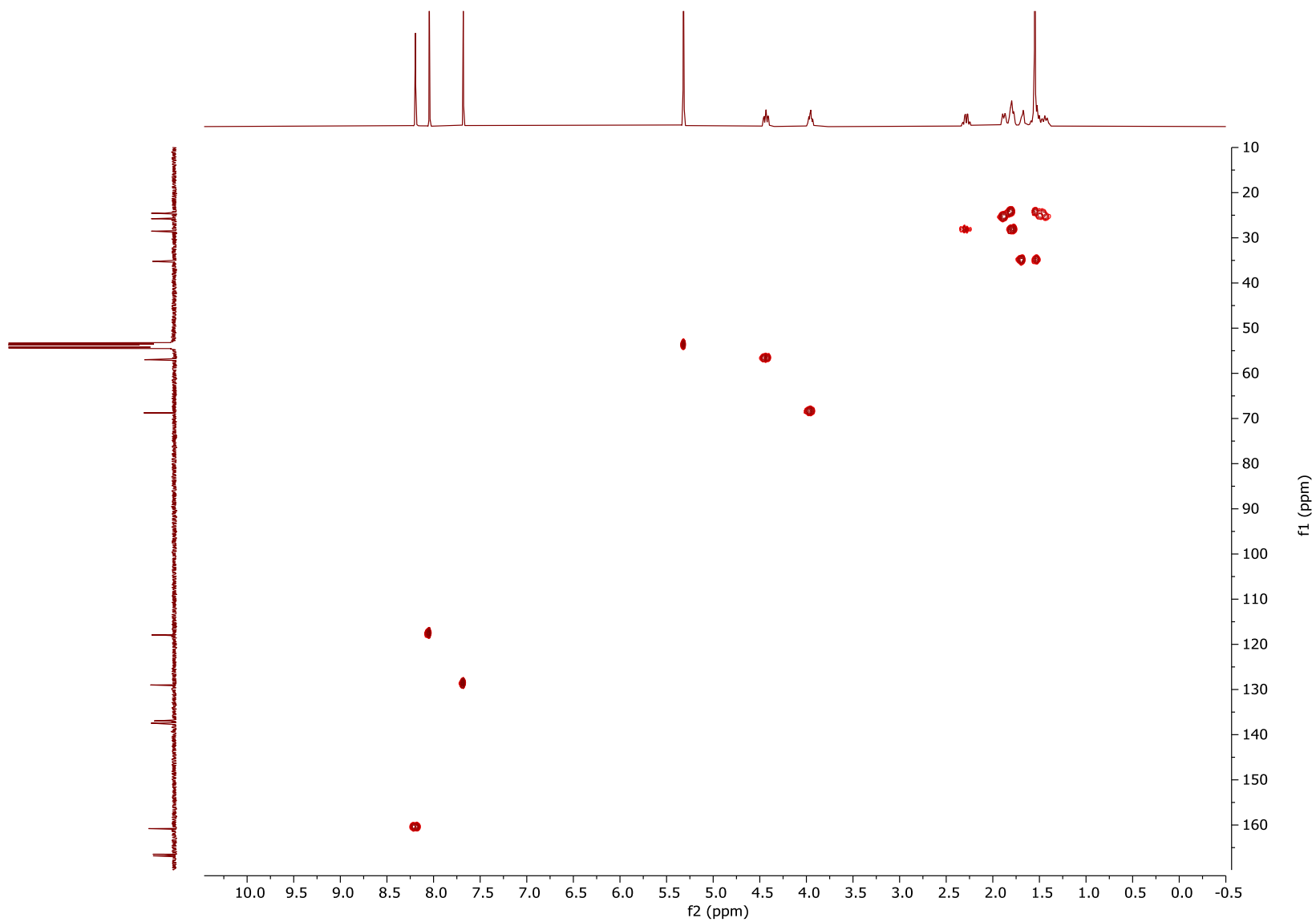


Figure S7. HR-ESI MS spectra of compound **1b**.

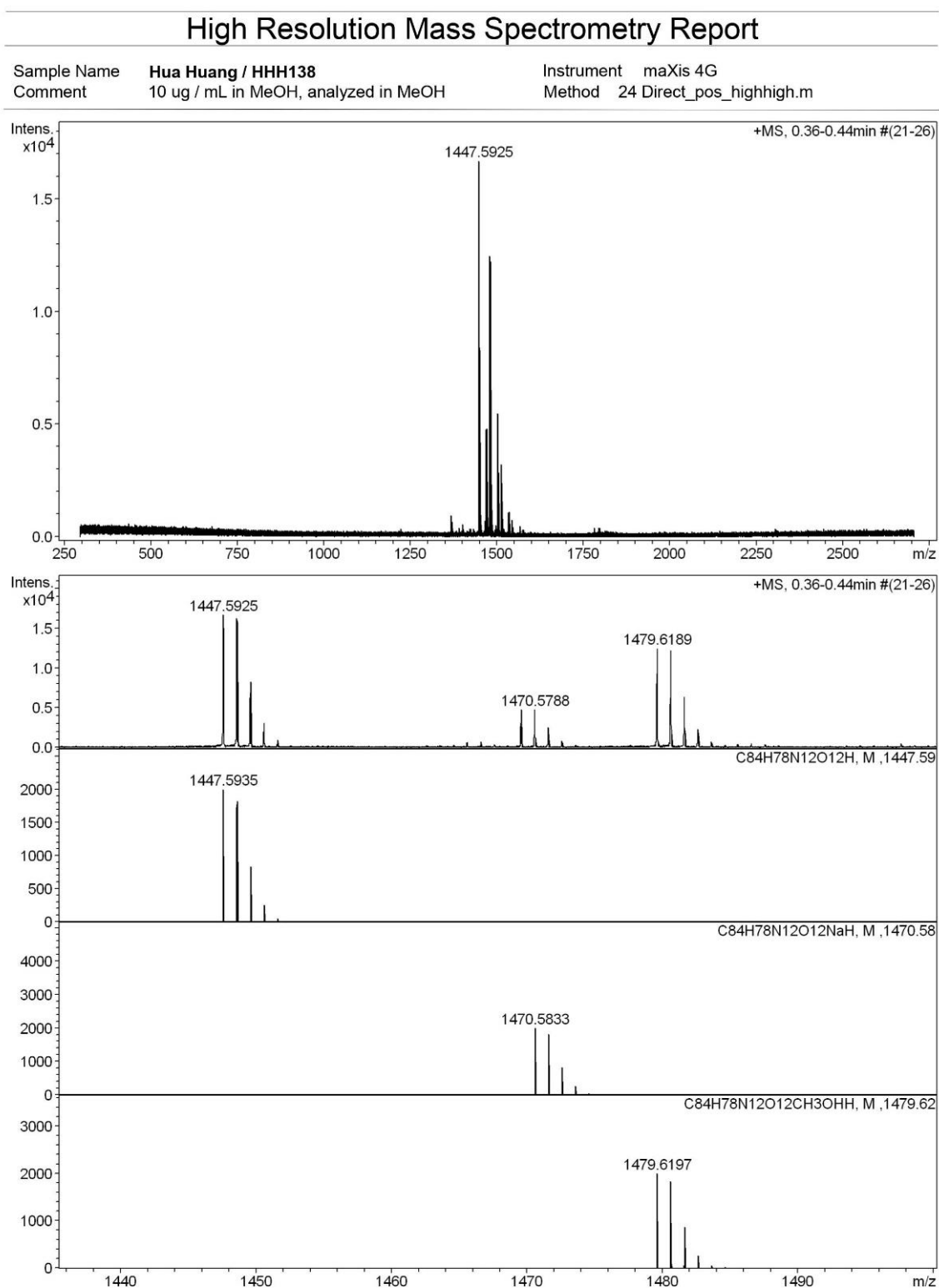


Figure S8. ^1H NMR spectrum of **1c** (400 MHz, CD_2Cl_2 , 298K).

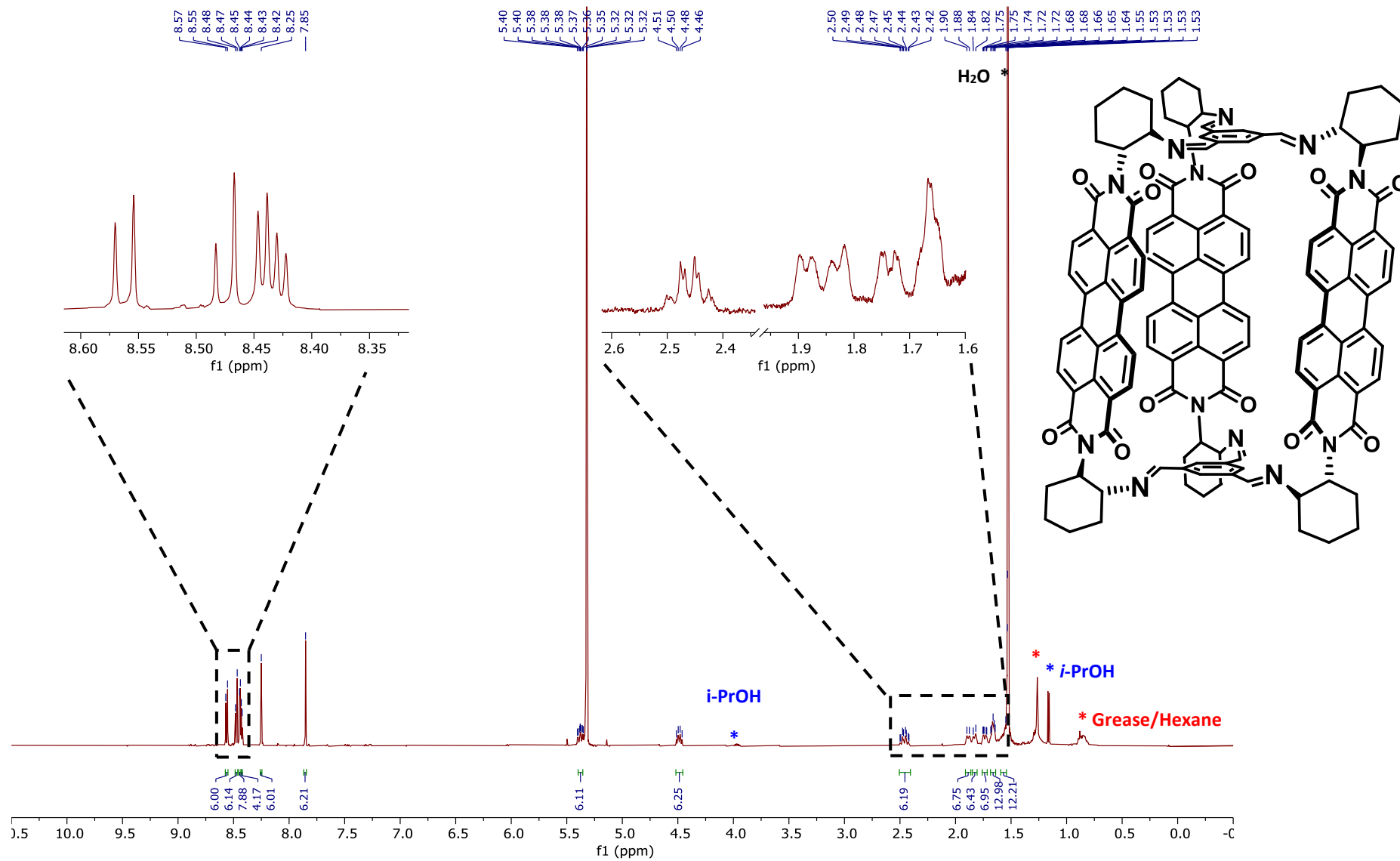


Figure S9. ^{13}C NMR spectrum of **1c** (151 MHz, CD_2Cl_2 , 298K).

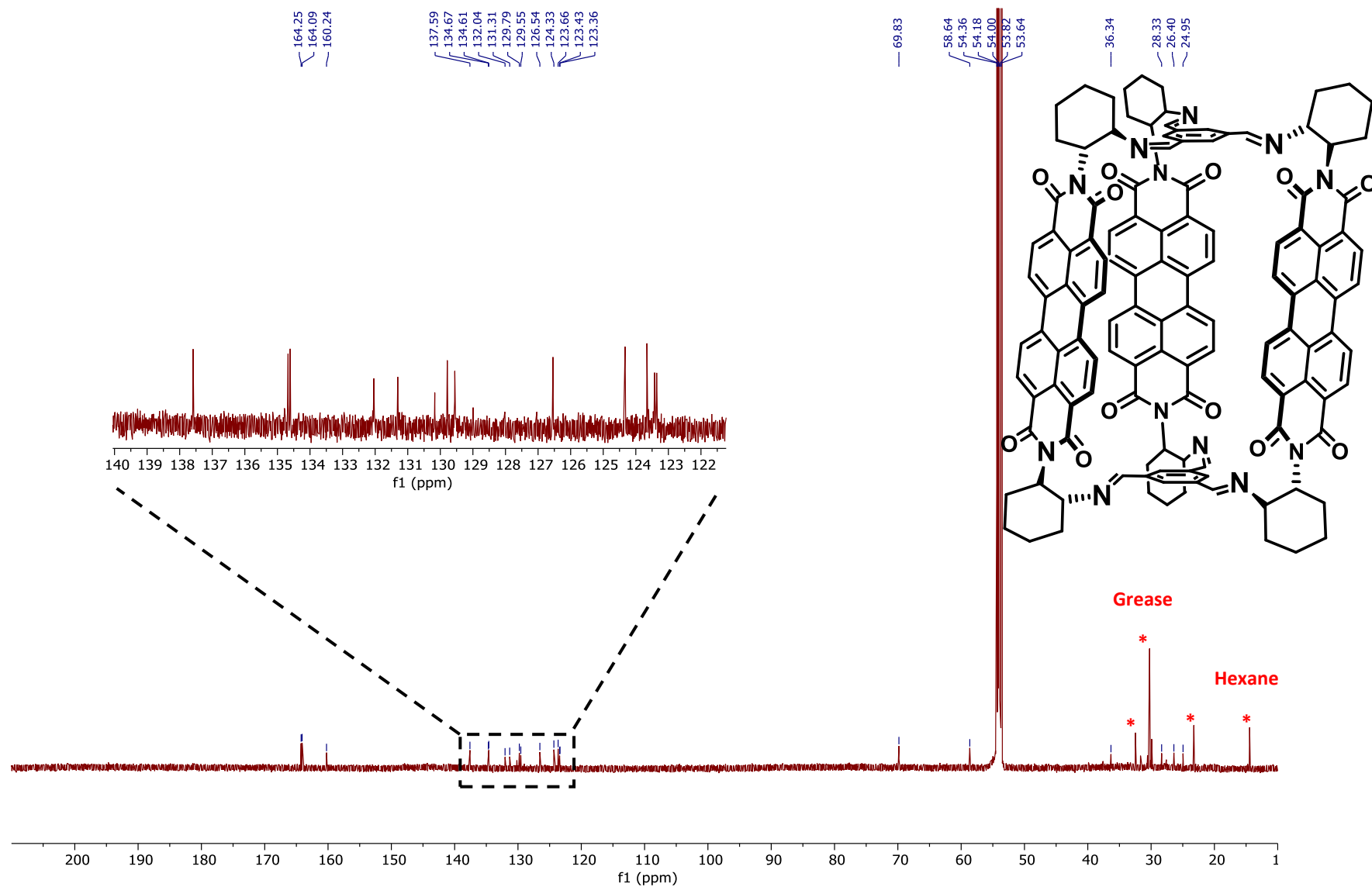


Figure S10. 2D ^1H - ^{13}C HSQC NMR spectrum of **1c** (151 MHz, 298K), full spectrum.

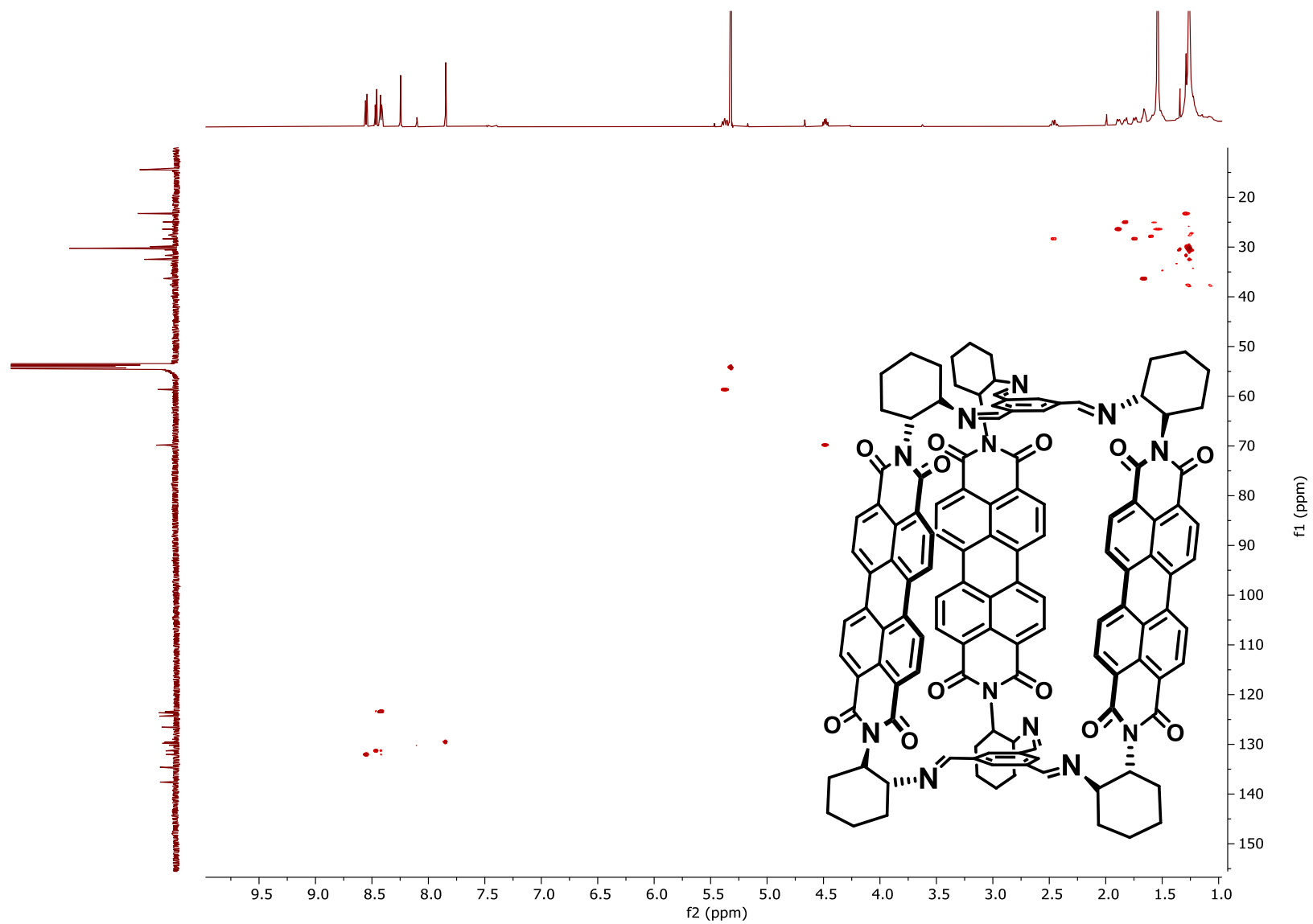


Figure S11. 2D ^1H - ^{13}C HSQC NMR spectrum of **1c** (151 MHz, CD_2Cl_2 , 298K), zoom in aromatic region.

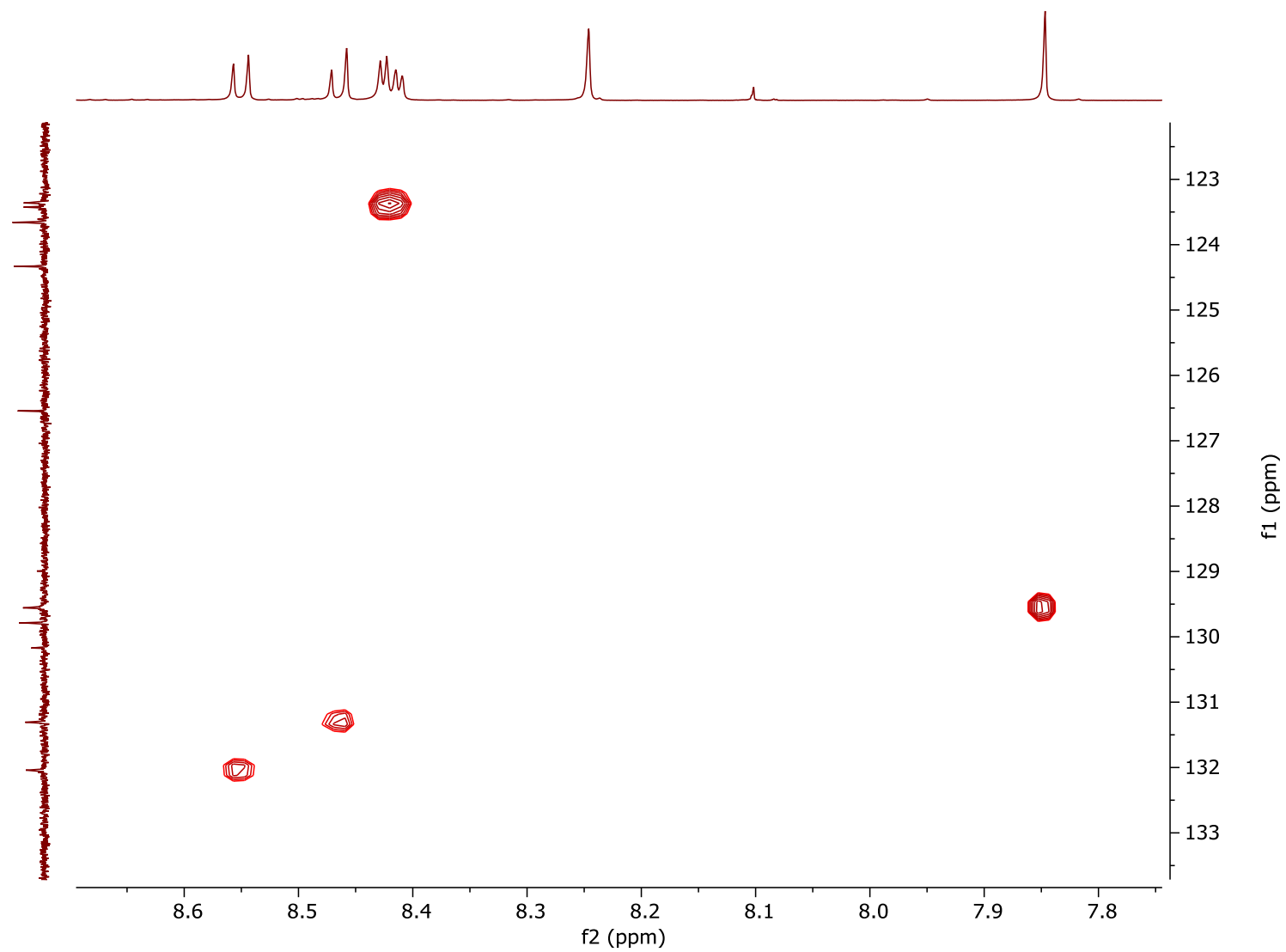


Figure S12. 2D ^1H - ^{13}C HMBC NMR spectrum of **1c** (151 MHz, CD_2Cl_2 , 298K), full spectrum.

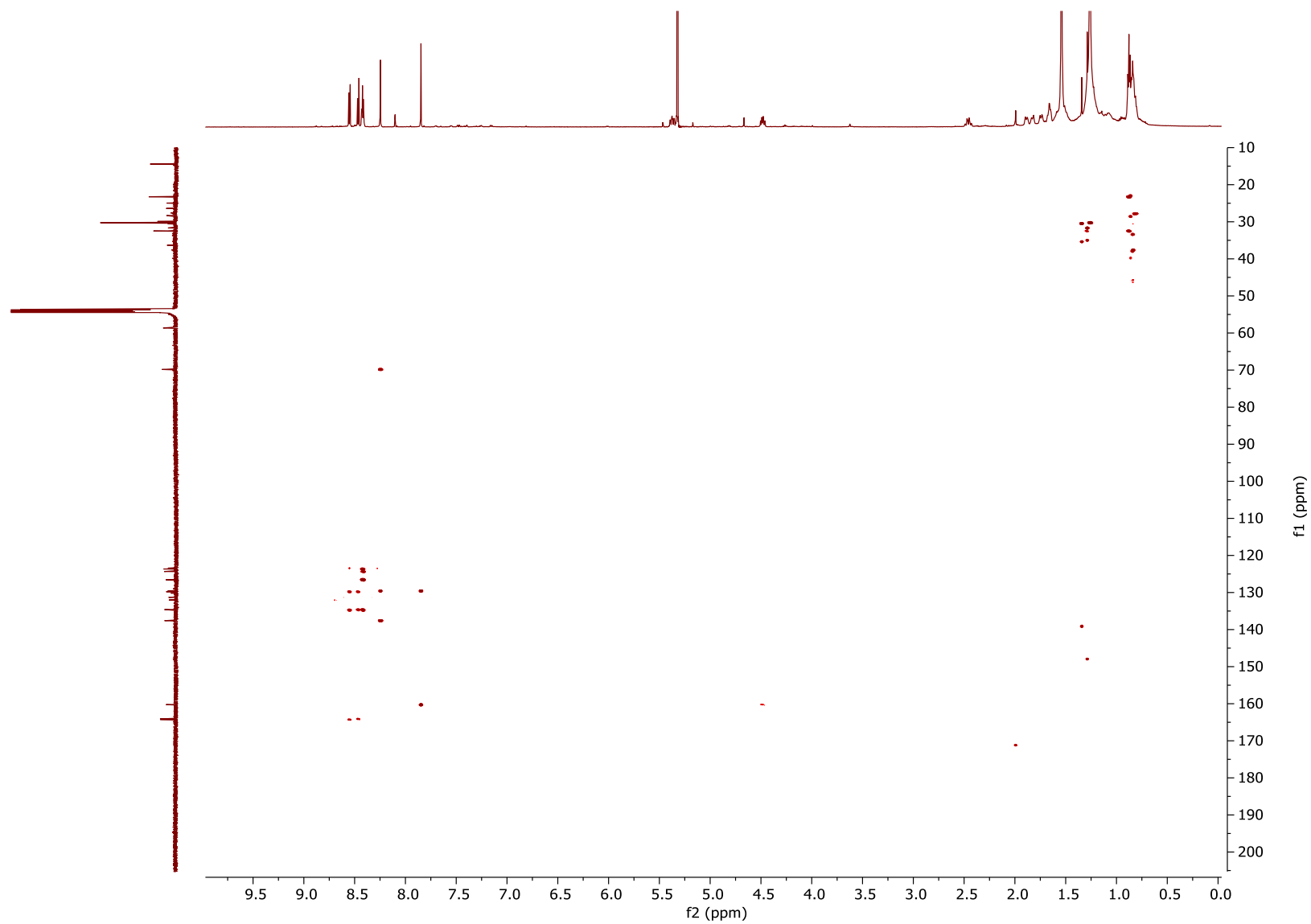


Figure S13. 2D ^1H - ^{13}C HMBC NMR spectrum of **1c** (151 MHz, CD_2Cl_2 , 298K), zoom in aromatic region.

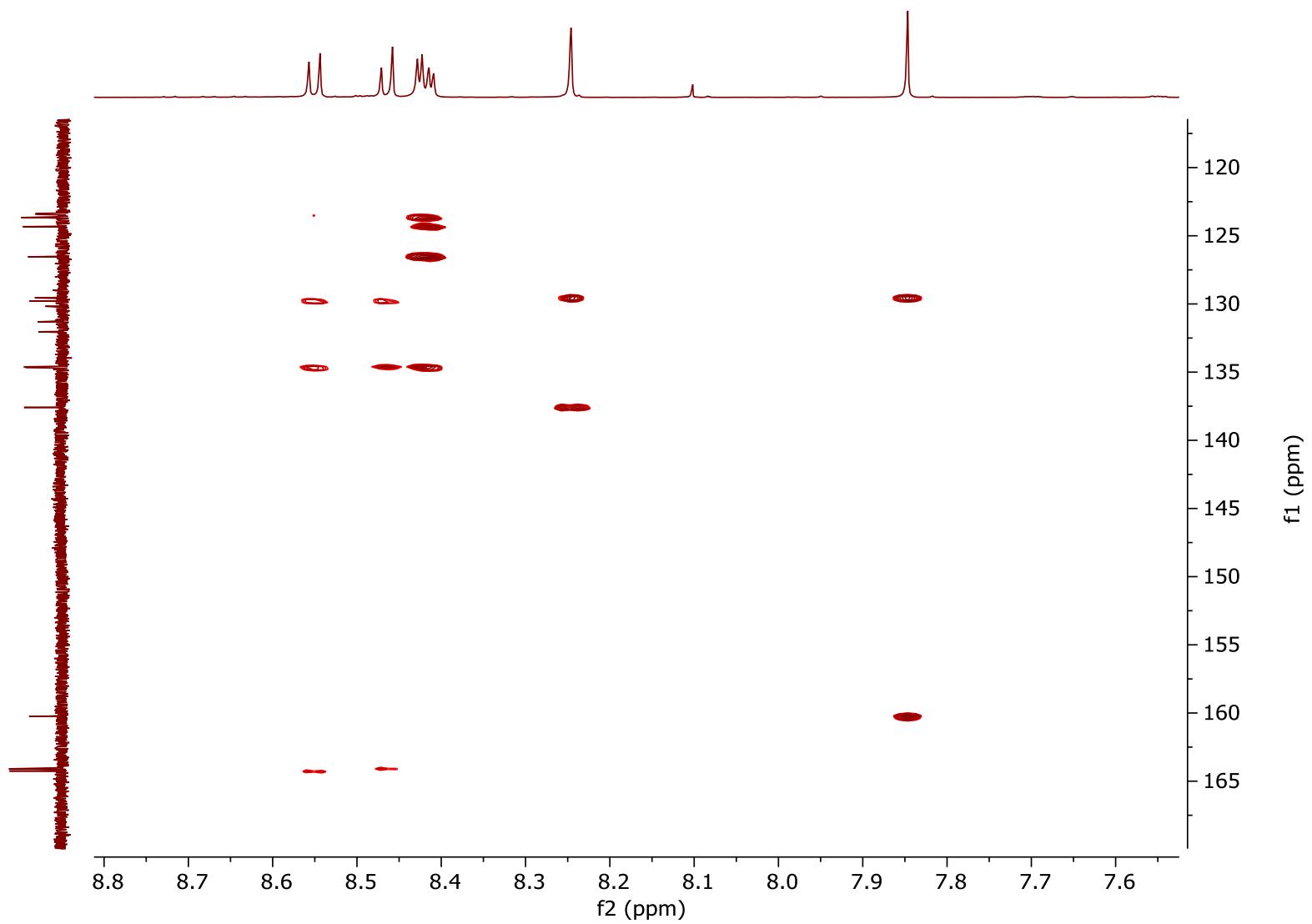


Figure S14. Full Assignment of the ^1H (black) and ^{13}C (red) NMR Shifts (in ppm) of **1c** in a CD_2Cl_2 solution.

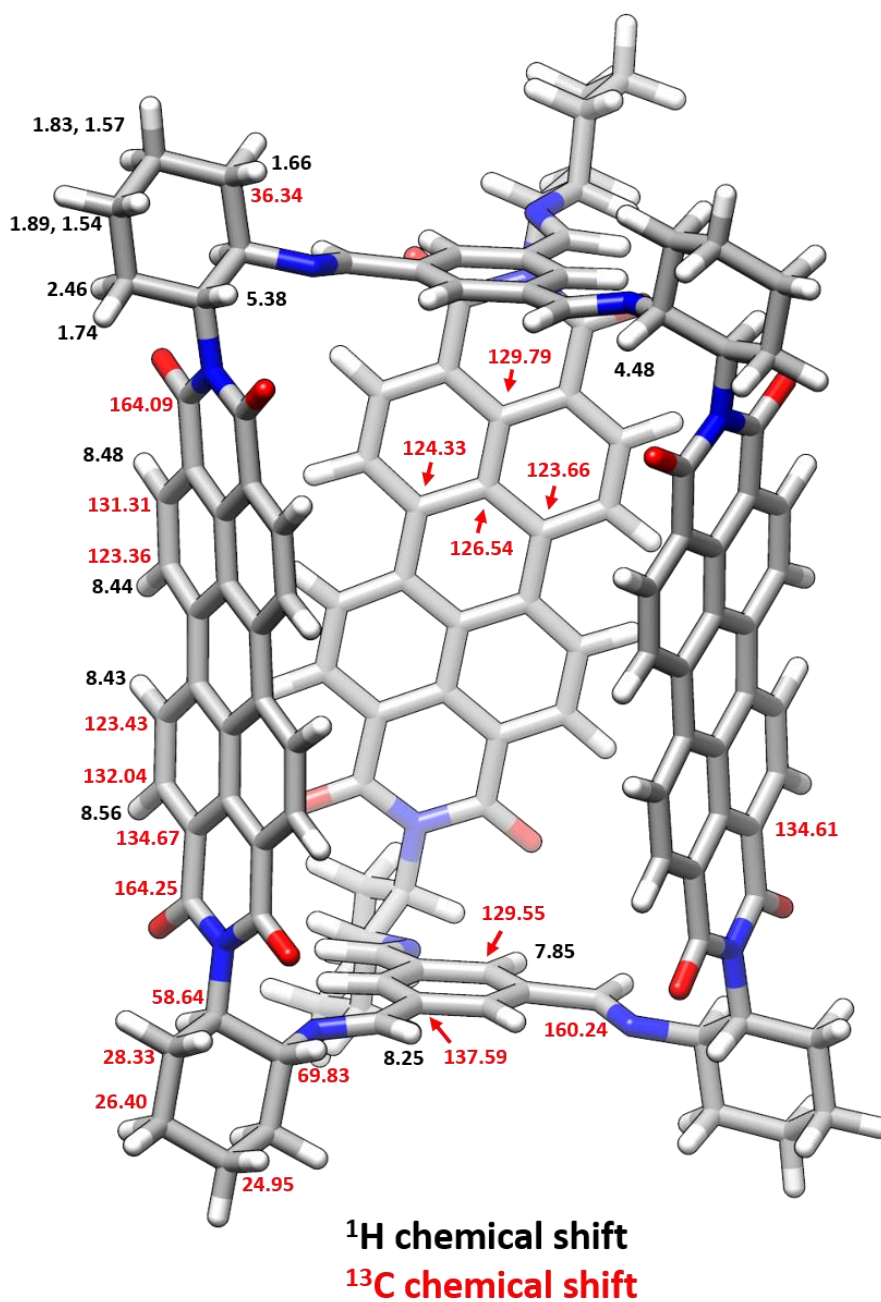


Figure S15. HR-ESI MS spectra of compound **1c**.

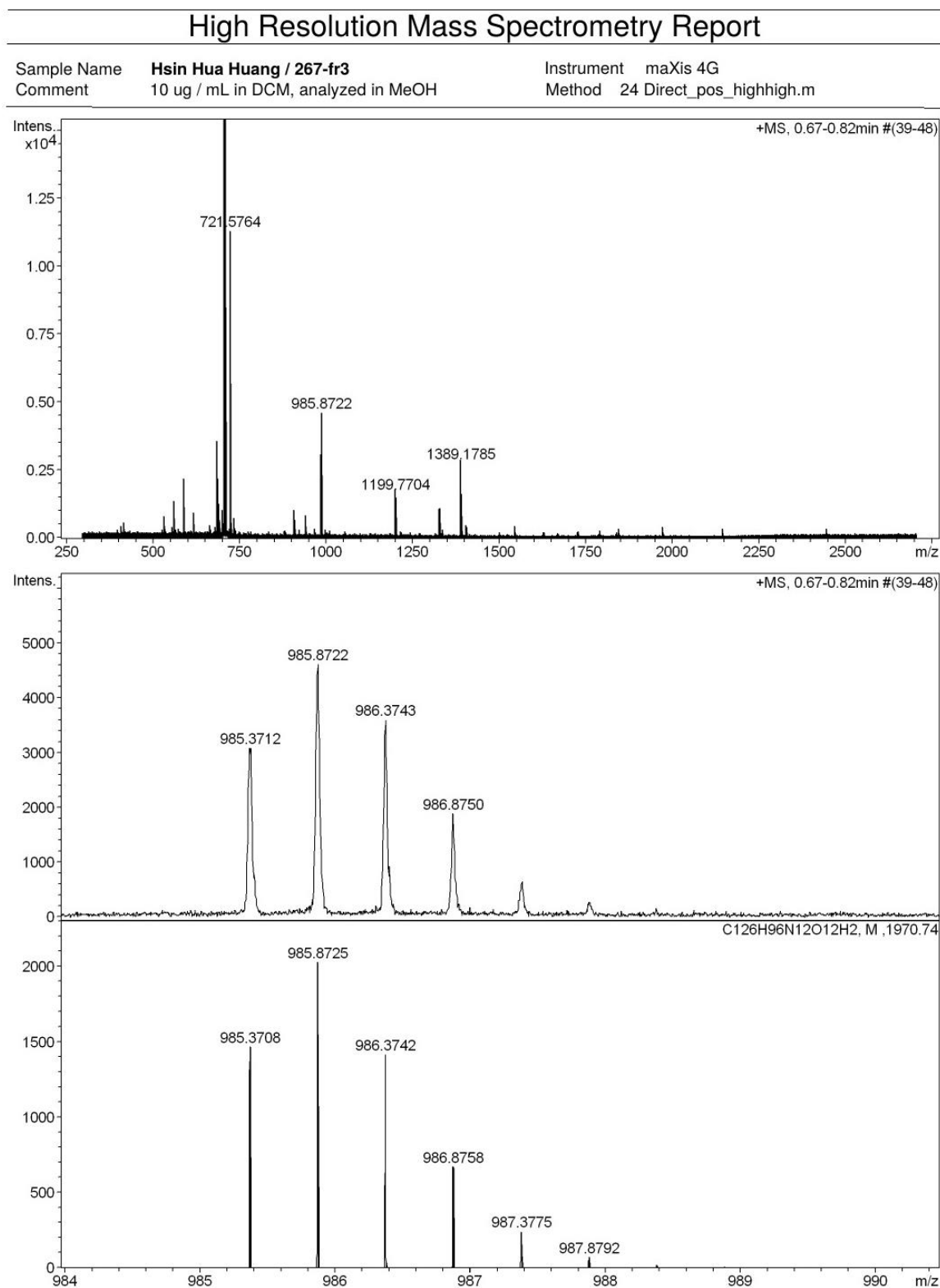


Figure S16. ^1H NMR spectrum of **2b** • 2TsOH (400 MHz, $\text{TFA-}d_1$, 298K).

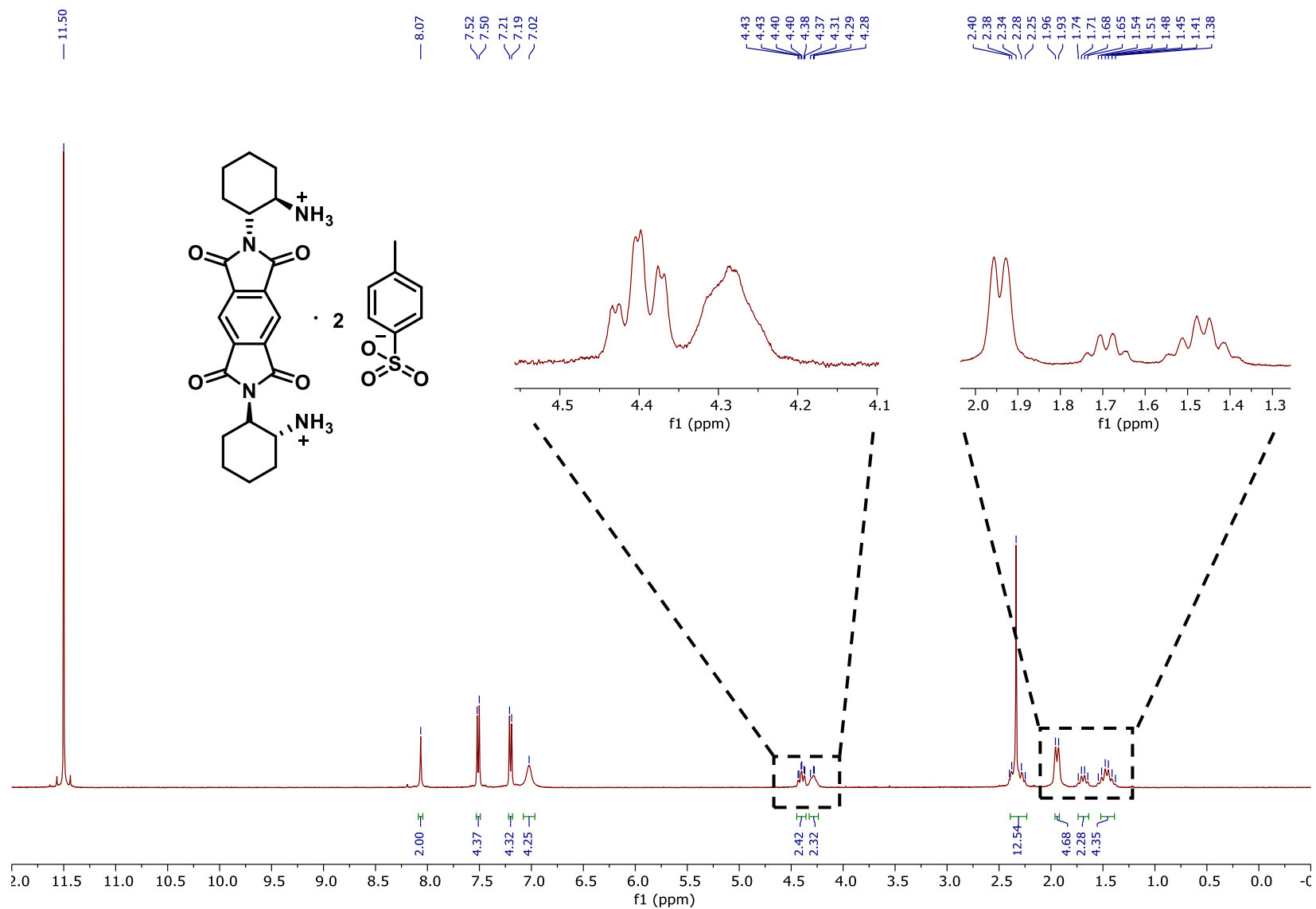


Figure S17. ^{13}C NMR spectrum of **2b** • 2TsOH (101 MHz, TFA- d_1 , 298K).

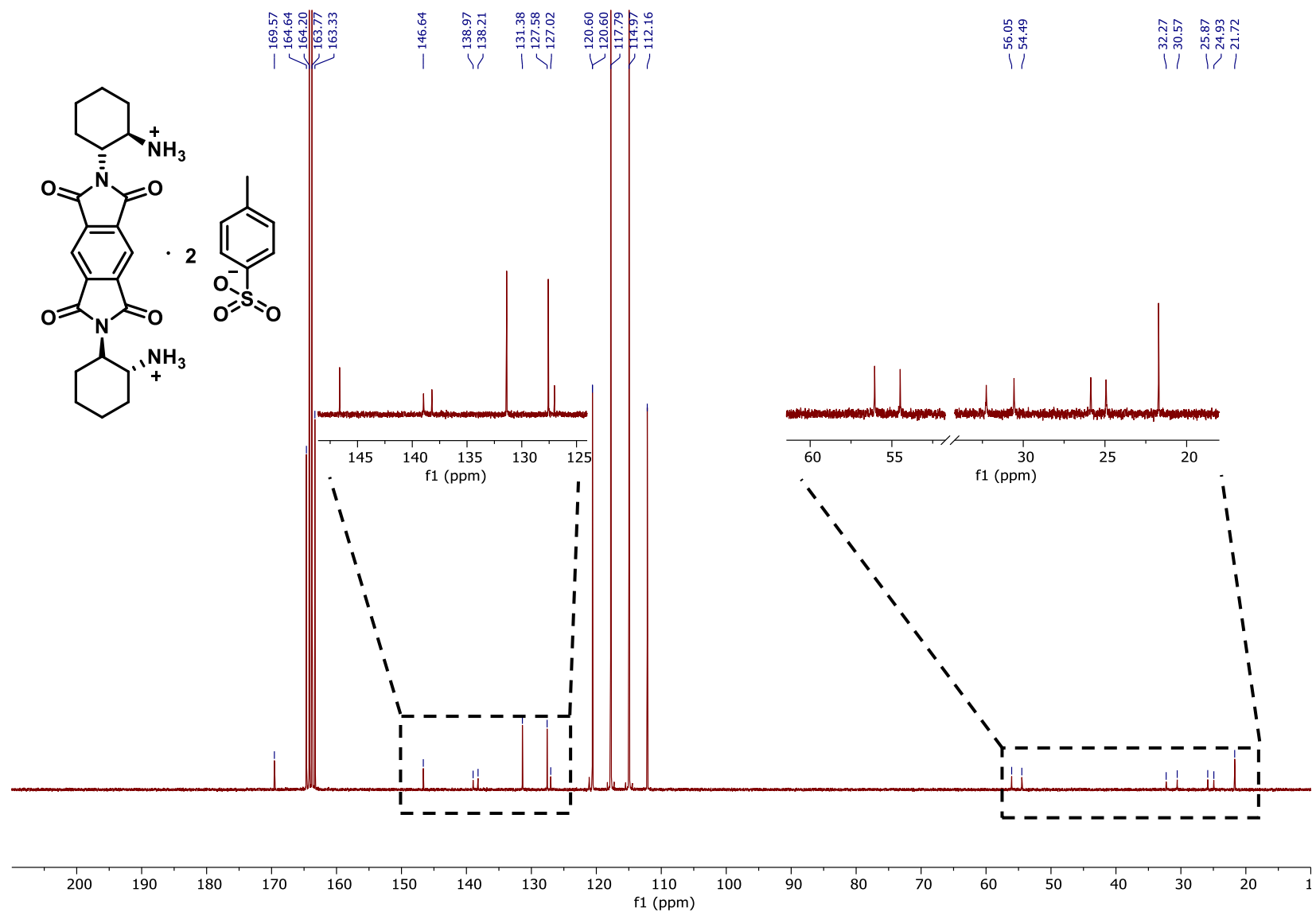


Figure S18. HR-ESI MS spectra of compound **2b** • 2TsOH.

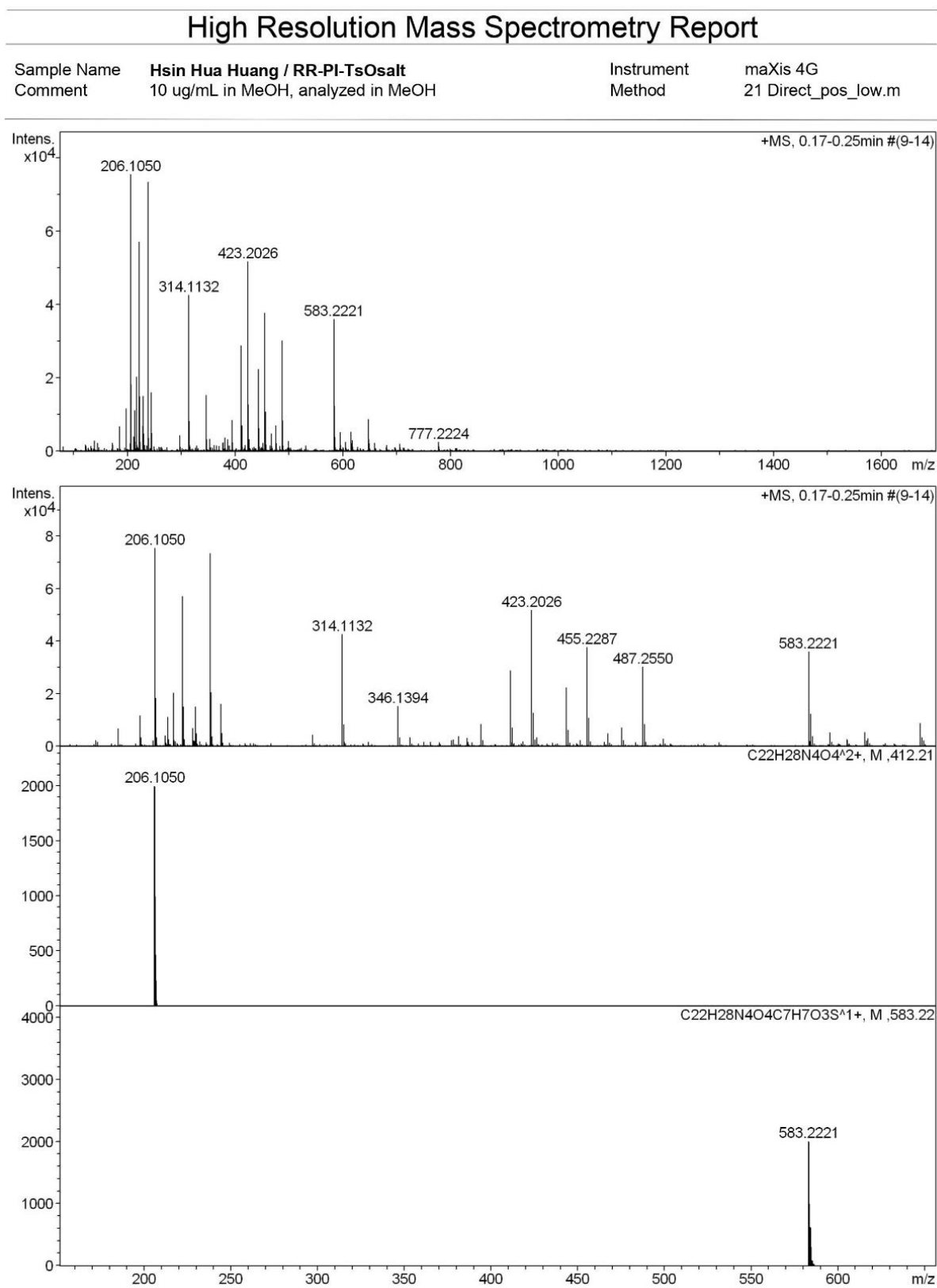


Figure S19. ^1H NMR spectrum of **2c** (400 MHz, $\text{TFA-}d_1$, 298K).

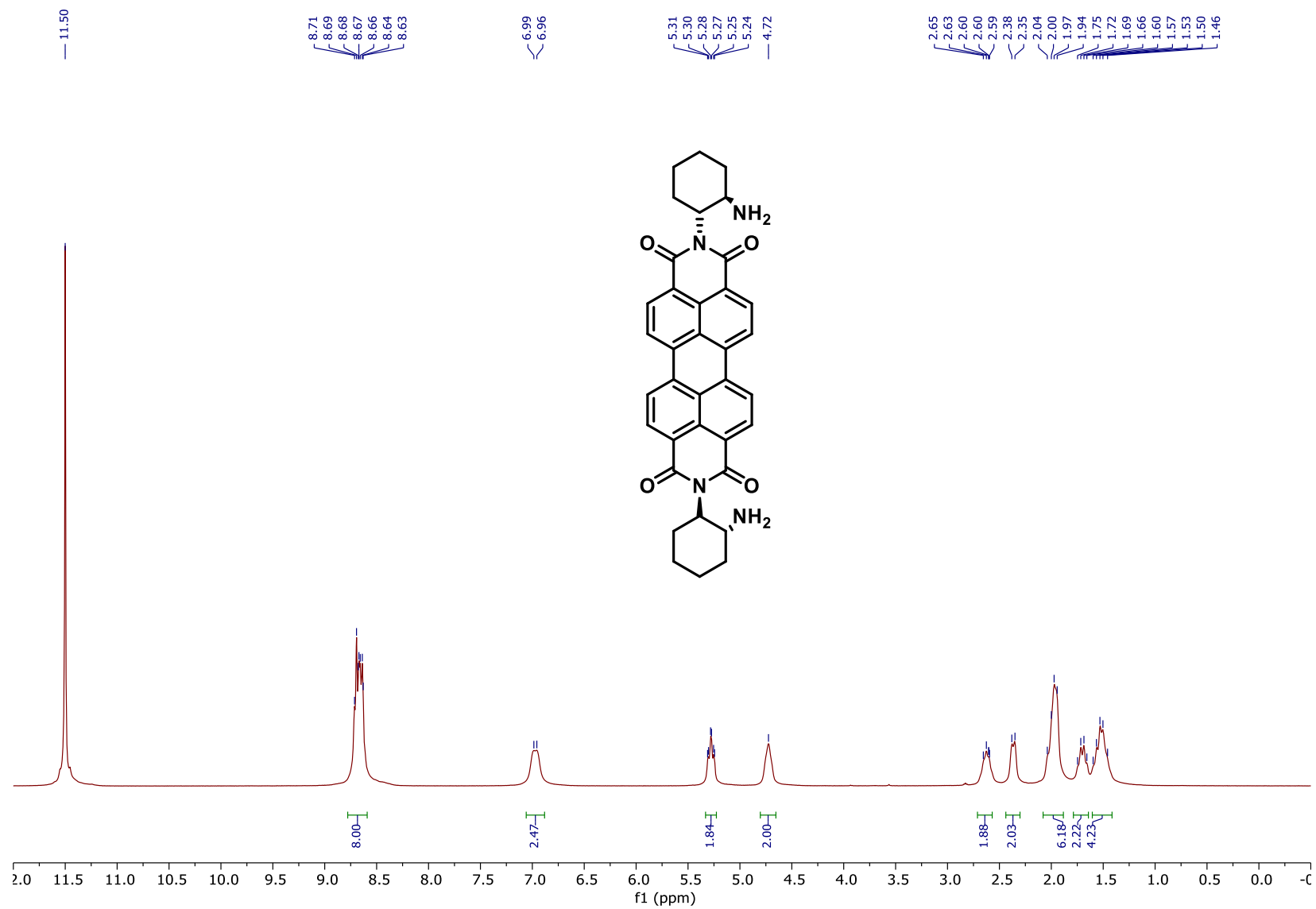


Figure S20. ^{13}C NMR spectrum of **2c** (101 MHz, $\text{TFA-}d_1$, 298K).

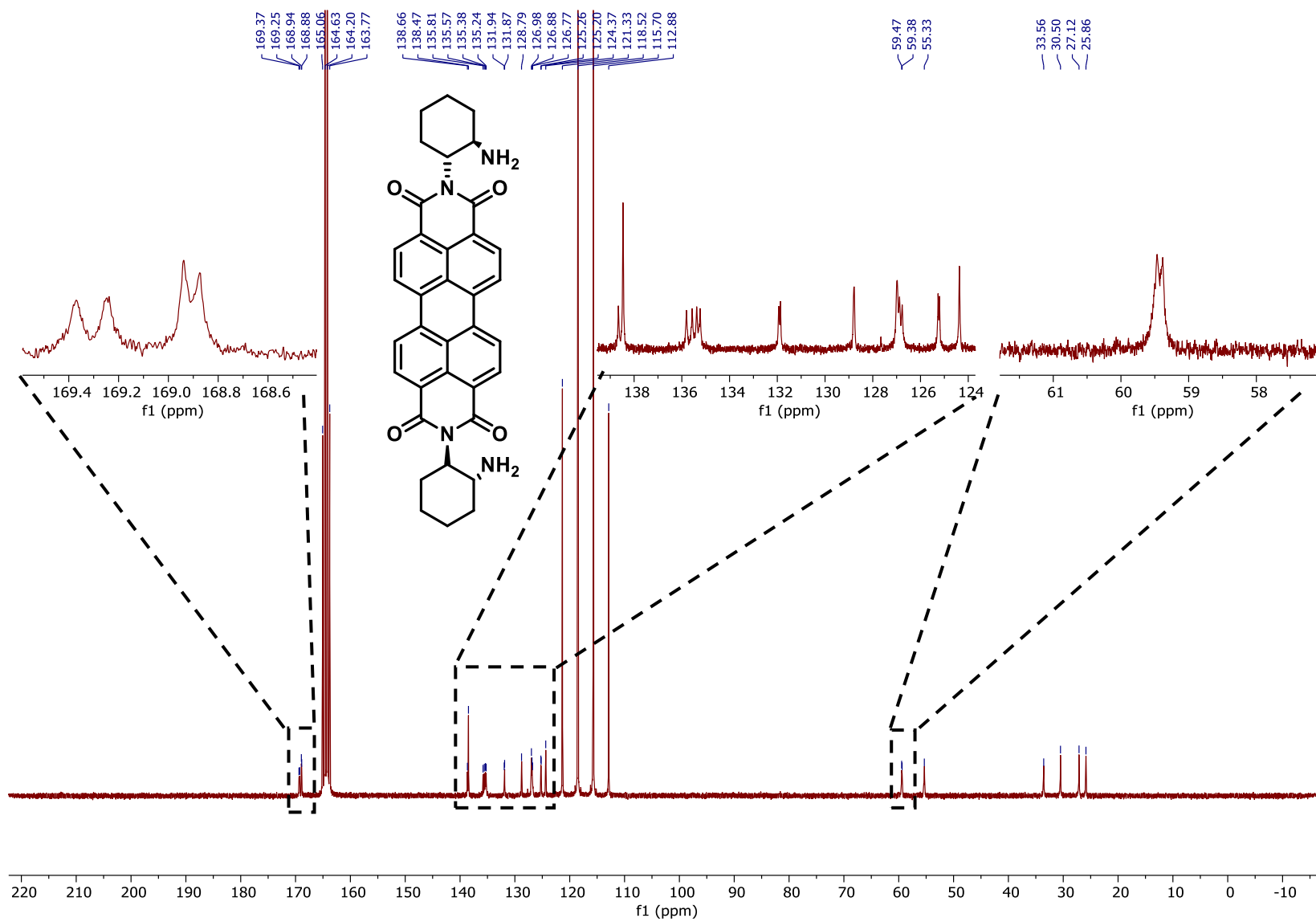


Figure S21. HR-ESI MS spectra of compound **2c**.

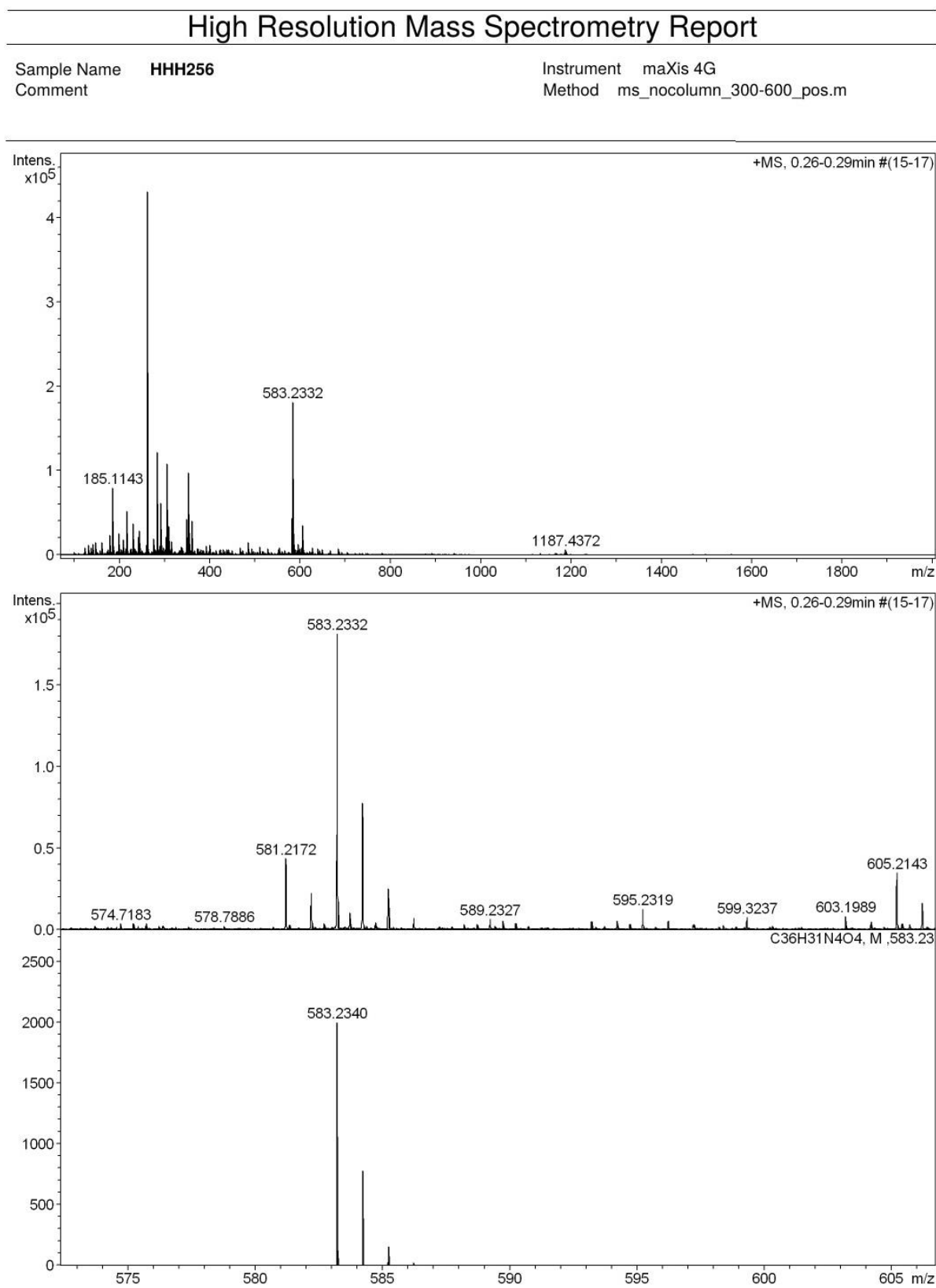


Figure S22. ^1H NMR spectrum of **4c** (600 MHz, CDCl_3 , 298K).

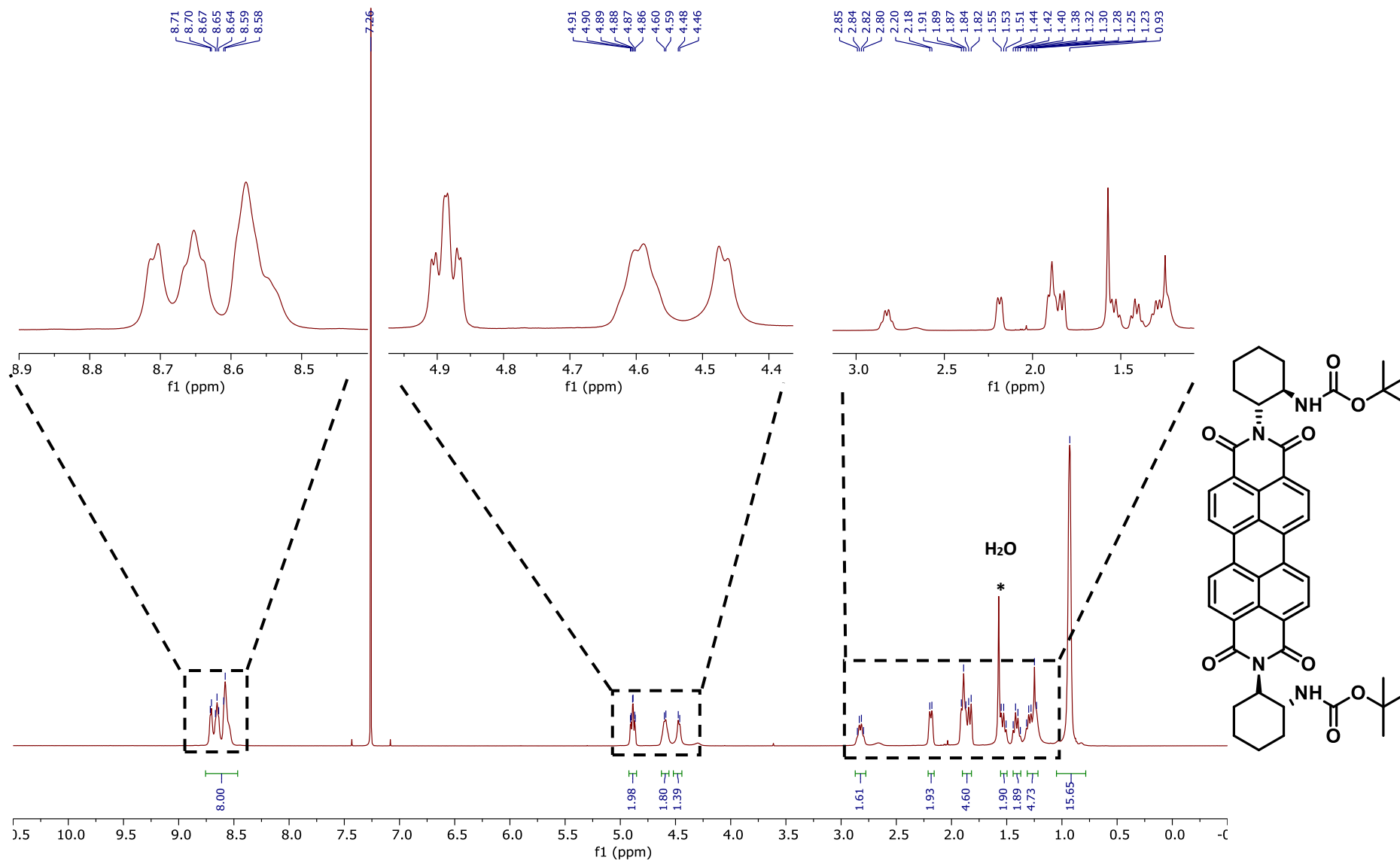


Figure S23. ^{13}C NMR spectrum of **4c** (151 MHz, CDCl_3 , 298K).

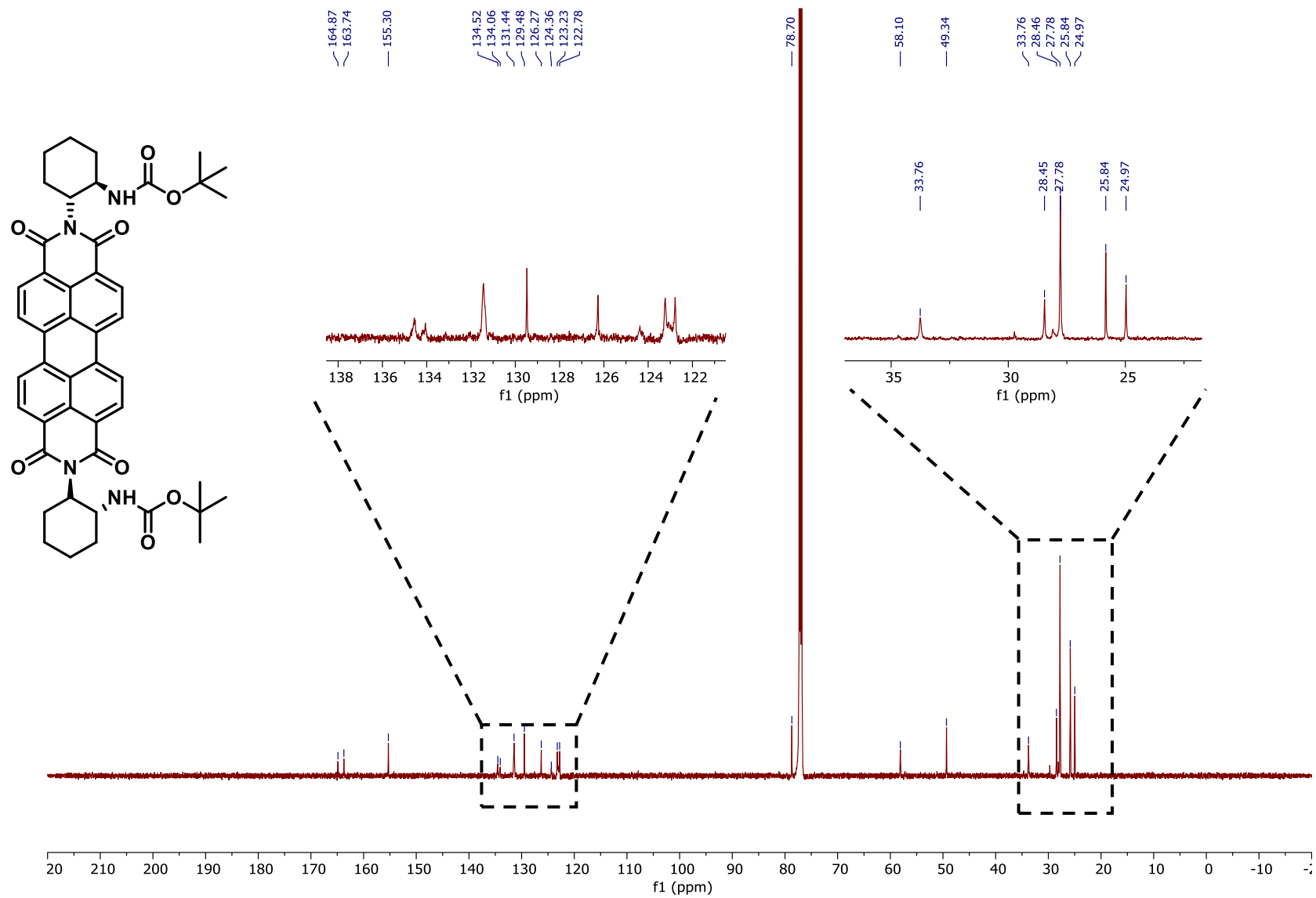


Figure S24. ^{13}C DEPT NMR spectrum of **4c** (151 MHz, CDCl_3 , 298K).

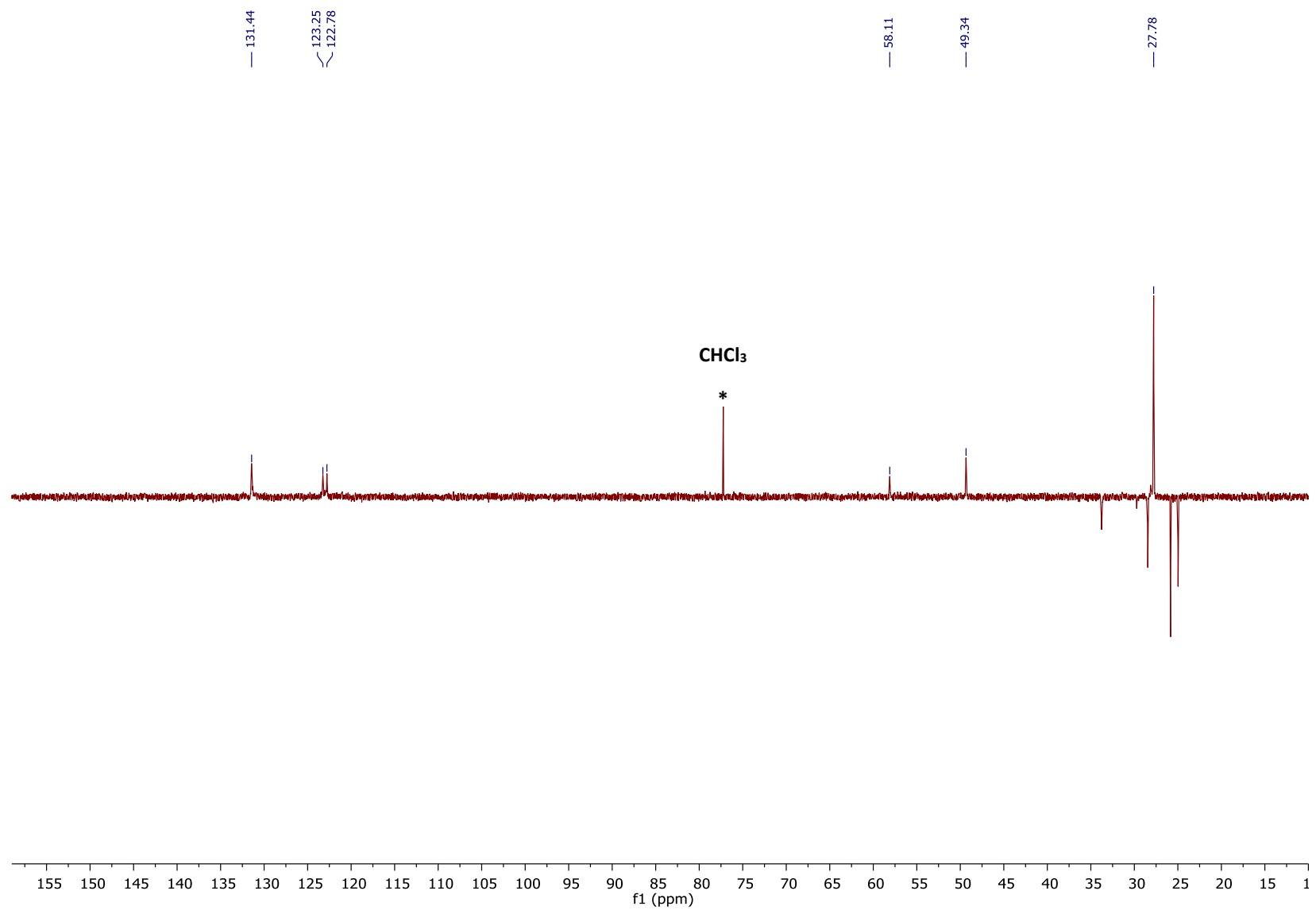


Figure S25. 2D ^1H - ^1H COSY NMR spectrum of **4c** (151 MHz, CDCl_3 , 298K).

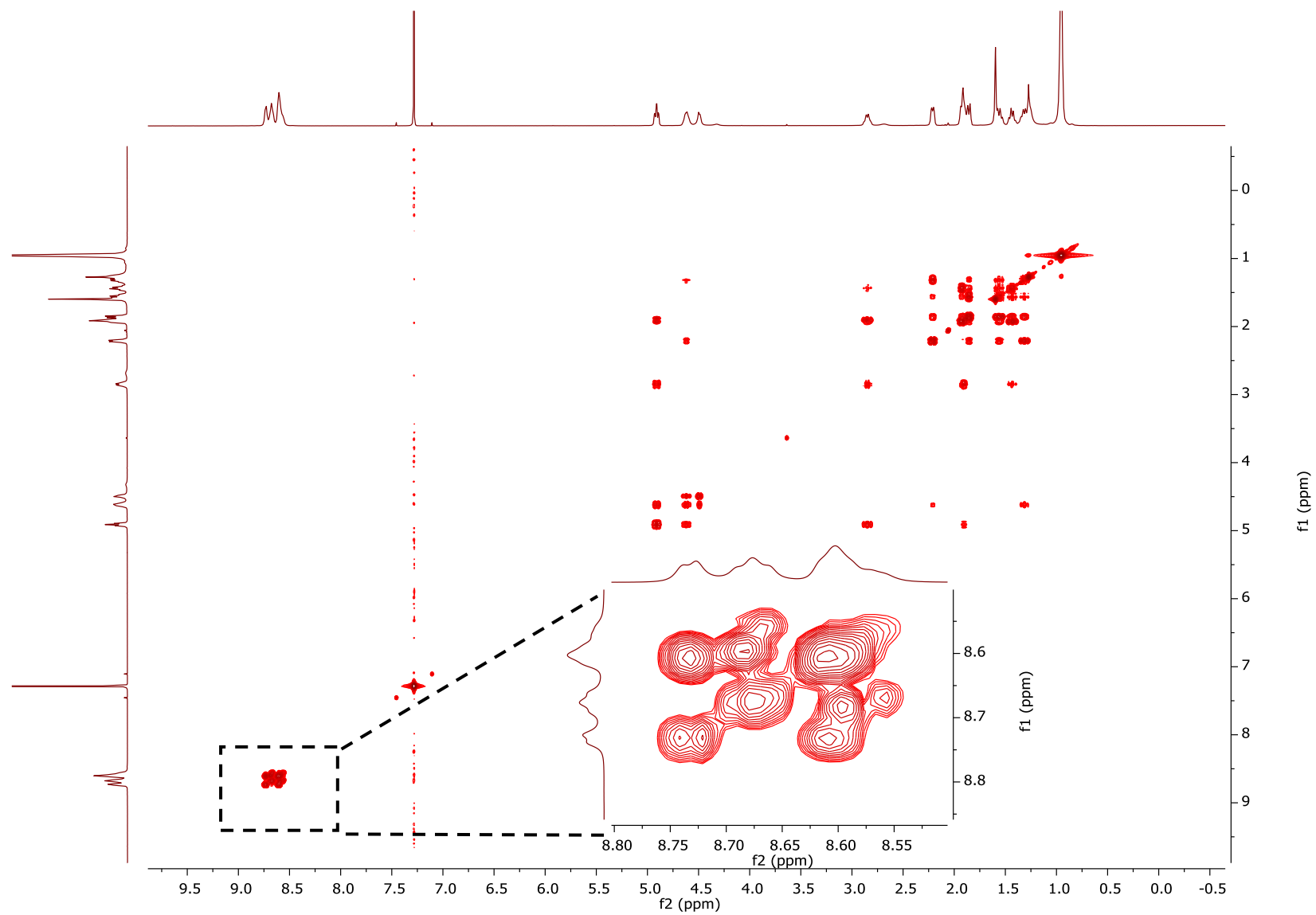


Figure S26. 2D ^1H - ^{13}C HMBC NMR spectrum of **4c** (151 MHz, CDCl_3 , 298K), full spectrum.

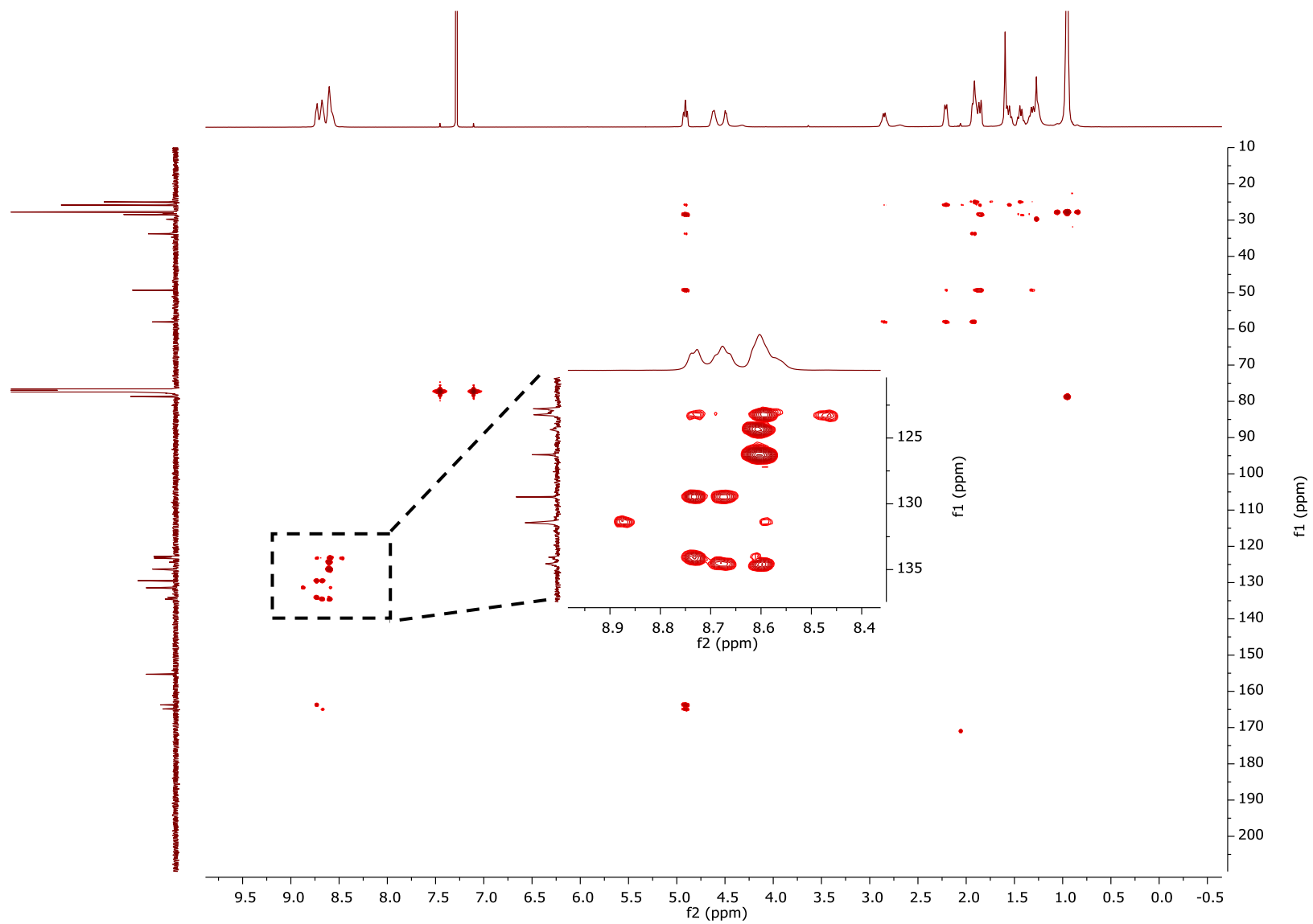


Figure S27. 2D ^1H - ^{13}C HMQC NMR spectrum of **4c** (151 MHz, CDCl_3 , 298K), full spectrum.

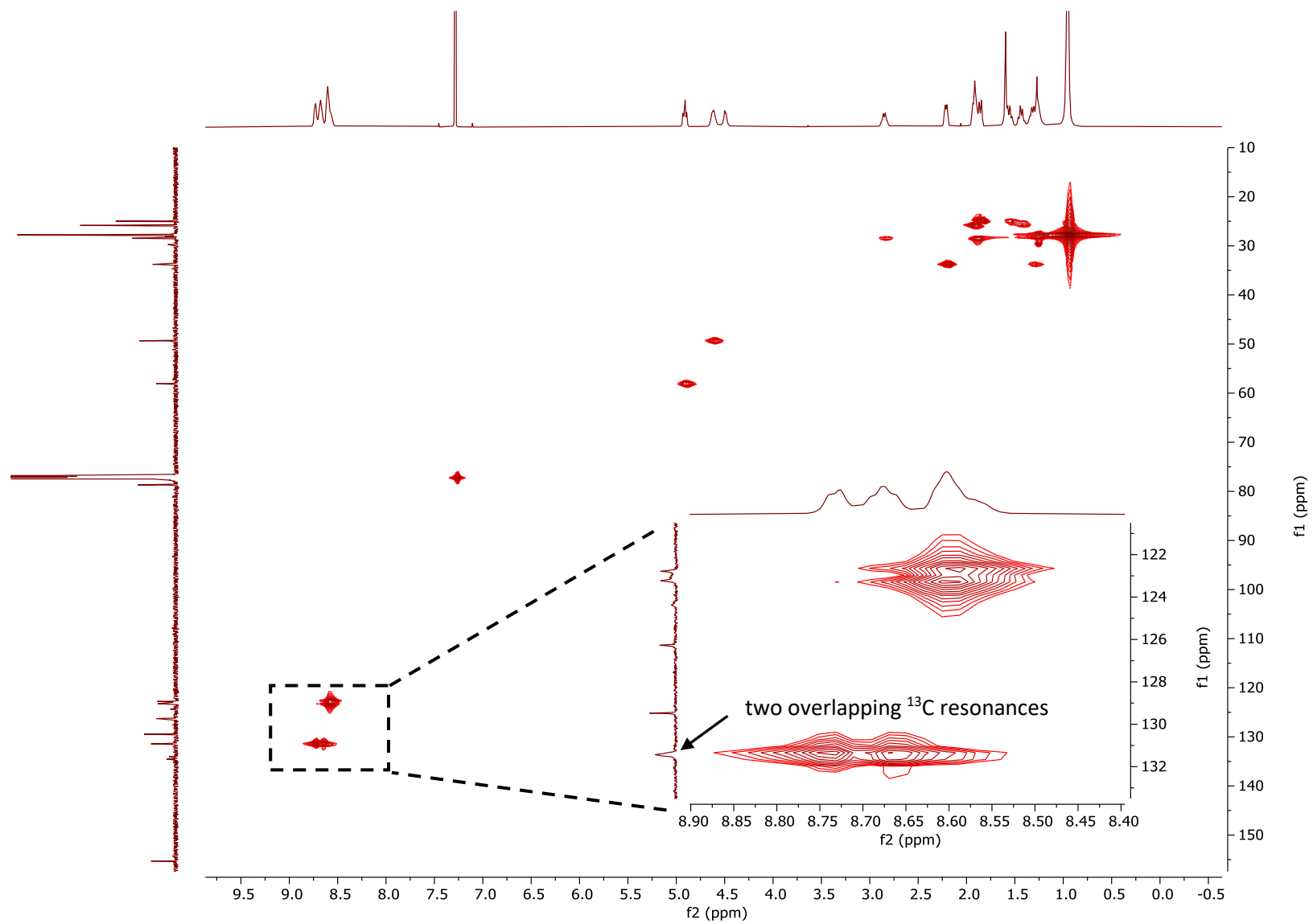


Figure S28. HR-ESI MS spectra of compound **4c**.

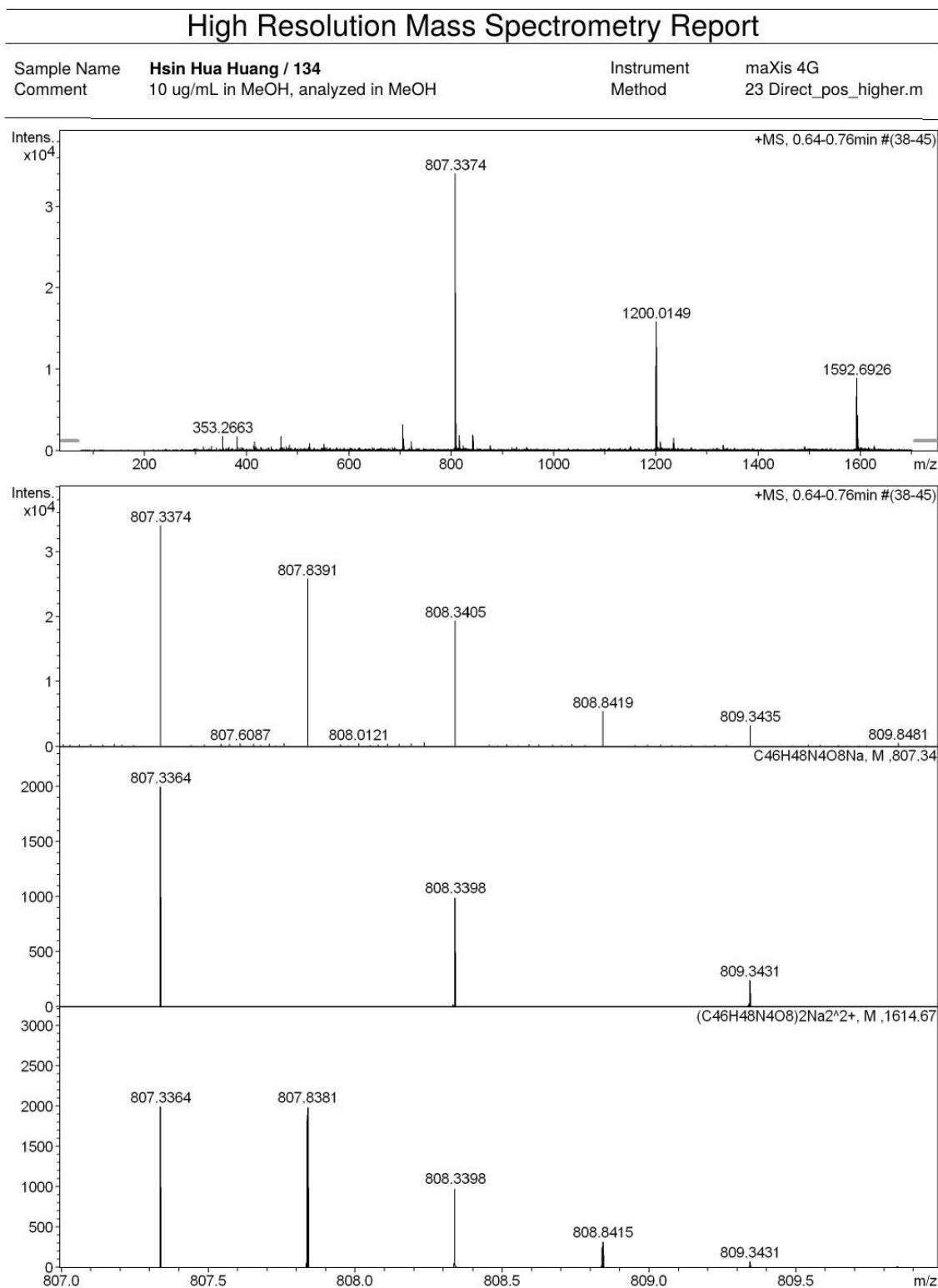


Figure S29. ^1H NMR spectrum of **3c** (600 MHz, CD_2Cl_2 , 298K).

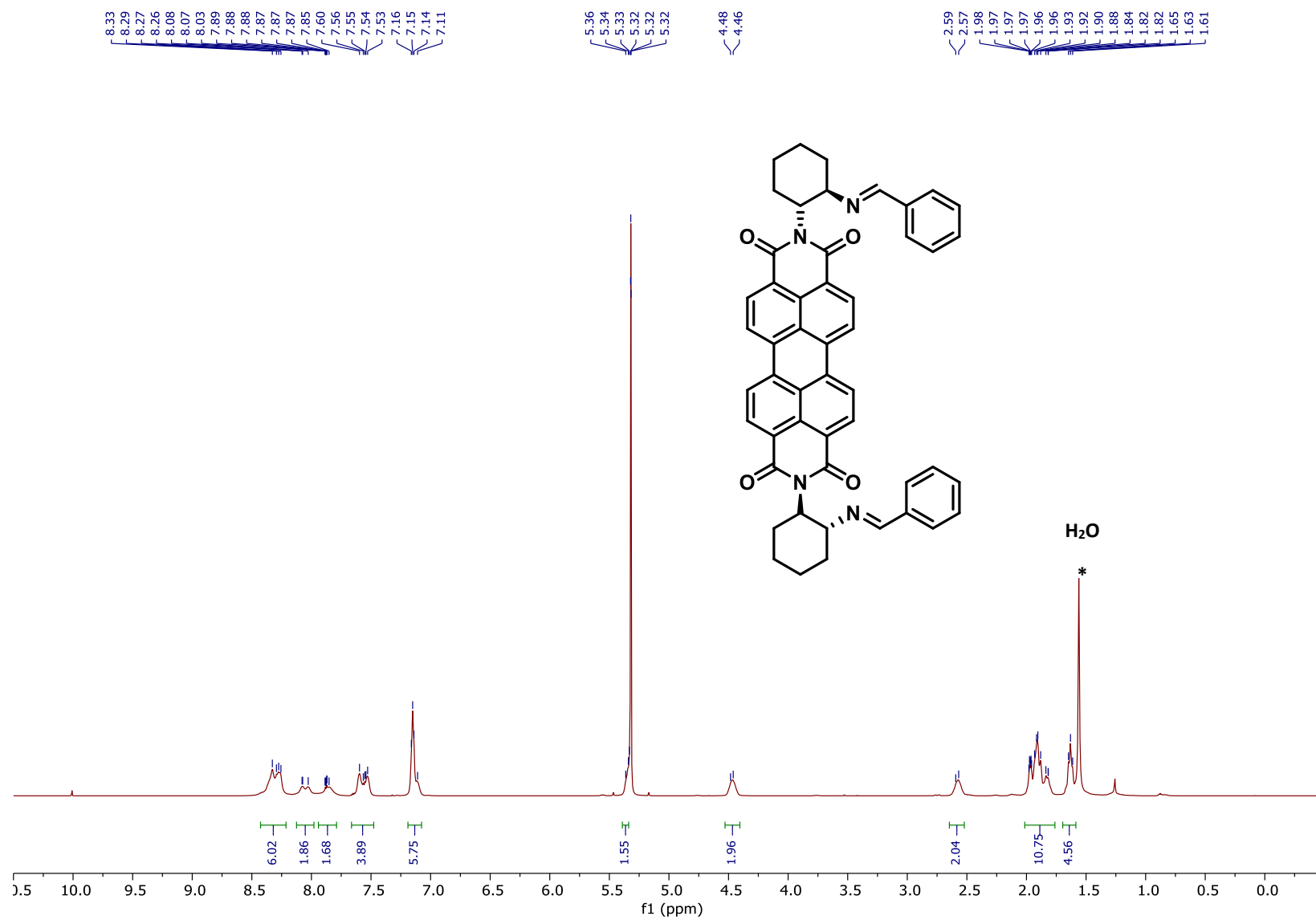


Figure S30. ^{13}C NMR spectrum of **3c** (151 MHz, CD_2Cl_2 , 298K).

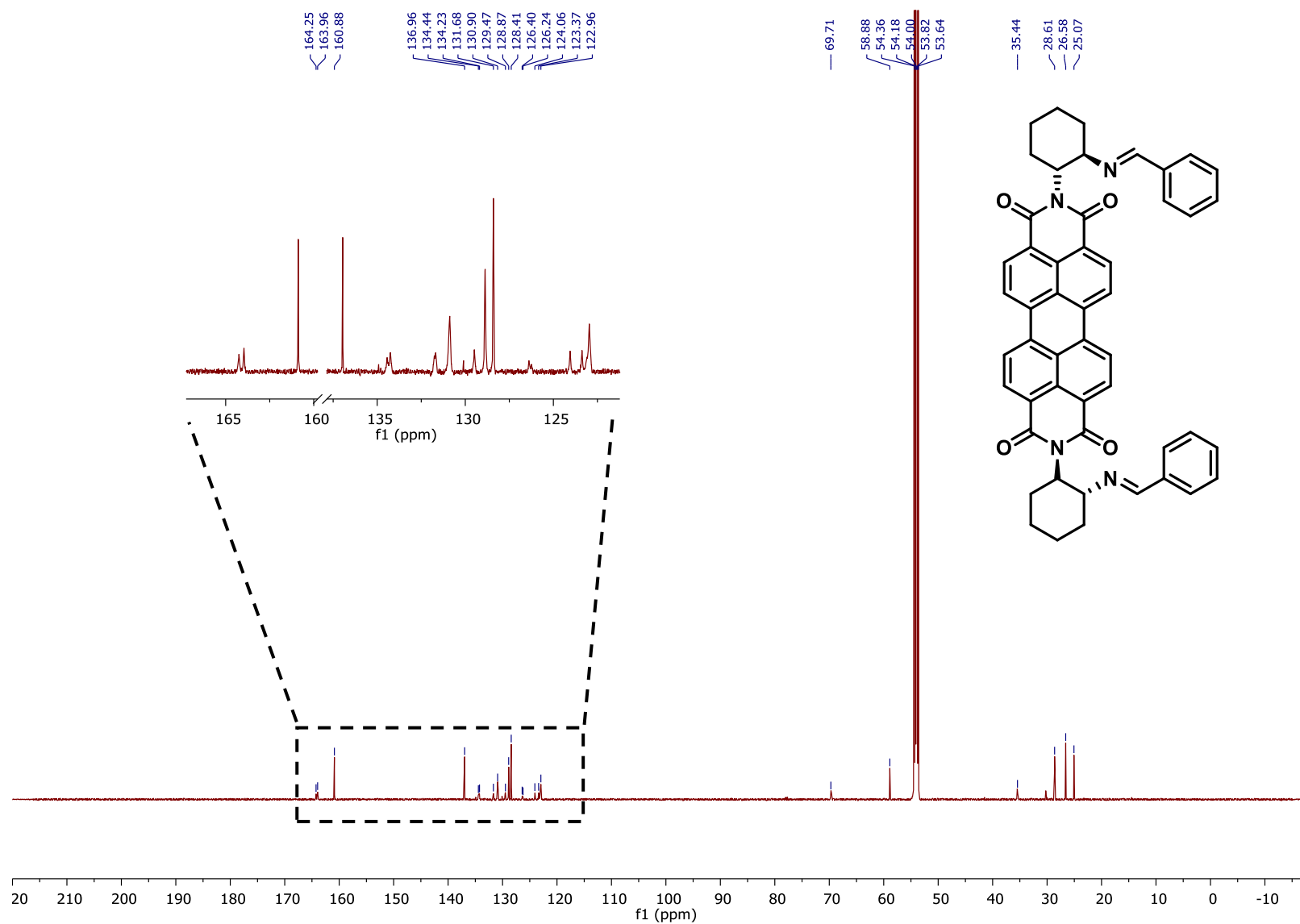


Figure S31. ^{13}C DEPT of **3c** (151 MHz, CD_2Cl_2 , 298K).

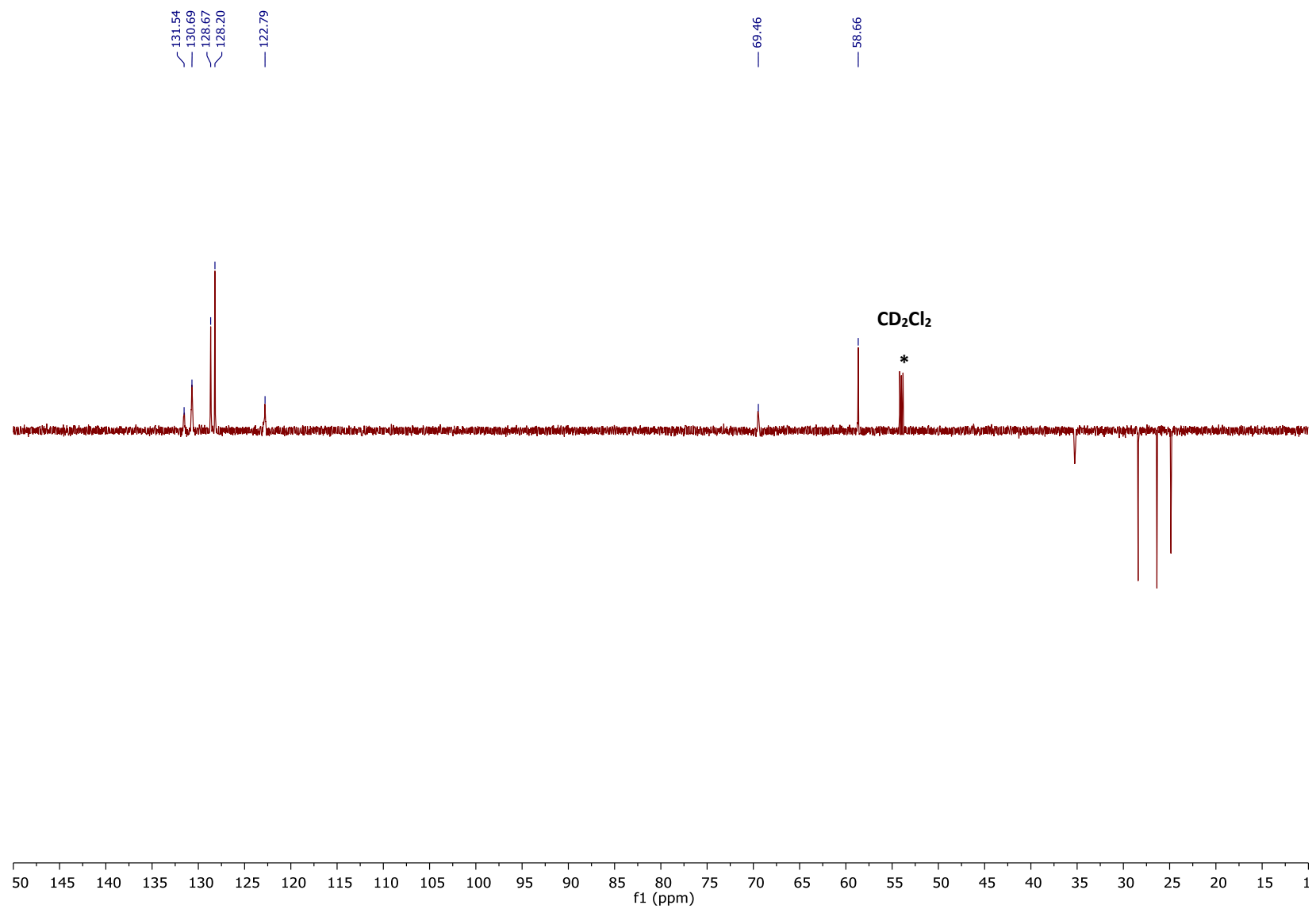


Figure S32. 2D ^1H - ^1H COSY NMR spectrum of **3c** (600 MHz, CD_2Cl_2 , 298K), full spectrum.

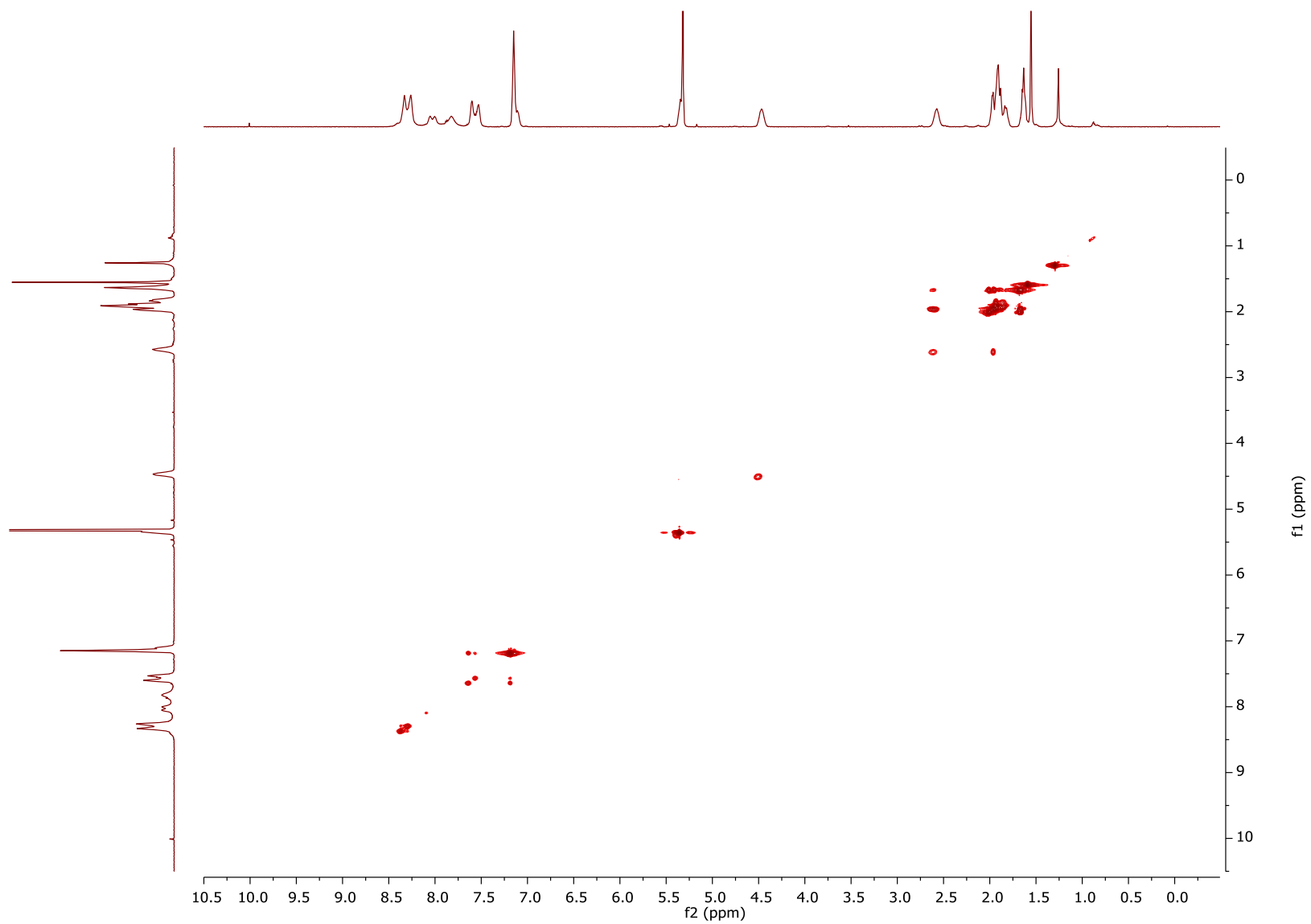


Figure S33. 2D ^1H - ^1H NOESY NMR spectrum of **3c** (600 MHz, CD_2Cl_2 , 298K), full spectrum.

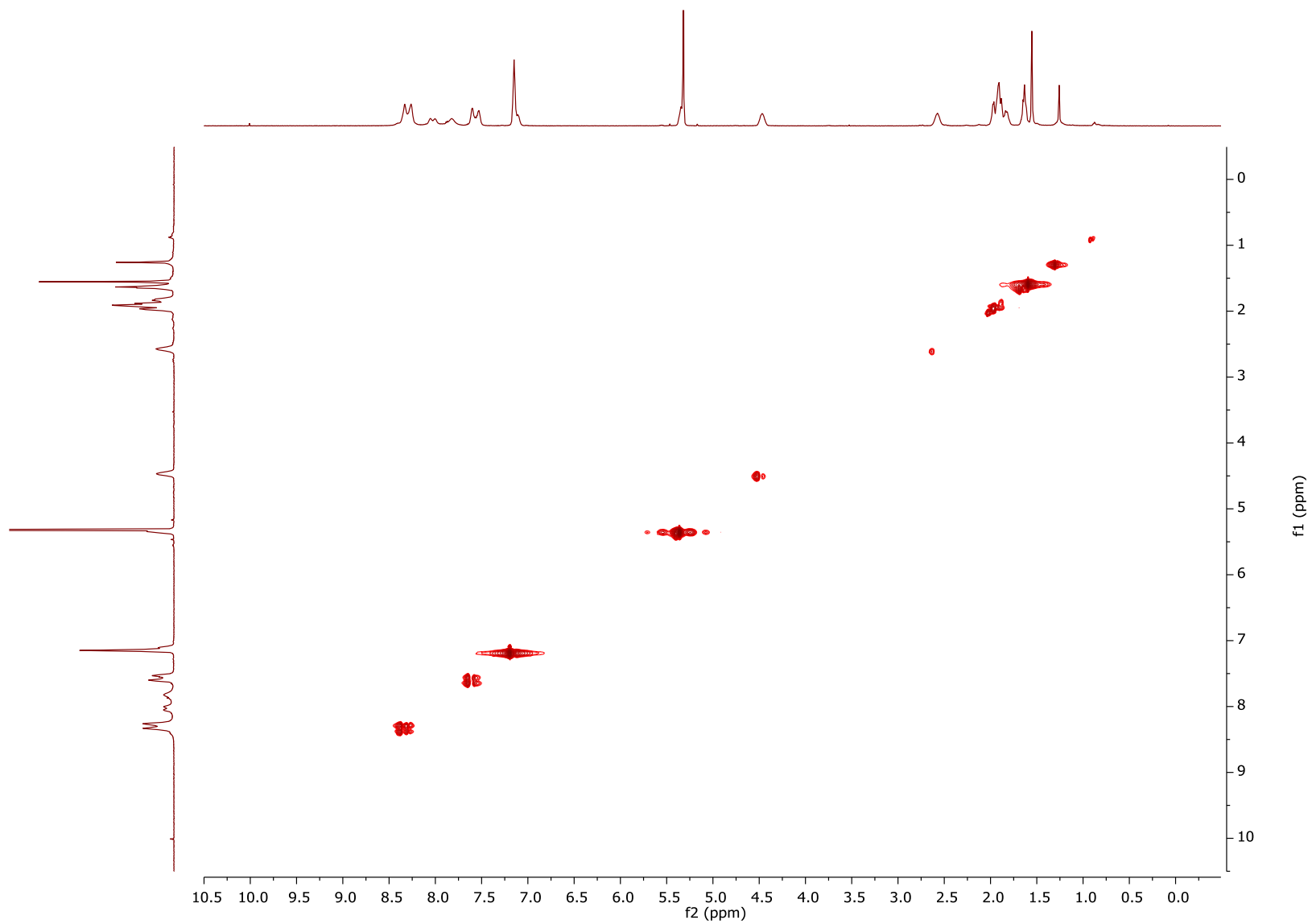


Figure S34. 2D ^1H - ^{13}C HMBC NMR spectrum of **3c** (600 MHz, CD_2Cl_2 , 298K), full spectrum.

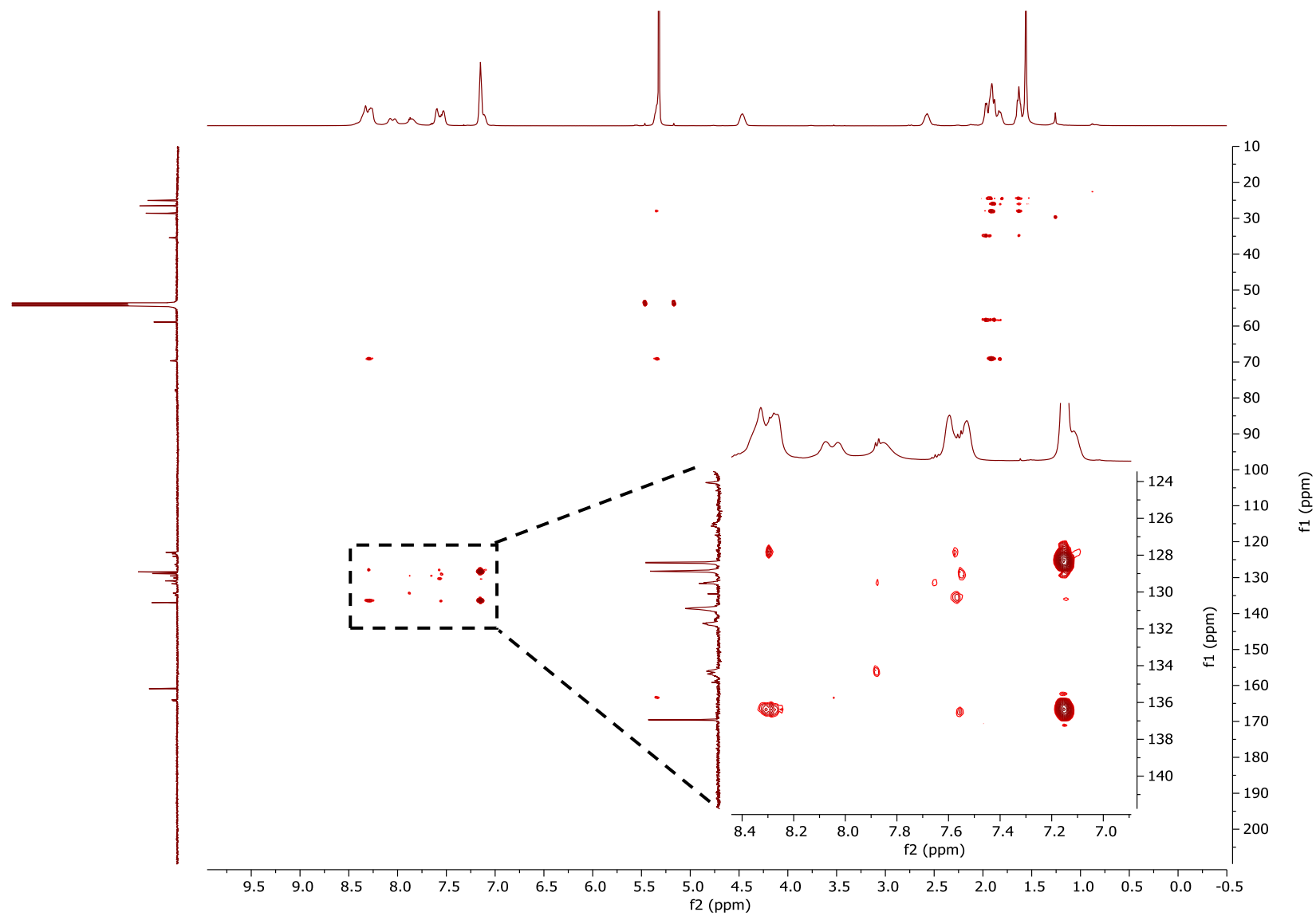


Figure S35. 2D ^1H - ^{13}C HSQC NMR spectrum of **3c** (600 MHz, CD_2Cl_2 , 298 K), full spectrum.

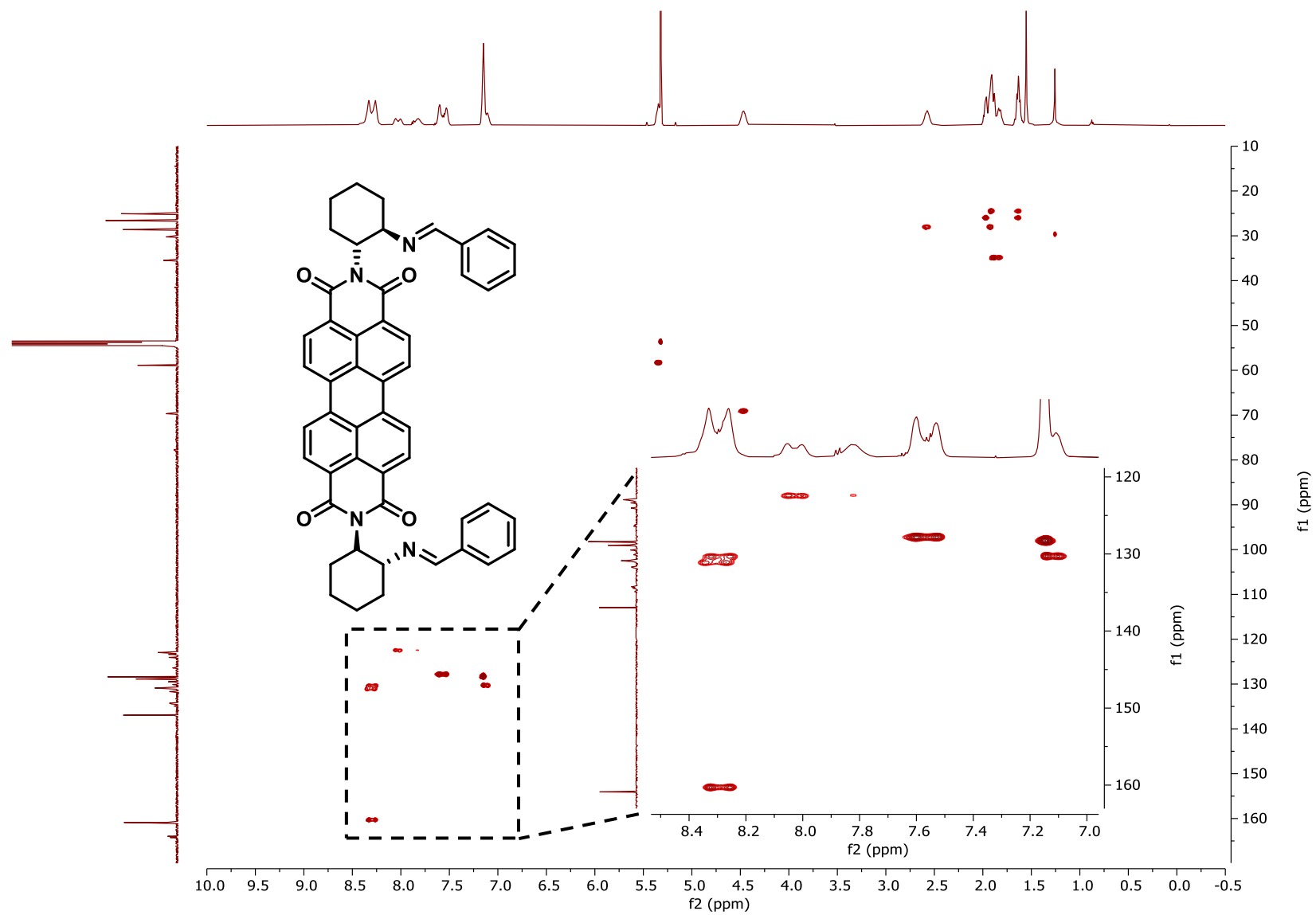


Figure S36. HR-ESI MS spectra of compound **3c**.

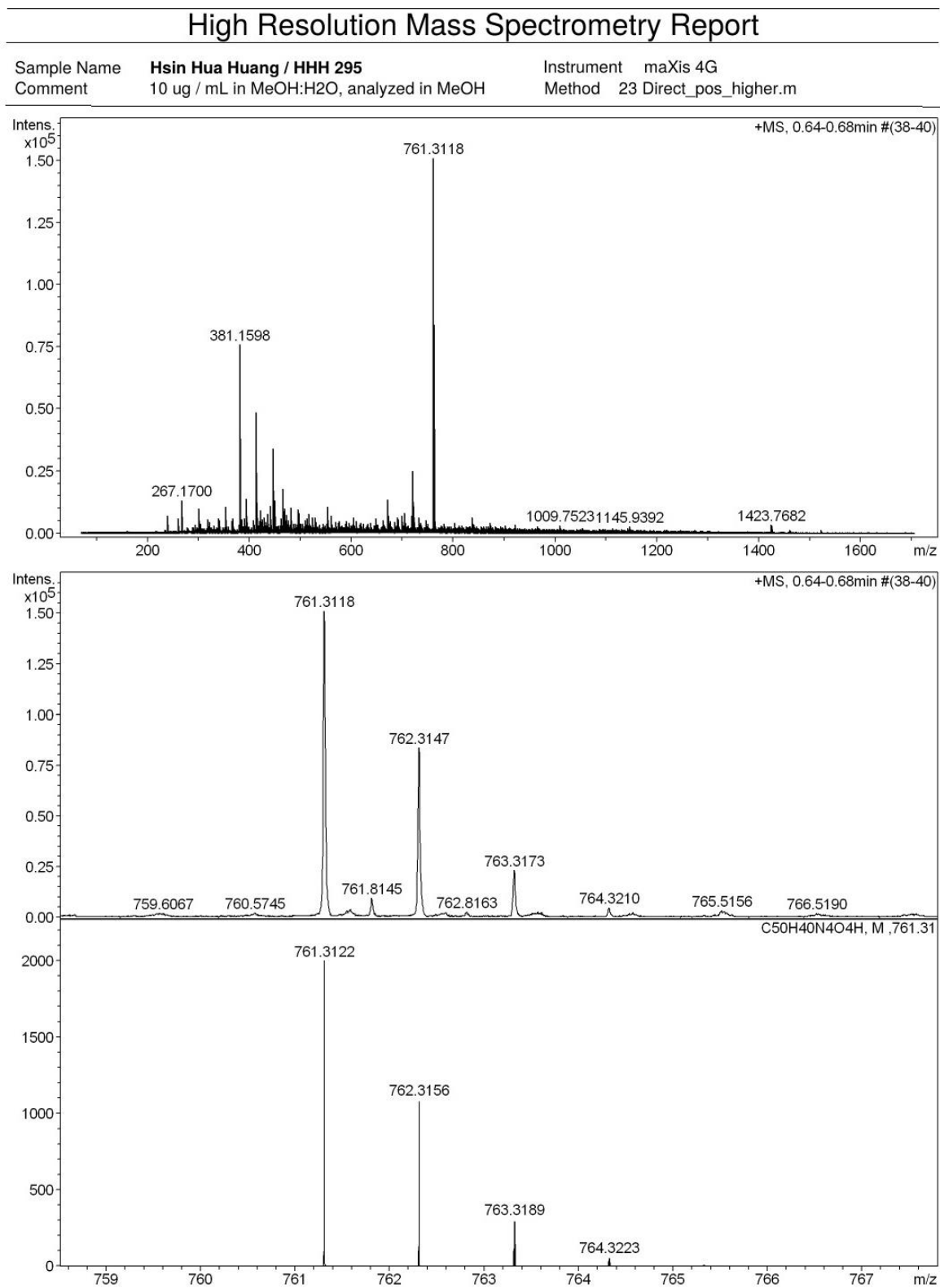


Figure S37. ^1H NMR spectrum of **5** (500 MHz, CDCl_3 , 298K).

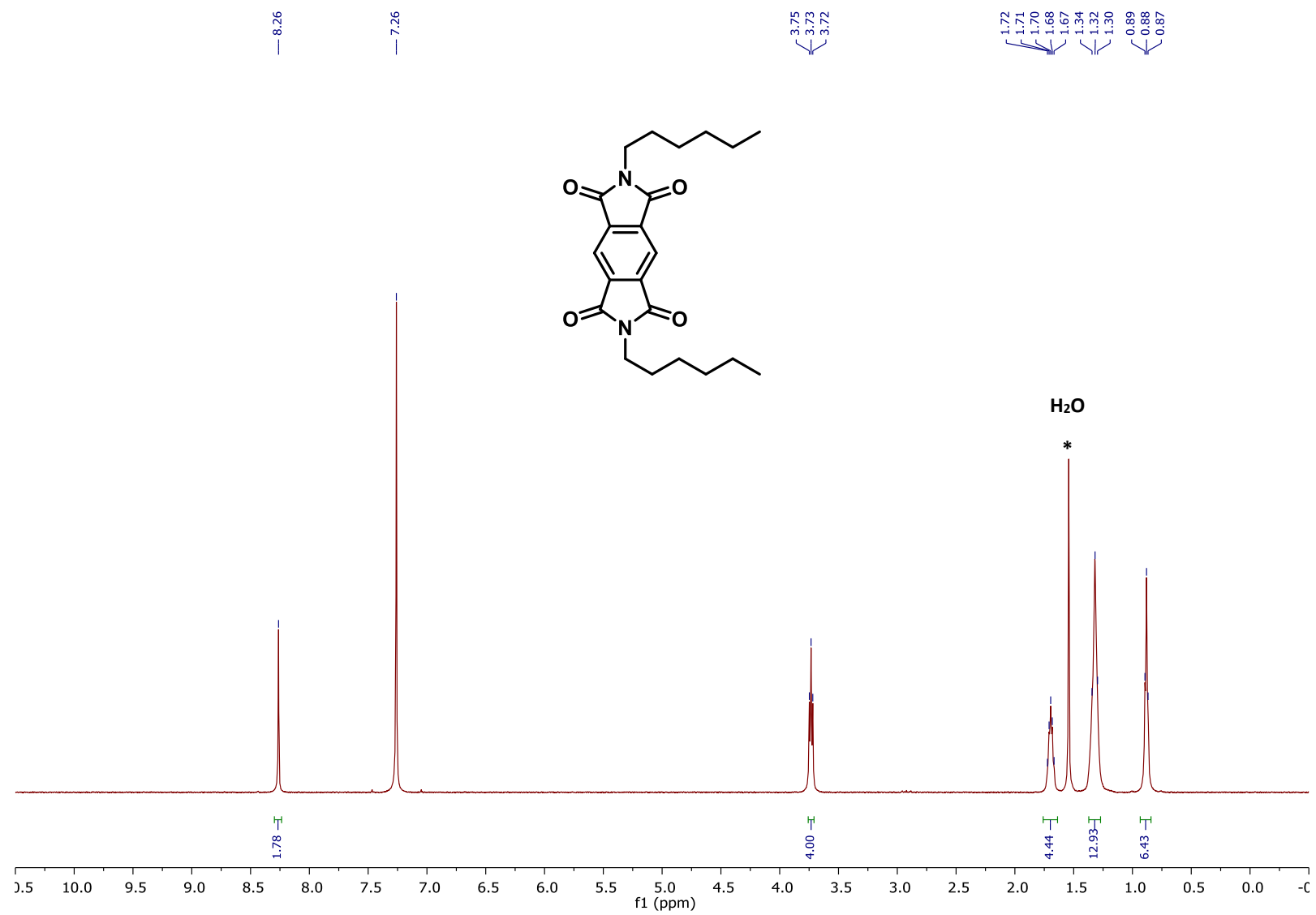
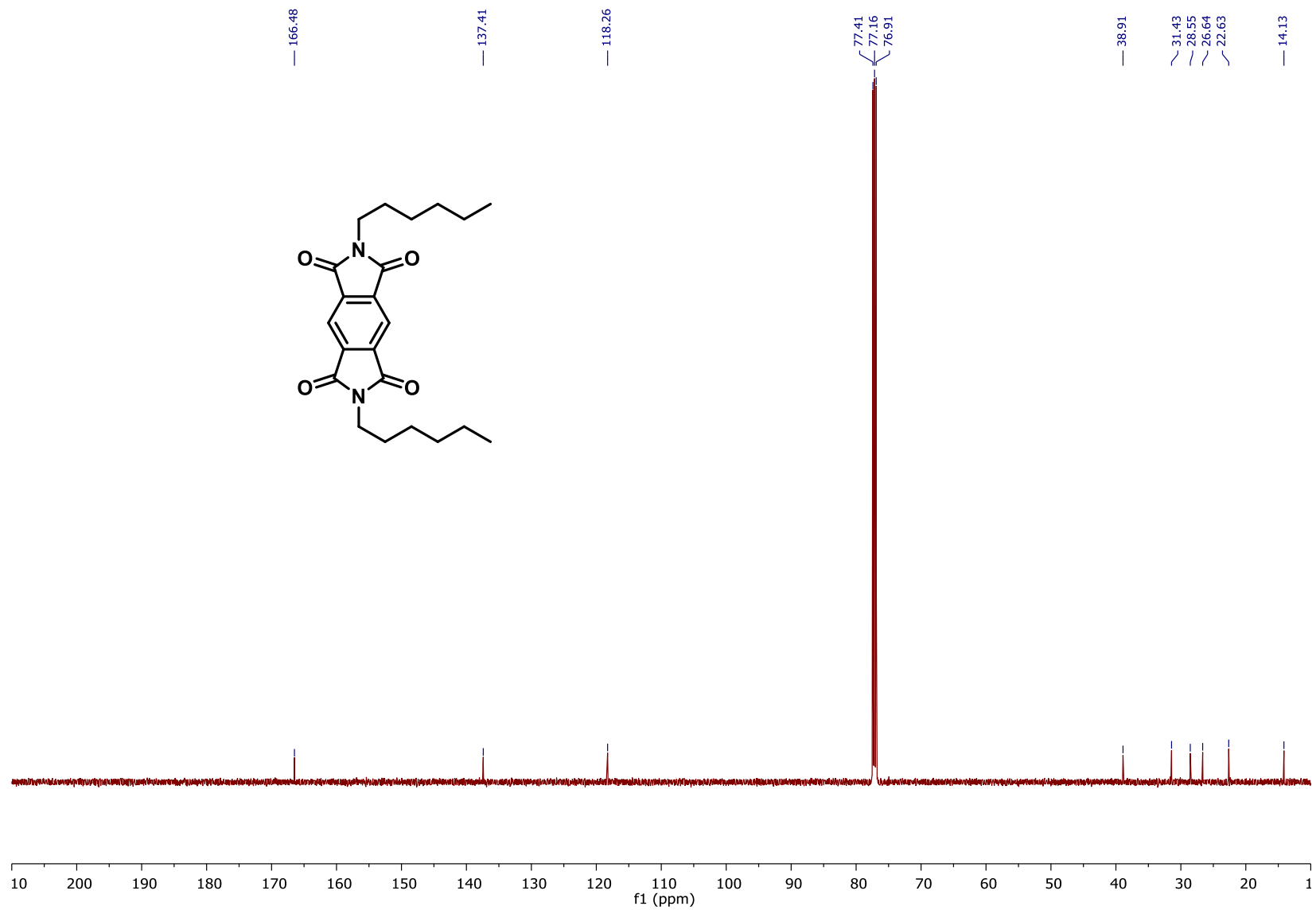


Figure S38. ^{13}C NMR spectrum of **5** (126 MHz, CDCl_3 , 298K).



Section E. UV-VIS Absorption and Fluorescence Spectroscopy

Figure S39. Normalized UV-VIS absorption spectra of **1b** and **5** in CH_2Cl_2 , $c \sim 0.1 - 0.2 \text{ mM}$.

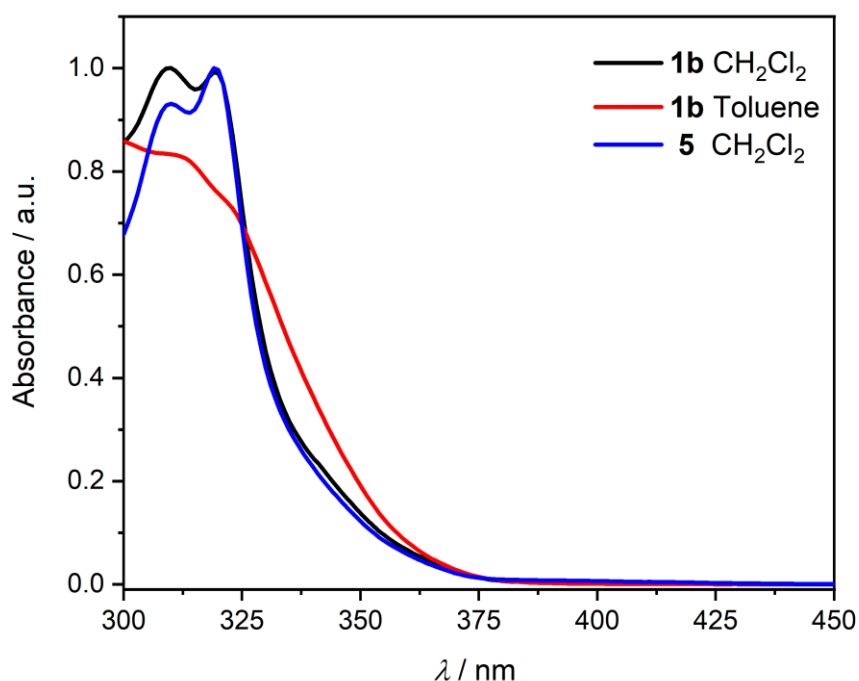


Figure S40. Normalized UV-VIS absorption (solid, black), excitation (solid, red; $\lambda_{\text{em}} = 577 \text{ nm}$) spectra of **1c** in CH_2Cl_2 ($c_{\text{abs}} \sim 0.01 - 0.02 \text{ mM}$) and emission (dash dot; $\lambda_{\text{exc}} = 487 \text{ nm}$) spectrum of **1c** in CH_2Cl_2 ($c_{\text{em}} \sim 0.1 - 0.2 \text{ }\mu\text{M}$).

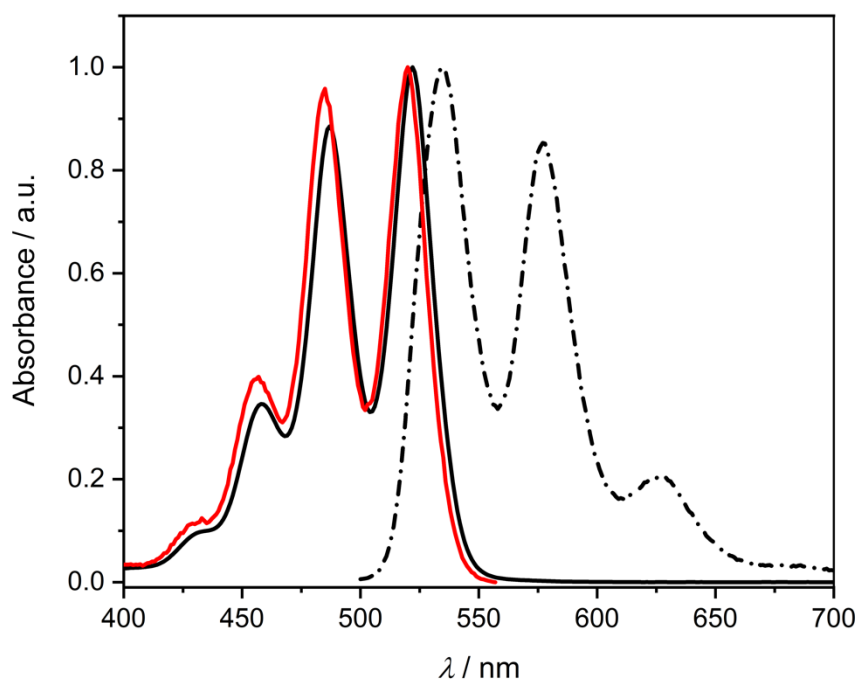


Figure S41. Normalized UV-VIS absorption (solid, black), excitation (solid, red; $\lambda_{\text{em}} = 574 \text{ nm}$) spectra of **3c** in CH_2Cl_2 ($c_{\text{abs}} \sim 0.01 - 0.02 \text{ mM}$) and emission (dash dot; $\lambda_{\text{exc}} = 489 \text{ nm}$) spectrum of **3c** in CH_2Cl_2 ($c_{\text{em}} \sim 0.1 - 0.2 \text{ }\mu\text{M}$).

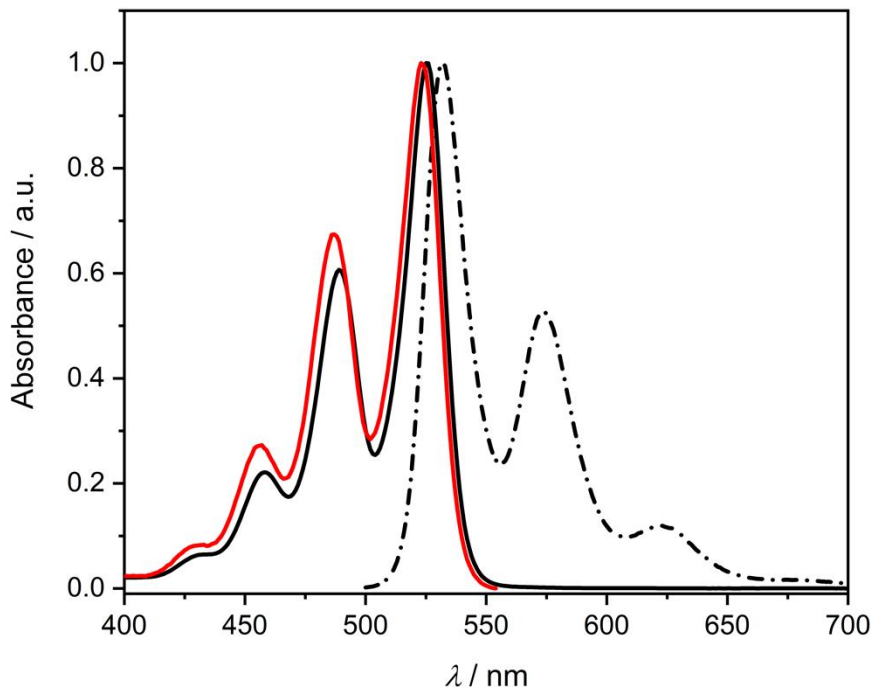


Figure S42. Comparison of the normalized UV-VIS absorption (solid) and emission (dash dot; $\lambda_{\text{exc}} = 489 \text{ nm}$) spectra of **1c** and **3c** in CH_2Cl_2 ($c_{\text{abs}} \sim 0.01 - 0.02 \text{ mM}$ and $c_{\text{em}} \sim 0.1 - 0.2 \text{ }\mu\text{M}$).

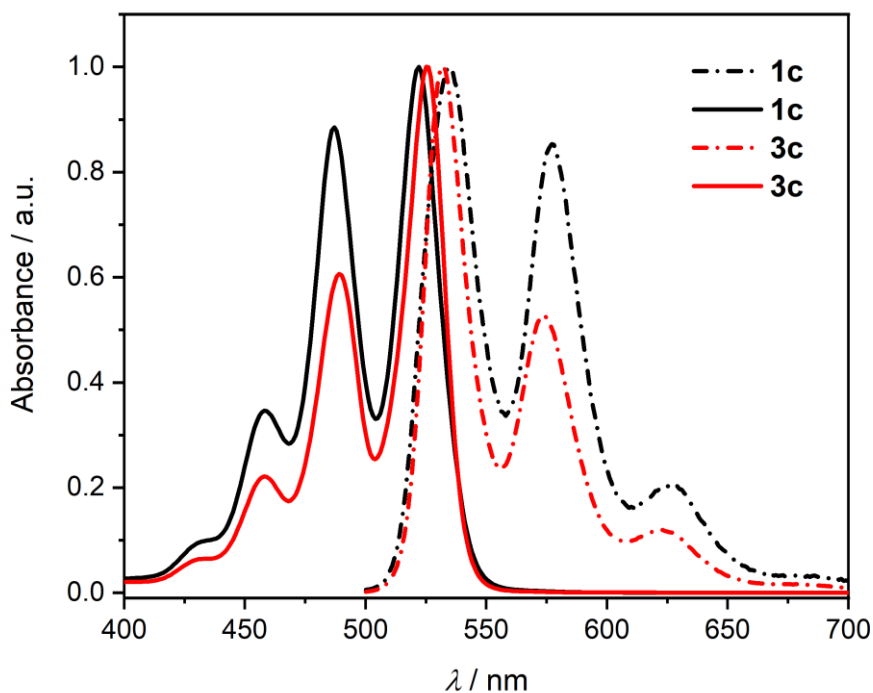


Figure S43. Comparison of the normalized UV-VIS absorption (solid) and emission (dash dot; $\lambda_{\text{exc}} = 487$ nm) spectra of **1c** in benzonitrile (black), CH_2Cl_2 (red), and toluene (blue); ($c_{\text{abs}} \sim 0.01 - 0.02$ mM and $c_{\text{em}} \sim 0.1 - 0.2$ μM).

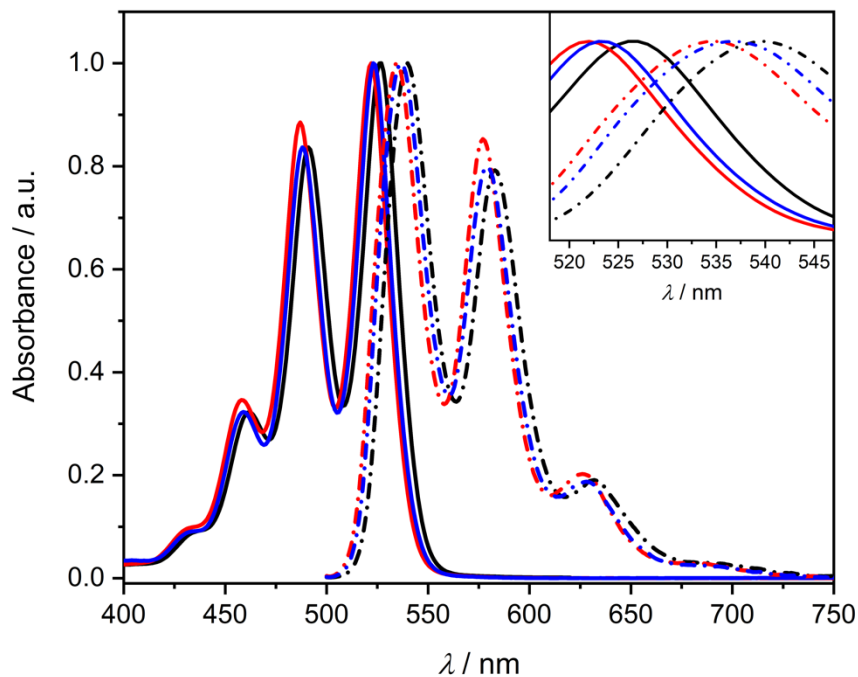
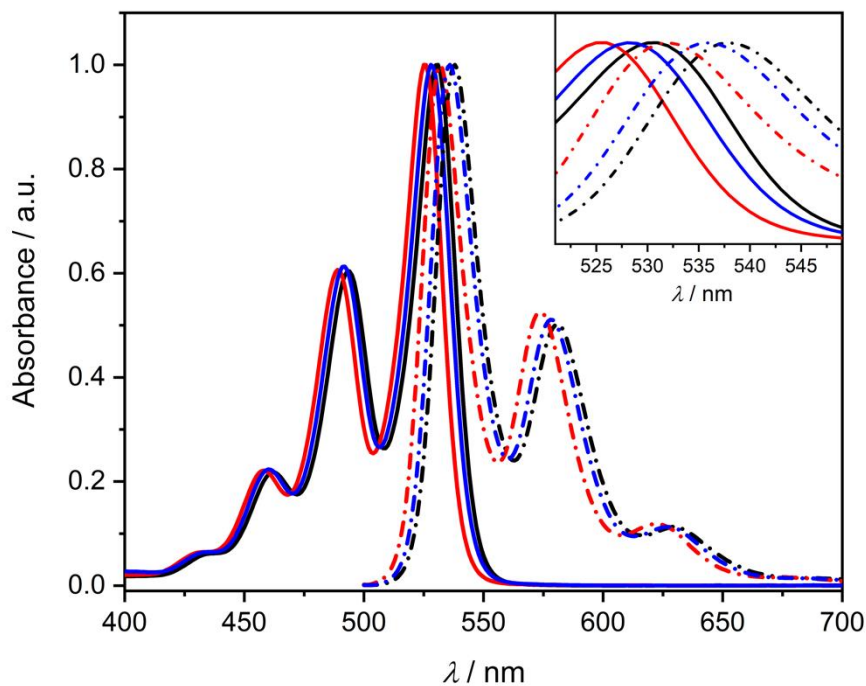


Figure S44. Comparison of the normalized UV-VIS absorption (solid) and emission (dash dot; $\lambda_{\text{exc}} = 489$ nm) spectra of **3c** in benzonitrile (black), CH_2Cl_2 (red), and toluene (blue); ($c_{\text{abs}} \sim 0.01 - 0.02$ mM and $c_{\text{em}} \sim 0.1 - 0.2$ μM).



Section F. Circular Dichroism (CD) Spectroscopy

Figure S45. CD spectra of (*RRR*)-**1b** (black) and (*SSS*)-**1b** (red) in CH₂Cl₂.

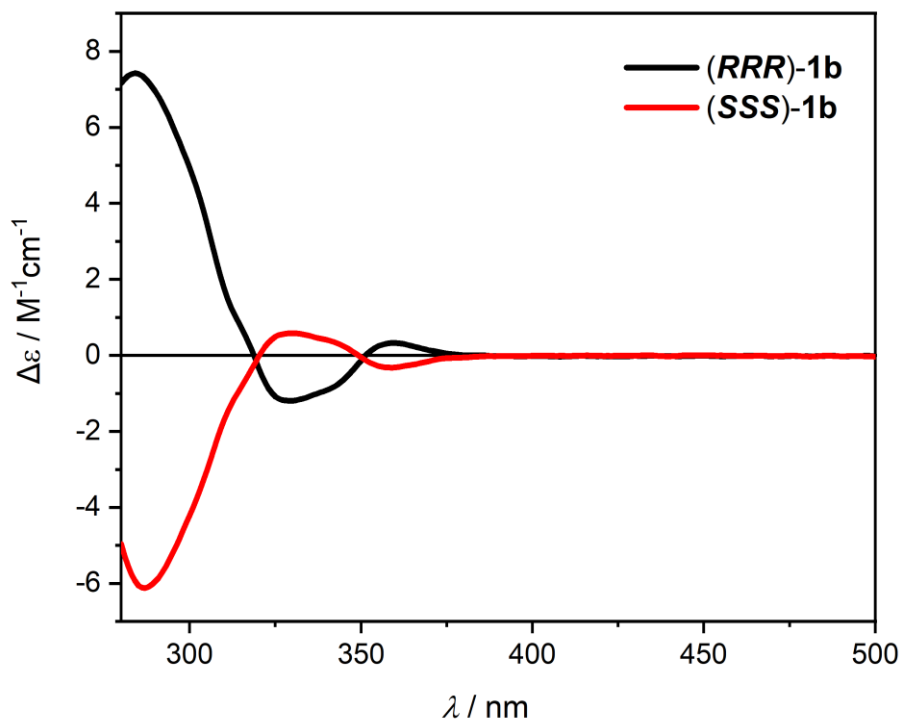


Figure S46. CD spectra of (*RRR*)-**1c** (black) and (*SSS*)-**1c** (red) in CH₂Cl₂

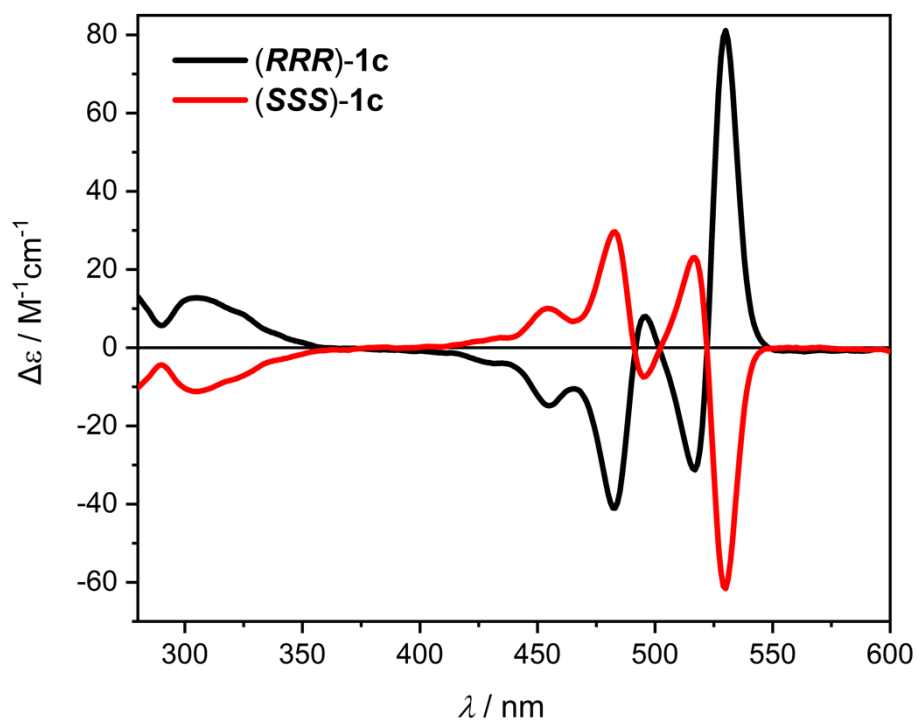
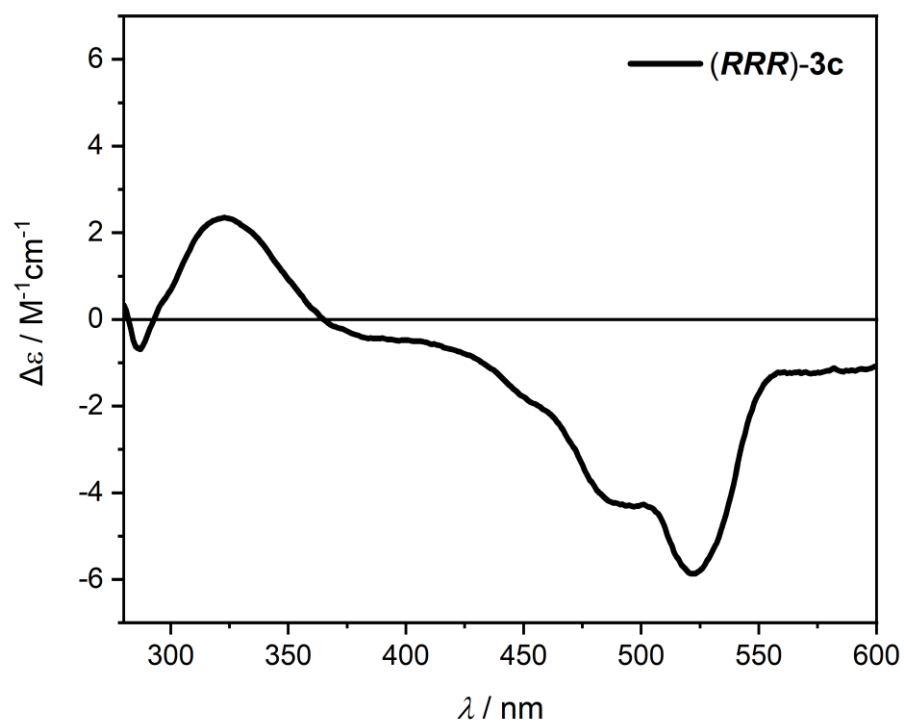


Figure S47. CD spectrum of (*RRR*)-**3c** in CH₂Cl₂.



Section G. Cyclic Voltammetry

Table S2. Redox and optical properties of **1a–c** and **3c** from cyclic voltammetry, UV-Vis and fluorescence spectroscopies.

	$E_{1/2}^{\text{red1}}$ ^a (V)	$E_{1/2}^{\text{red2}}$ ^a (V)	$\lambda_{\text{abs},0-0}$ ^b (nm)	$\lambda_{\text{abs},0-1}$ ^c (nm)	$\lambda_{\text{em},0-0}$ ^b (nm)	$\lambda_{\text{em},0-1}$ ^c (nm)	E_{0-0} ^d (eV)	E_{LUMO} ^e (eV)	E_{HOMO} ^f (eV)
1a	-1.13 ^g	-1.60 ^g	382	361 (0.90)	– ^h	– ^h	3.11 ⁱ	-3.67	-6.78 ⁱ
1b	-1.36	– ^h	320	– ^h	– ^h	– ^h	3.06 ⁱ	-3.44	-6.50 ⁱ
1c	-1.05	-1.27	527	487 (0.89)	535	578 (0.85)	2.35	-3.75	-6.10
3c	-1.09 (-1.06) ^j	-1.28 (-1.32) ^j	529	489 (0.60)	532	574 (0.53)	2.34	-3.71	-6.05

^aHalf-wave potentials of the first and the second reduction waves of CH₂Cl₂ solutions (*c* ~ 1 mM; ~100 mM Bu₄NPF₆ as electrolyte) at 100 mV s⁻¹ scan rate vs ferrocenium/ferrocene couple used as an internal standard. ^bThe first vibronic transition for CH₂Cl₂ solutions. ^cThe second vibronic transition for CH₂Cl₂ solutions; the numbers in parentheses are ratios of the intensities of the 0–0 and 0–1 vibronic transitions. ^dThe first electronic transition energy between ground vibrational states: $E_{0-0} = (1240 \text{ eV nm})/\lambda_{\text{inter}}$, where λ_{inter} is the intersection of the normalized absorption and emission curves (Figures S40 and S41). ^e $E_{\text{LUMO}} = -4.8 \text{ eV} - e \times E_{1/2}^{\text{red}}$. ^f $E_{\text{HOMO}} = E_{\text{LUMO}} - E_{0-0}$. ^gRedox potentials were taken from reference 12. ^hNot available. ⁱThe onset of the absorption was used to compute the energy. ^jFor a solution of **3c** in benzonitrile.

Figure S48. Cyclic voltammograms of a CH_2Cl_2 solution of **1b** ($c \sim 1$ mM; ~ 100 mM Bu_4NPF_6 as electrolyte) at different scan rates with ferrocene as an internal standard.

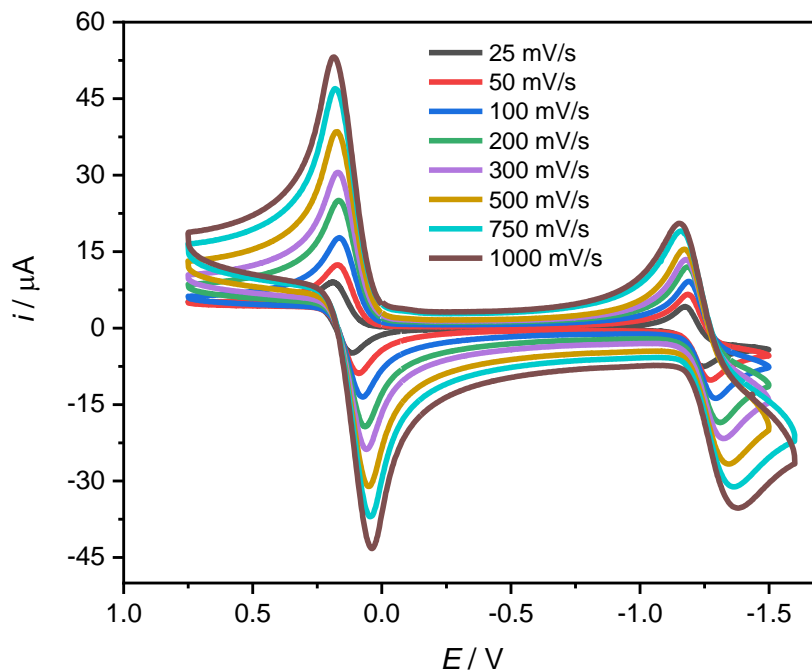


Figure S49. Cyclic voltammograms of a CH_2Cl_2 solution of **1c** ($c \sim 1$ mM; ~ 100 mM Bu_4NPF_6 as electrolyte) at different scan rates with ferrocene as an internal standard.

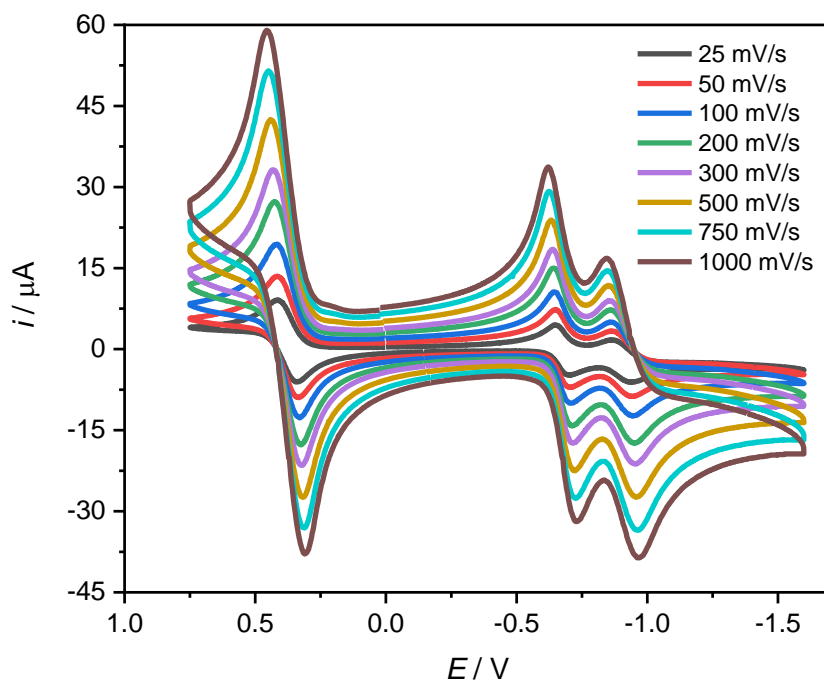


Figure S50. Cyclic voltammograms of a CH_2Cl_2 solution of **3c** ($c \sim 1 \text{ mM}$; $\sim 100 \text{ mM}$ Bu_4NPF_6 as electrolyte) at different scan rates with ferrocene as an internal standard.

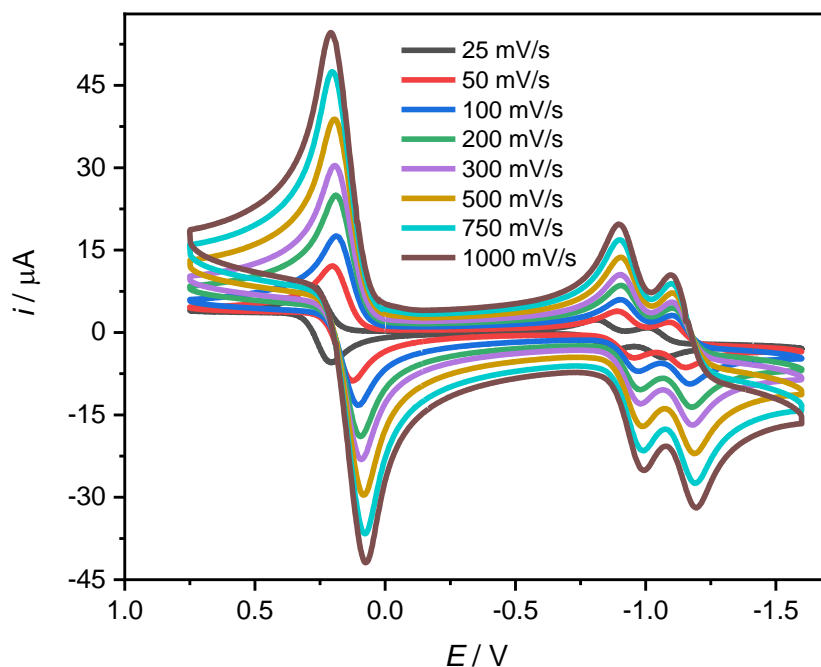


Figure S51. Cyclic voltammetry trace of a CH_2Cl_2 solution of **1b** ($c \sim 1 \text{ mM}$; $\sim 100 \text{ mM}$ Bu_4NPF_6 as electrolyte) at 100 mVs^{-1} scan rate with ferrocene as an internal standard.

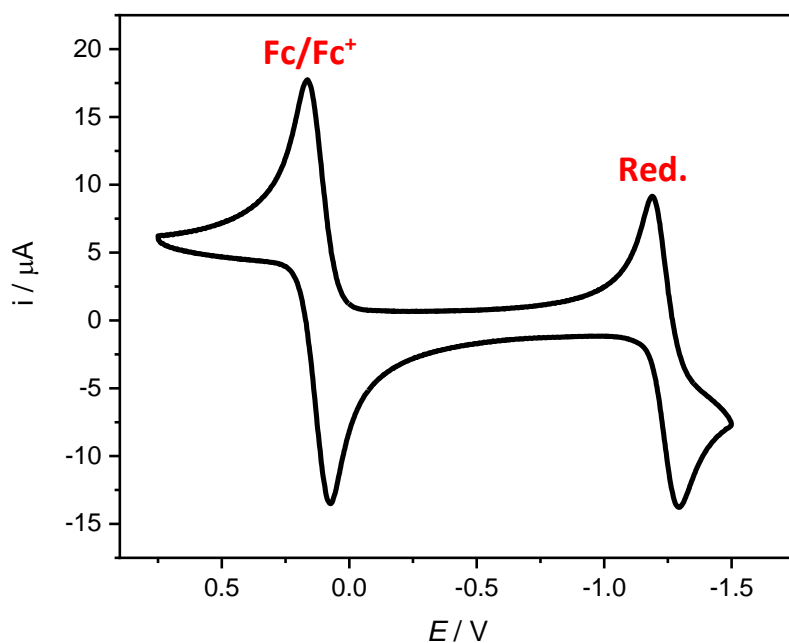


Figure S52. Cyclic voltammetry trace of a CH₂Cl₂ solution of **1c** (*c* ~1 mM; ~100 mM Bu₄NPF₆ as electrolyte) at 100 mVs⁻¹ scan rate with ferrocene as an internal standard.

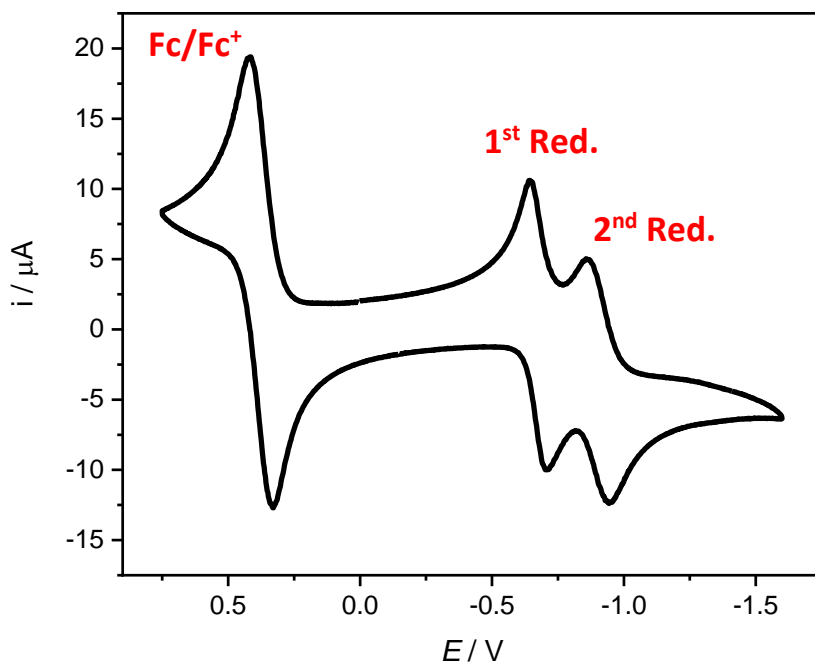


Figure S53. Cyclic voltammetry trace of a CH₂Cl₂ solution of **3c** (*c* ~1 mM; ~100 mM Bu₄NPF₆ as electrolyte) at 100 mVs⁻¹ scan rate with ferrocene as an internal standard.

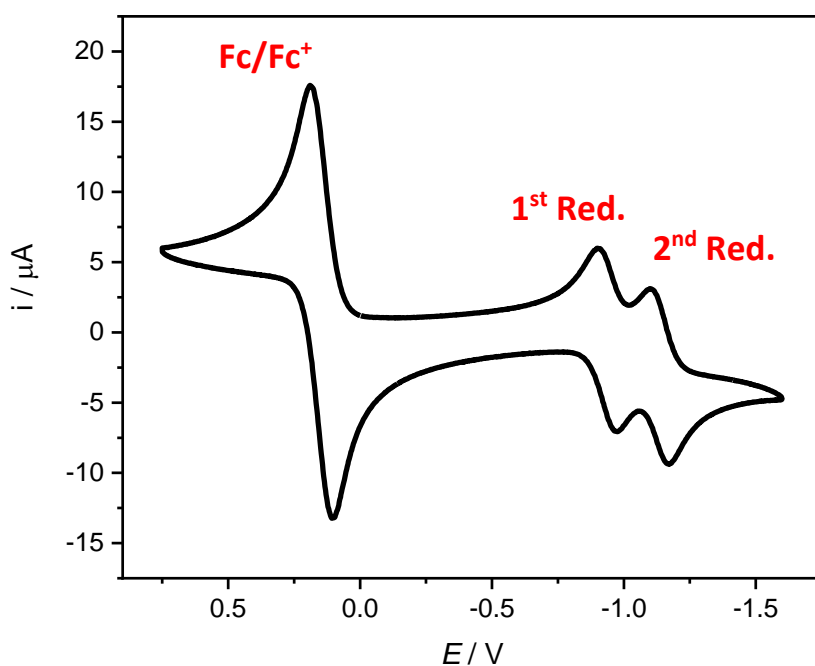
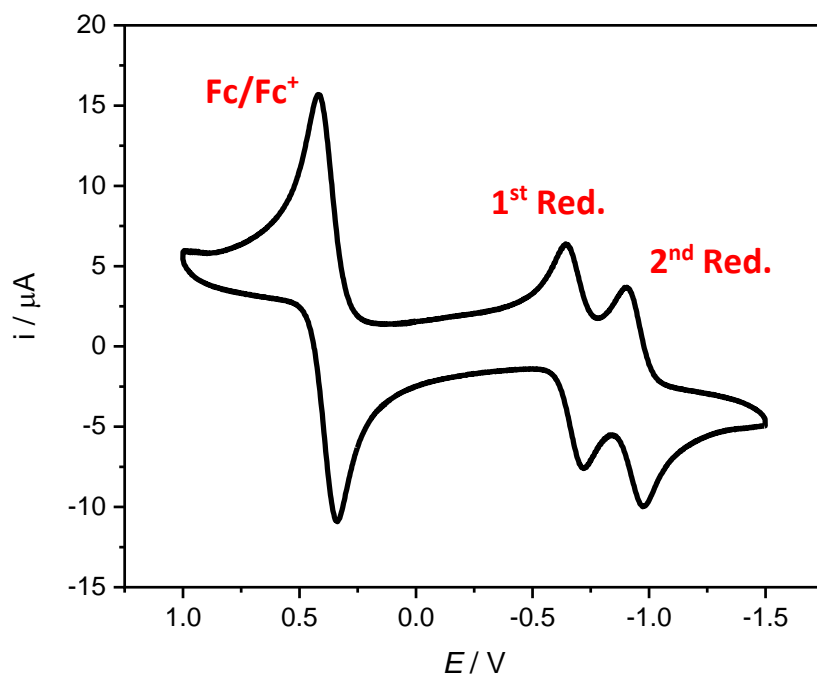


Figure S54. Cyclic voltammety trace of a benzonitrile solution of **3c** ($c \sim 1$ mM; ~ 100 mM Bu_4NPF_6 as electrolyte) at 100 mVs^{-1} scan rate with ferrocene as an internal standard.



Section H. Single-crystal X-Ray Diffraction

Crystal structure determination of (RRR)-1b crystallized from nitrobenzene; CCDC 2031730.

Colorless needle-shaped single crystals of $C_{119}H_{109.1}N_{12}O_{23}$ [(RRR)-1b] were grown by a slow vapour diffusion of methanol into a nitrobenzene solution of the cage over the course of several days.

Refinement special details: Most of the solvent molecules are disordered and non-fully occupied. Restraints had to be used.

Crystal Data $C_{119}H_{109.1}N_{12}O_{23}$, $M_r = 2075.28$, monoclinic, $C2$ (No. 5), $a = 31.9058(6)$ Å, $b = 17.2344(3)$ Å, $c = 20.9913(4)$ Å, $\beta = 102.3150(10)^\circ$, $\alpha = \gamma = 90^\circ$, $V = 11277.0(4)$ Å³, $T = 130$ K, $Z = 4$, $Z' = 1$, $m(\text{GaK}_\alpha) = 0.451$, 60720 reflections measured, 21729 unique ($R_{\text{int}} = 0.0365$) which were used in all calculations. The final wR_2 was 0.2617 (all data) and R_1 was 0.0879 ($I > 2(I)$).

Crystal structure determination of (SSS)-1b crystallized from nitrobenzene; CCDC 2031731.

Colorless needle-shaped crystals of $C_{115.5}H_{108.1}N_{17}O_{23.2}$ [(SSS)-1b] were grown by a slow vapour diffusion of methanol into a nitrobenzene solution of the cage over the course of several days.

Refinement special details: there is a lot of solvent molecules in the structure. Many of them are not fully occupied and had to be restrained to be chemically reasonable.

Crystal Data $C_{115.5}H_{108.1}N_{17}O_{23.2}$, $M_r = 2105.48$, monoclinic, $C2$ (No. 5), $a = 31.8864(19)$ Å, $b = 17.2148(10)$ Å, $c = 20.9689(12)$ Å, $\beta = 102.403(3)^\circ$, $\alpha = \gamma = 90^\circ$, $V = 11241.6(11)$ Å³, $T = 130$ K, $Z = 4$, $Z' = 1$, $m(\text{CuK}_\alpha) = 0.728$, 74017 reflections measured, 19234 unique ($R_{\text{int}} = 0.0374$) which were used in all calculations. The final wR_2 was 0.2145 (all data) and R_1 was 0.0713 ($I > 2(I)$).

Crystal structure determination of (SSS)-1b crystallized from toluene.

Colorless single crystals of (SSS)-**1b** were grown by a slow vapour diffusion of hexane into a toluene solution of the cage over the course of several days.

Special details: R value is relatively high, likely due to additional disorder from solvent.

Crystal Data C_{94.5}H₉₀N₁₂O₁₂, monoclinic, C3 (No. 146), $a = 26.1643(8)$ Å, $b = 26.1643(8)$ Å, $c = 13.1415(9)$ Å, $\gamma = 102^\circ$, $\alpha = \beta = 90^\circ$, $V = 7791.01$ Å³, $T = 130$ K, $Z = 3$, $Z' = 0$, $R_1 = 17.94\%$.

Crystal structure determination of (RRR)-1c and (SSS)-1c crystallized from nitrobenzene.

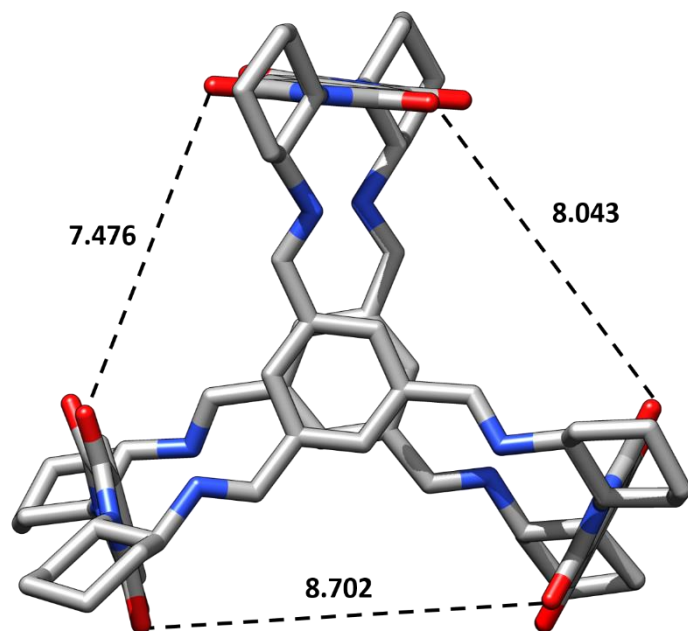
Reddish single crystals of (RRR)-**1c** and (SSS)-**1c** were grown by a slow vapour diffusion of methanol into a nitrobenzene solution of the cage over the course of several days.

Special details: There is a large void in the structure of **1c** filled with solvent molecules. The structure of **1c** can be defined, however, the high-quality factors of R_1 and wR_2 were hard to reach due to the large disorder from solvent.

Crystal Data C₁₂₆H₉₆N₁₂O₁₂, monoclinic, C2 (No. 5), $a = 18.4386(7)$ Å, $b = 27.3379(7)$ Å, $c = 18.7116(5)$ Å, $\beta = 107.150(3)^\circ$, $\alpha = \gamma = 90^\circ$, $V = 9012.62$ Å³, $T = 130$ K, $Z = 2$, $Z' = 0$, $R_1 = 14.38\%$.

Figure S55. XRD structures and structural parameters of (*SSS*)-**1b** from single crystals grown by diffusion of methanol vapour to nitrobenzene solutions within several days. Color code: Grey–carbon, red–oxygen, blue–nitrogen. Hydrogen atoms and solvent molecules are omitted for clarity. The C–C distances (in Å) between a) the carbonyl groups edges and b) the central carbons of PMDI units in (*SSS*)-**1b**, respectively, are shown.

a.



b.

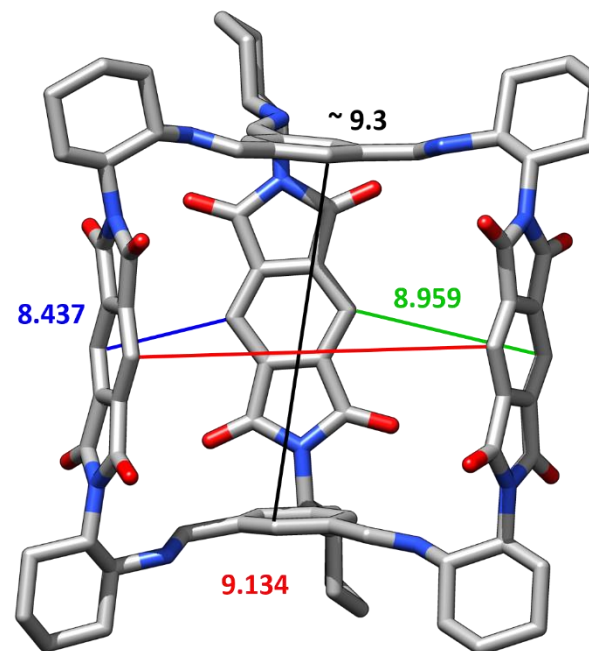


Figure S56. A side view of the crystallographic solid-state superstructure of (*SSS*)-**1b** determined by XRD of single crystals of (*SSS*)-**1b** grown from a) toluene and b) nitrobenzene. Color code: Grey–carbon, red–oxygen, blue–nitrogen. Hydrogen atoms and solvent molecules are omitted for clarity. Note that solvent molecules occupy both the cavities of the cages and the voids/channels between different cages.

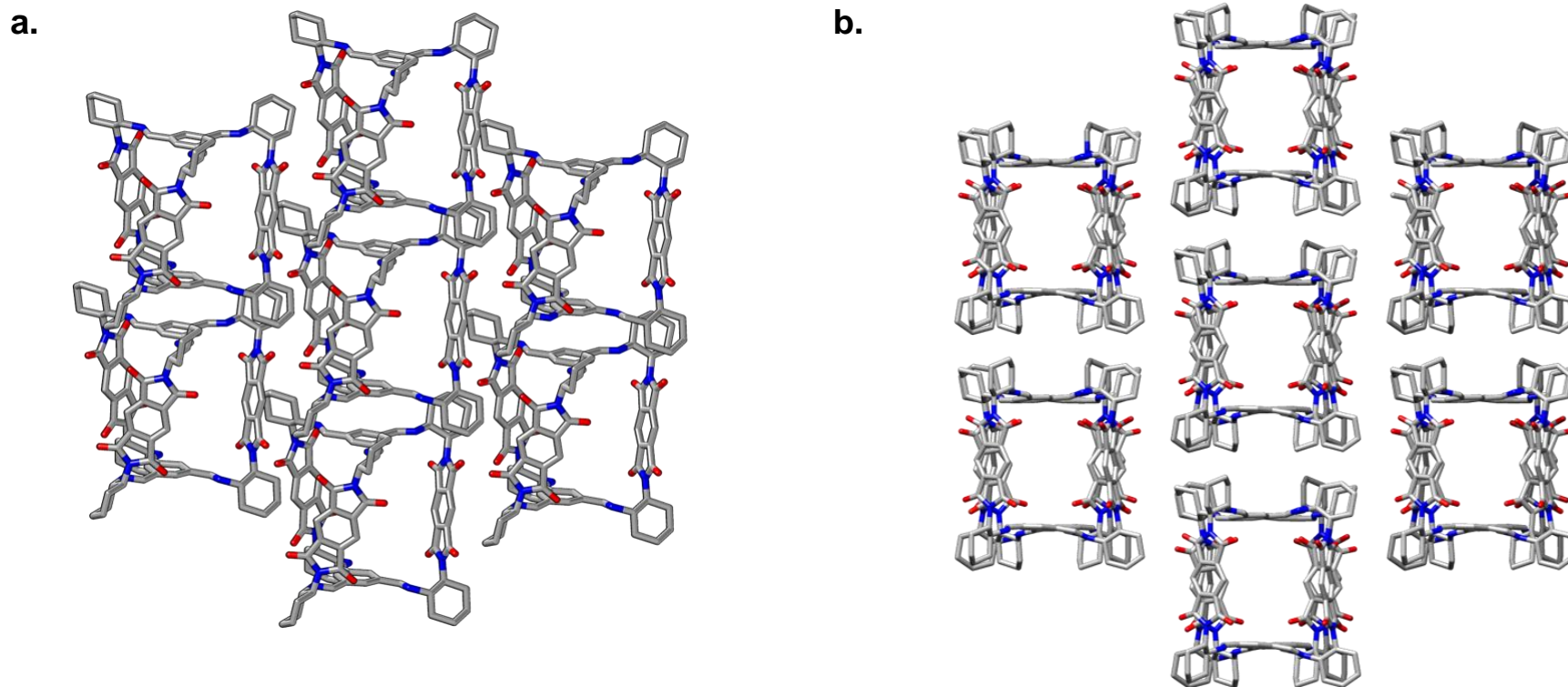
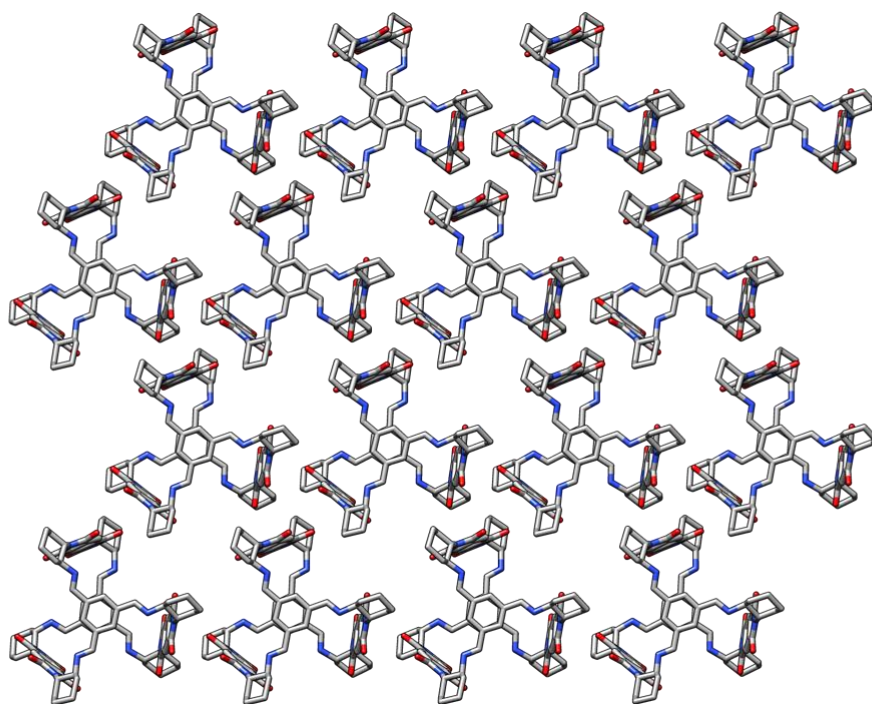


Figure S57. A top view of the crystallographic solid-state superstructure of (SSS)-**1a** determined by XRD of single crystals of (SSS)-**1b** grown from a) toluene and b) nitrobenzene. Colour code: Grey–carbon, red–oxygen, blue–nitrogen. Hydrogen atoms and solvent molecules are omitted for clarity. Note that solvent molecules occupy both the cavities of the cages and the voids/channels between the different cages (toluene and nitrobenzene, respectively).

a.



b.

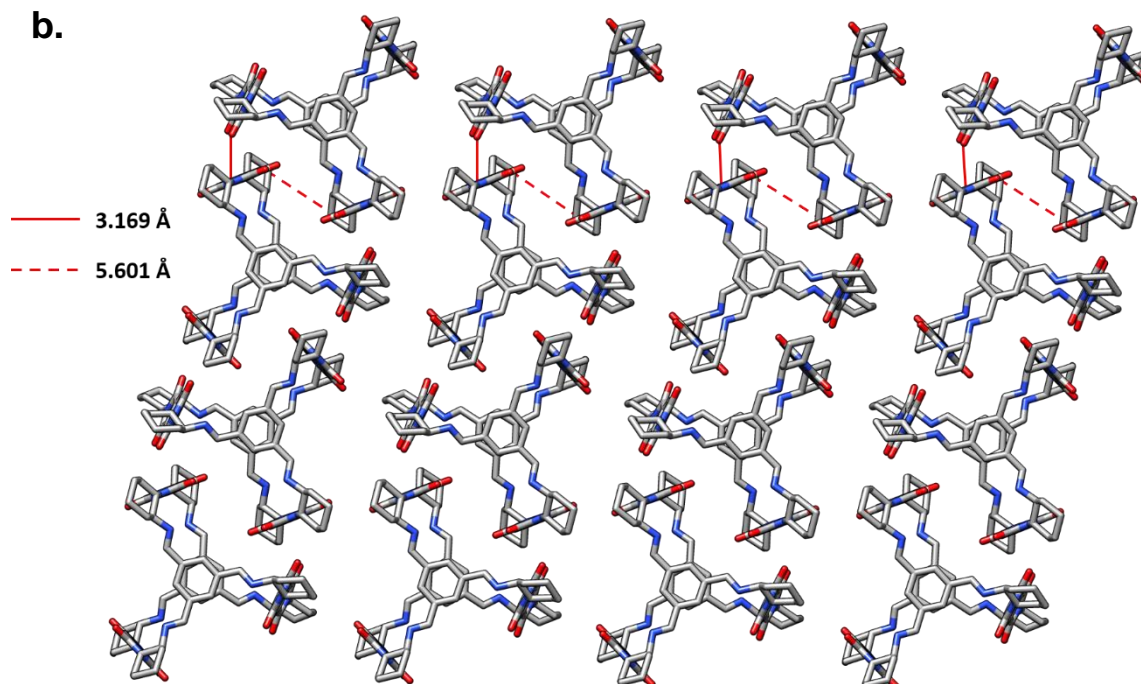
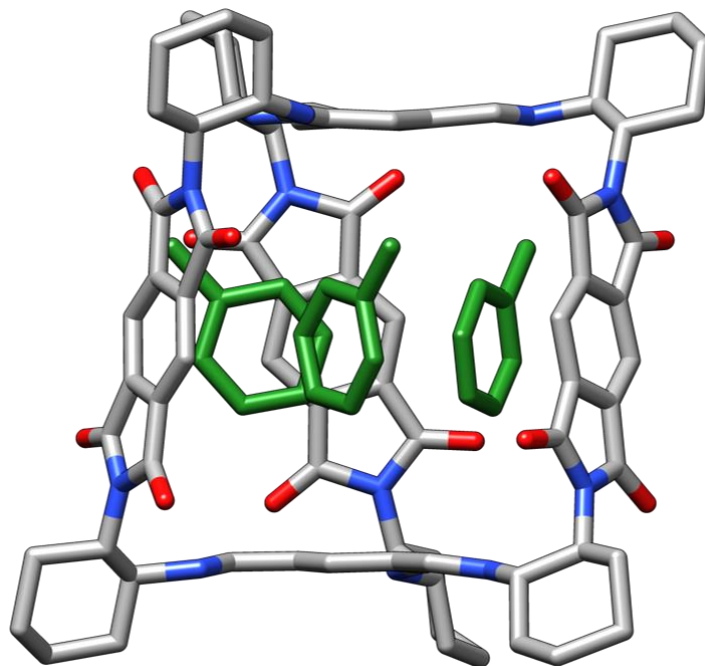


Figure S58. Structure of crystallographic cages in solid (*SSS*)-**1b** obtained by XRD of a single crystal of (*SSS*)-**1b** grown from a) toluene and b) nitrobenzene. Grey–carbon, red–oxygen, blue–nitrogen. Hydrogen atoms are omitted for clarity. Toluene molecules that occupy the cavity of the cage are highlighted in green. Nitrobenzene molecules are highlighted in purple.

a.



b.

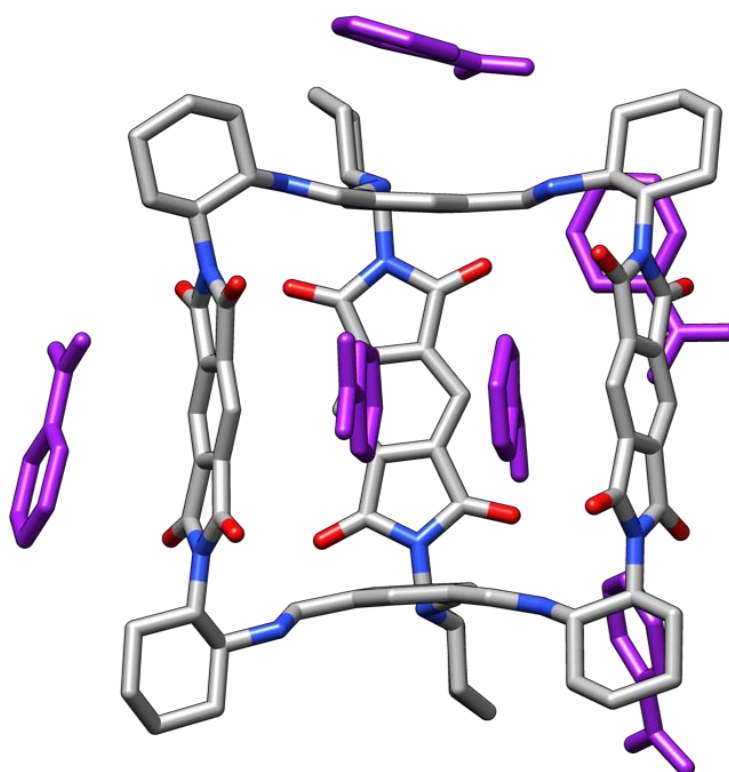


Figure S59. a) A side and b) a top view of the crystallographic solid-state superstructure of **1c** determined by XRD of single crystals of **1c** grown from nitrobenzene. Grey–carbon, red–oxygen, blue–nitrogen. Hydrogen atoms and solvent molecules are omitted for clarity.

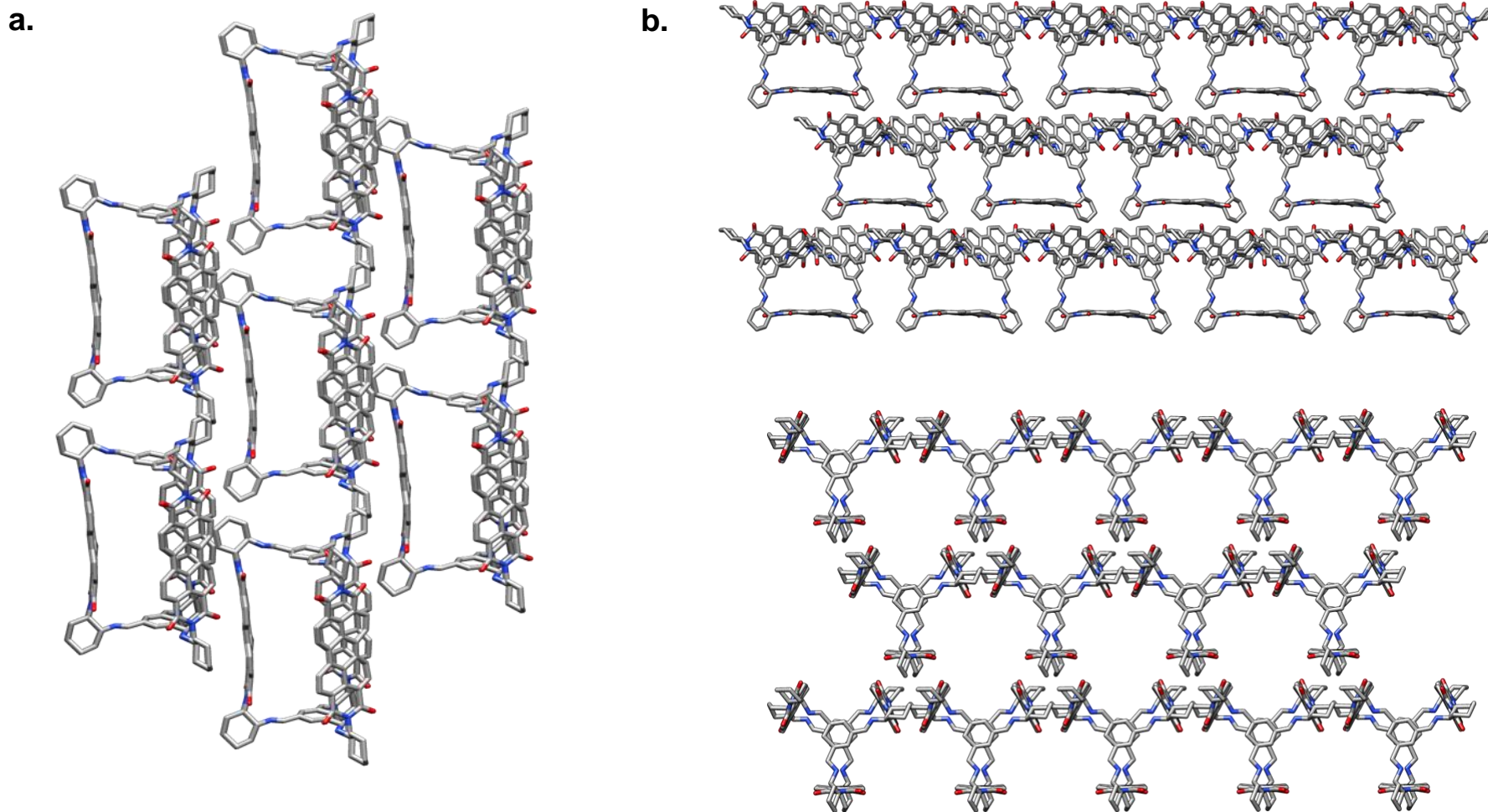


Table S3. Energy required to distort the gas phase geometries of cages **1** into their solid-state structures.^a

	E^b / kcal mol ⁻¹		
	B3LYP	BMK	M06-2X
1a	8.9	7.5	7.7
1b	8.8	8.4	8.4
1c	– ^c	– ^c	– ^c

^aCalculated as the difference between the energy of the fully optimized geometries of cages **1** in D_3 point group of symmetry at B3LYP/6-31G(d) level of theory (gas phase) and the partially optimized crystal structures taken from the single crystals grown by methanol vapor diffusion into nitrobenzene solutions of cages **1**. The partial optimization relaxed the coordinates of hydrogen atoms and the bond lengths between the heavy atoms (C, N, O). ^bThe energy (in kcal mol⁻¹) was obtained with the respective functional and 6-31+G(2d,p) basis set. Zero-point vibrational energy correction is (and cannot be) included. ^cThe energy could not be accurately predicted because the crystals structure of **1c** is not resolved with sufficient accuracy (see X-Ray crystallography analysis in the Supporting Information).

Section I. Gas Adsorption

Gas Selectivity Calculation. All adsorption isotherms are fitted using single-site Langmuir model or a dual-site Langmuir model. And the selectivity of CO₂/N₂ are calculated based on Idea Adsorbed Solution Theory (IAST). All calculations were performed in Mathematica.¹⁴

Fitting CO₂ isotherms and Calculation of Heat of Adsorption (Q_{st}). The dual-site Langmuir-Freundlich expression is used to fit all CO₂ and CH₄ isotherm data at 273 K, 298 K and 323 K, where n is the amount adsorbed (mmol g⁻¹), n_{sat} is the saturation loading (mmol g⁻¹), b_i is the Langmuir parameter (bar^{- v_i}), p is the pressure, and v_i is a constant for site 1 and 2

$$n = \frac{n_{sat,1}b_1p^{v_1}}{1 + b_1p^{v_1}} + \frac{n_{sat,2}b_2p^{v_2}}{1 + b_2p^{v_2}}$$

The isosteric heat of adsorption, $-Q_{st}$ was calculated for each material with the fitting plots and using Clausius-Clapeyron relation, where R is the ideal gas constant, p is the pressure, and T is the temperature.

$$-Q_{st} = RT^2 \left(\frac{\partial \ln p}{\partial T} \right)_n$$

Figure S60. Ar adsorption (filled) and desorption (empty) isotherms of **1a** and **1b** crystalline samples obtained from nitrobenzene (a,b) and from MeOH/THF (c,d).

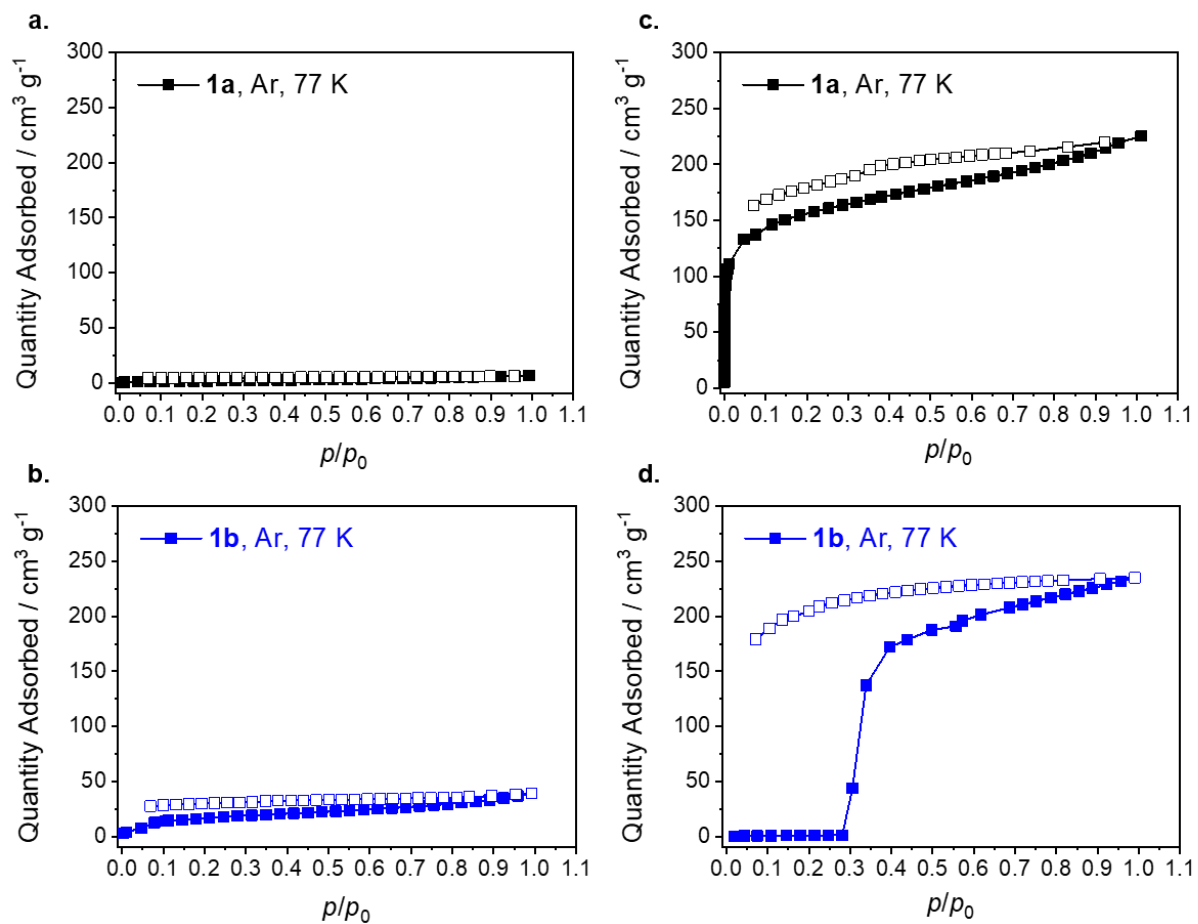


Figure S61. CO₂/N₂ IAST selectivity of **1a** (a) and **1b** (b).

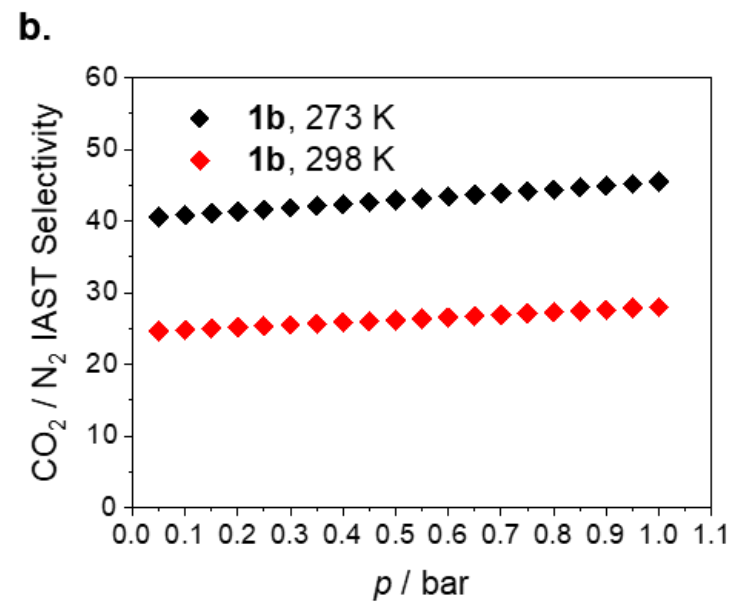
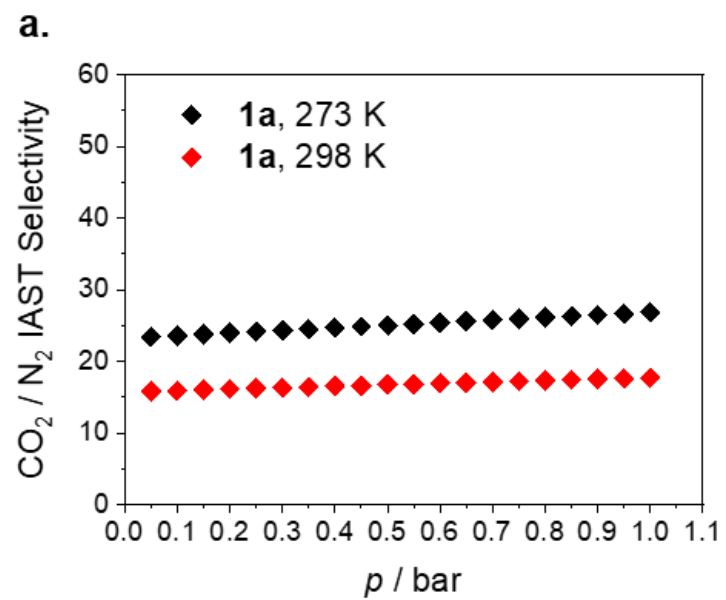


Table S4. CO₂, N₂ adsorption isotherms **1a** and **1b** at 273, 298 and 323 K up to 1 bar.

Sample	CO ₂ ^a			Q_{st}^b (kJ mol ⁻¹)	N ₂ ^a			CO ₂ /N ₂ Selectivity ^c	
	273 K (mmol g ⁻¹)	298 K (mmol g ⁻¹)	323 K (mmol g ⁻¹)		273 K (mmol g ⁻¹)	298 K (mmol g ⁻¹)	323 K (mmol g ⁻¹)	273 K (1 bar)	298 K (1 bar)
Cage 1a	2.91	1.84	1.15	27.0	0.31	0.19	0.050	26.9	17.8
Cage 1b	2.00	1.26	0.78	27.5	0.16	0.83	0.014	45.5	28.0

^aGas uptake at 1 bar ^bat zero coverage. ^cIAST Selectivity.

Figure S62. CH₄ adsorption and heat of adsorption (CH₄ Q_{st}) of **1a** (a,b) and **1b** (c,d).

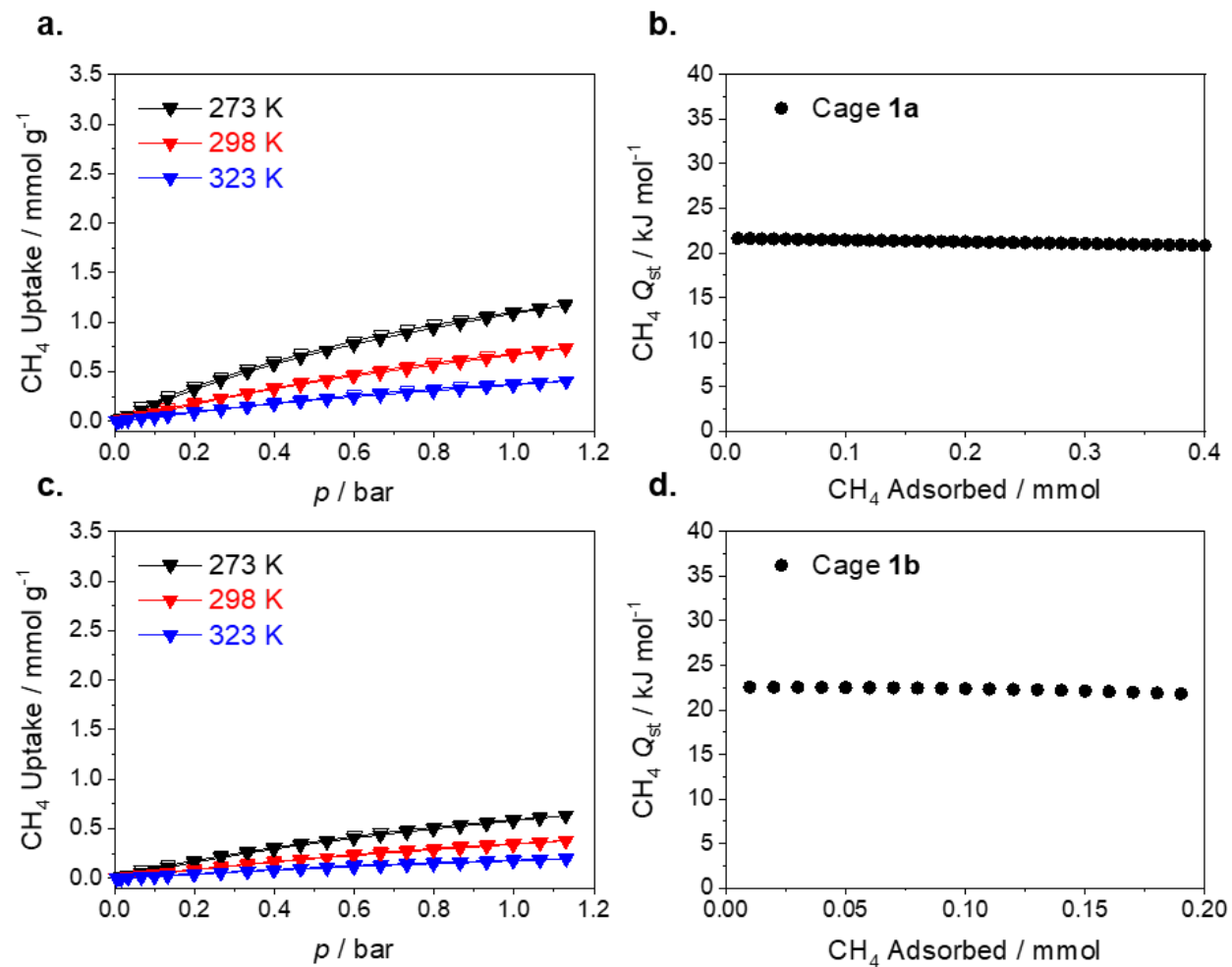


Table S5. CH₄ adsorption of **1a** and **1b**.

Sample	CH ₄ ^a			Q_{st}^b (kJ mol ⁻¹)
	273 K (mmol g ⁻¹)	298 K (mmol g ⁻¹)	323 K (mmol g ⁻¹)	
Cage 1a	1.09	0.67	0.36	21.6
Cage 1b	0.6	0.36	0.18	22.6

^aGas uptake is 1 bar ^bat zero coverage.

Figure S63. (a) BET linear plot and (b) Rouquerol plot for **1a**.

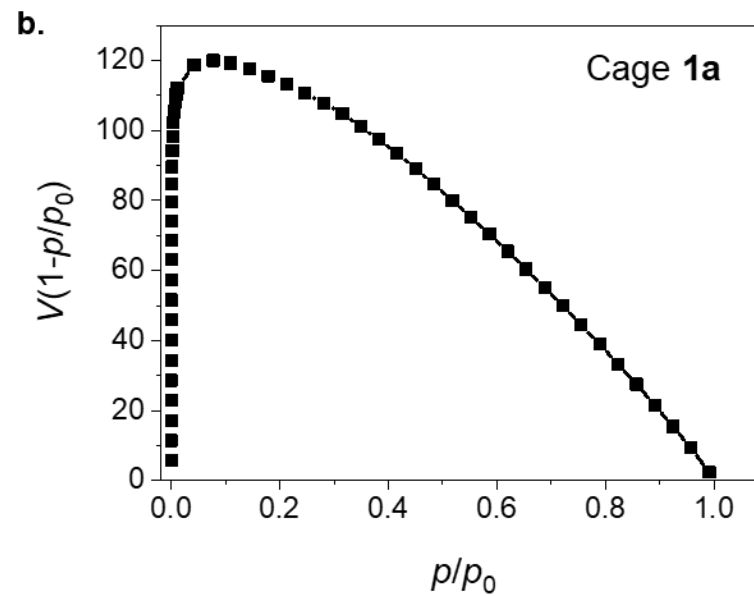
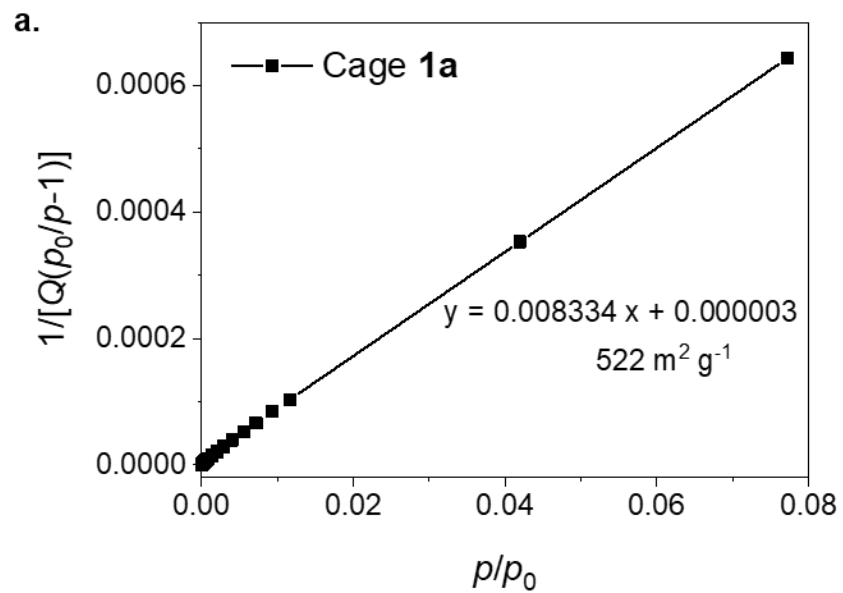
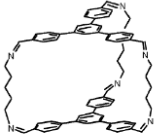
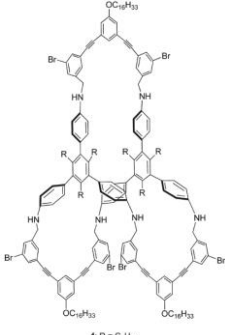
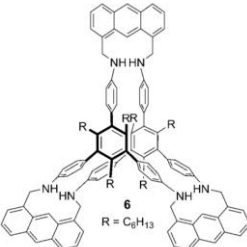
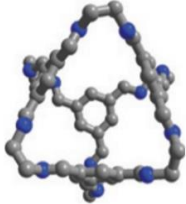
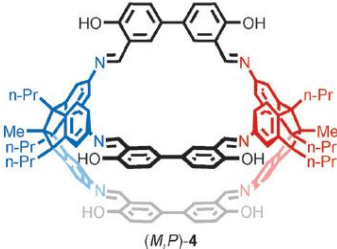
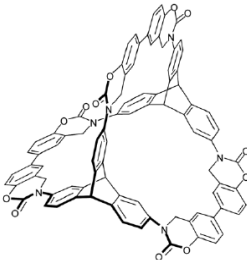
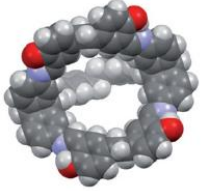
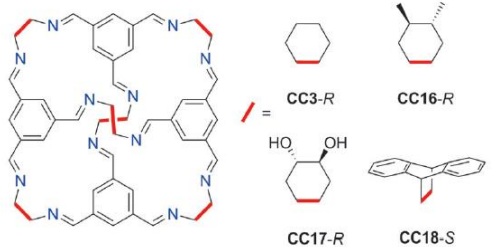
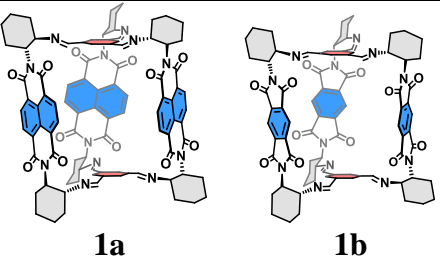


Table S6. The summary of CO₂ adsorption for porous organic cages reported in the literature.

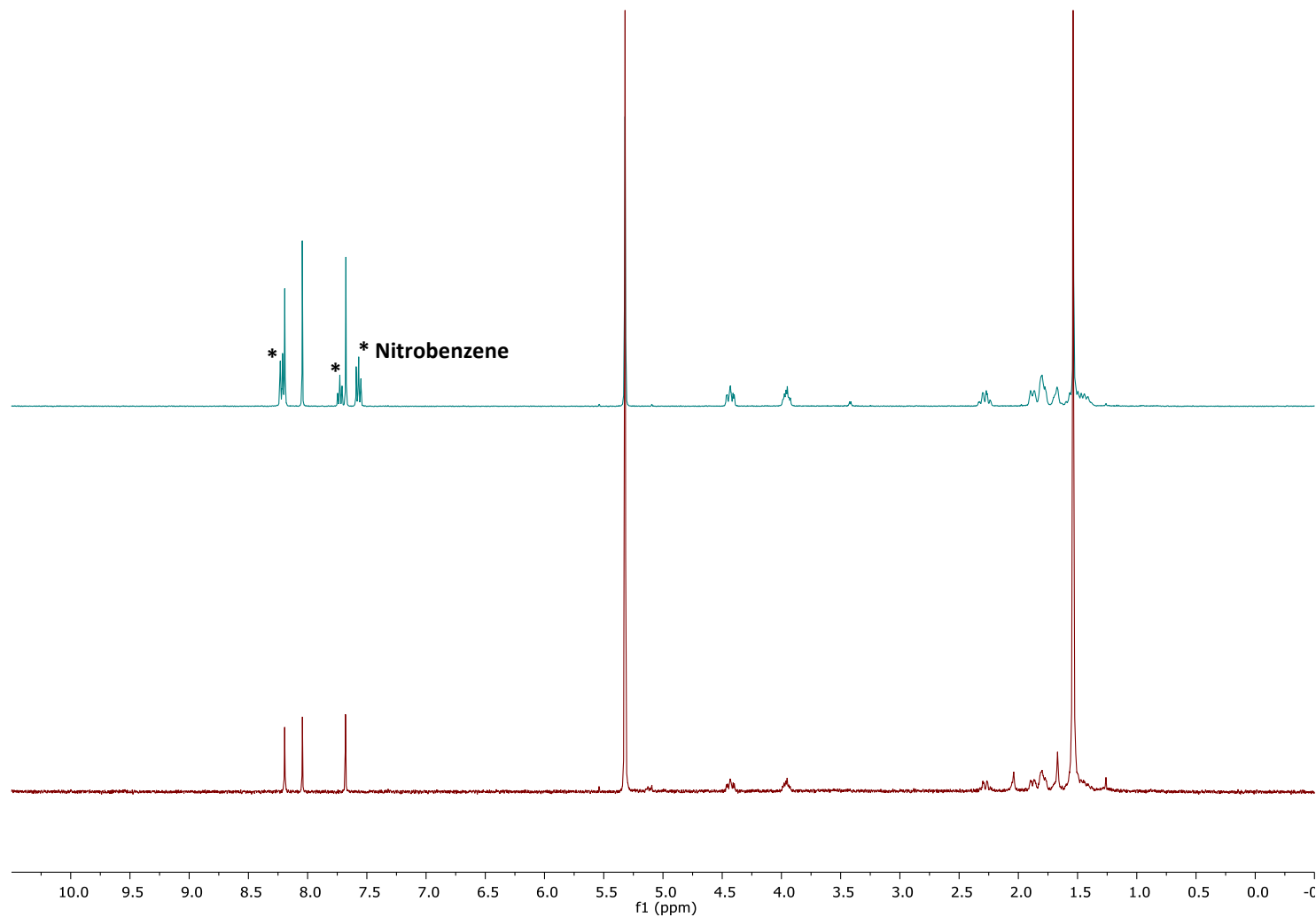
Cage	S_{ABET} (m ² g ⁻¹)	CO ₂ (mmol g ⁻¹)	Q _{st} (kJ mol ⁻¹)	N ₂ (mmol g ⁻¹)	CO ₂ /N ₂ Selectivity	Ref
[2 + 3] cage  5	99	0.9 (300 K, 1.2 bar)	—	0.08 (300 K, 1.2 bar)	11 (1 bar)	15
[2 + 3] cage  4: R = C ₁₂ H ₂₅	Non porous (<10)	0.1 - 0.25 (293 K, 1.0 bar)	—	0.008 - 0.006 (293 K, 1.0 bar)	38 - 138	16
[2 + 3] cage  6 R = C ₁₂ H ₂₅	—	0.16 - 0.19 (293 K, 1.0 bar)	—	0.002 - 0.0048 (293 K, 1.0 bar)	39.2 - 73.0	17

Cage	S_{ABET} ($\text{m}^2 \text{g}^{-1}$)	CO_2 (mmol g^{-1})	Q_{st} (kJ mol^{-1})	N_2 (mmol g^{-1})	CO_2/N_2 Selectivity	Ref
[4 + 6] Cage 	23 - 624	1.27 - 3.0 (275 K, 1.0 bar)	—	—	—	18
[2 + 3] Cage  (<i>M,P</i>)-4	211-918	2.5 - 3.5 (273 K, 1.0 bar)	25 - 31	0.35 - 0.43 (273 K, 1.0 bar)	17.5 - 25.3 (273 K) ^a	19
[2 + 3] cage 	105	2.55 (273 K, 1 bar)	60.1	0.48 (273 K, 1 bar)	13.9 (273 K) ^a	20

Cage	S_{ABET} ($\text{m}^2 \text{g}^{-1}$)	CO_2 (mmol g^{-1})	Q_{st} (kJ mol^{-1})	N_2 (mmol g^{-1})	CO_2/N_2 Selectivity	Ref
[2 + 3] cage 	30,744	2.7 - 3.3 (298 K, 1 bar)	—	—	—	21
[4 + 6] Cage 	10 - 1023	1.03 - 2.00 (273 K, 1 bar)	—	—	—	22
[2 + 3] Cage 	522 (1a)	2.00 - 2.91 (273 K, 1 bar)	27.0 -27.5	0.16 - 0.31	26.9 (1a), 45.5 (1b) (273 K)	Our work

^aSelectivity is calculated from Henry law constant.

Figure S64. ^1H NMR spectrum of crystalline sample of (*RRR*)-**1b** obtained from nitrobenzene before (top) and after (bottom) the sample activation for the BET measurement (400 MHz, CD_2Cl_2 , 298K) demonstrating that majority of nitrobenzene was removed under dynamic vacuum during the sample activation process.



Section J. TCSPC and Quantum Yields

Figure S65. TCSPC spectra of degassed CH_2Cl_2 samples ($c \sim 0.1\text{--}0.2 \mu\text{M}$) of **1c** (black, fit: red) and **3c** (blue, fit: red).

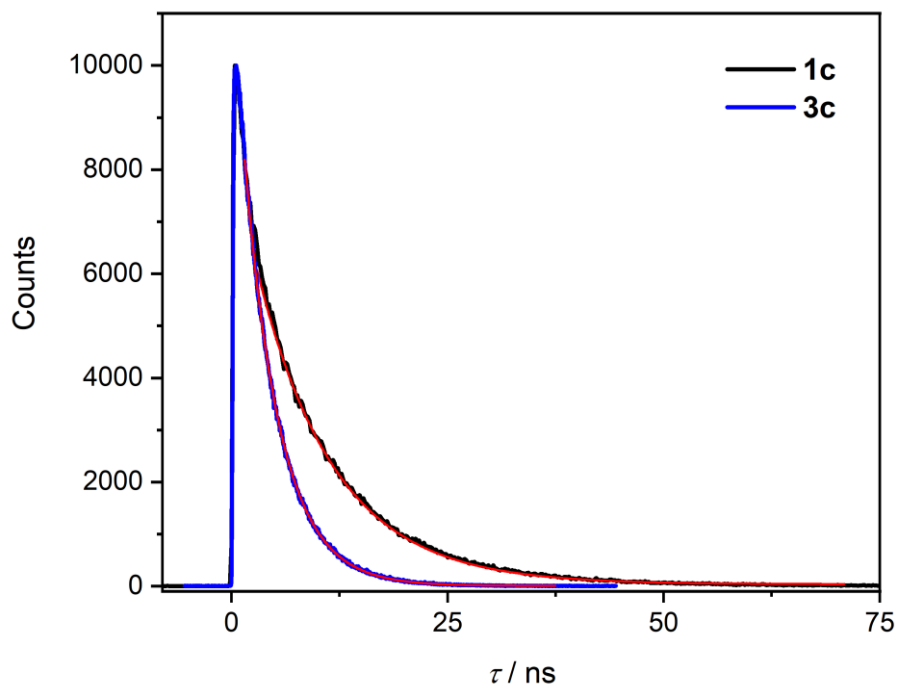


Figure S66. TCSPC spectra of degassed samples ($c \sim 0.1\text{--}0.2 \mu\text{M}$) of **3c**. Toluene (black, fit: red), CH_2Cl_2 (blue, fit: red) and benzonitrile (green, fit: red).

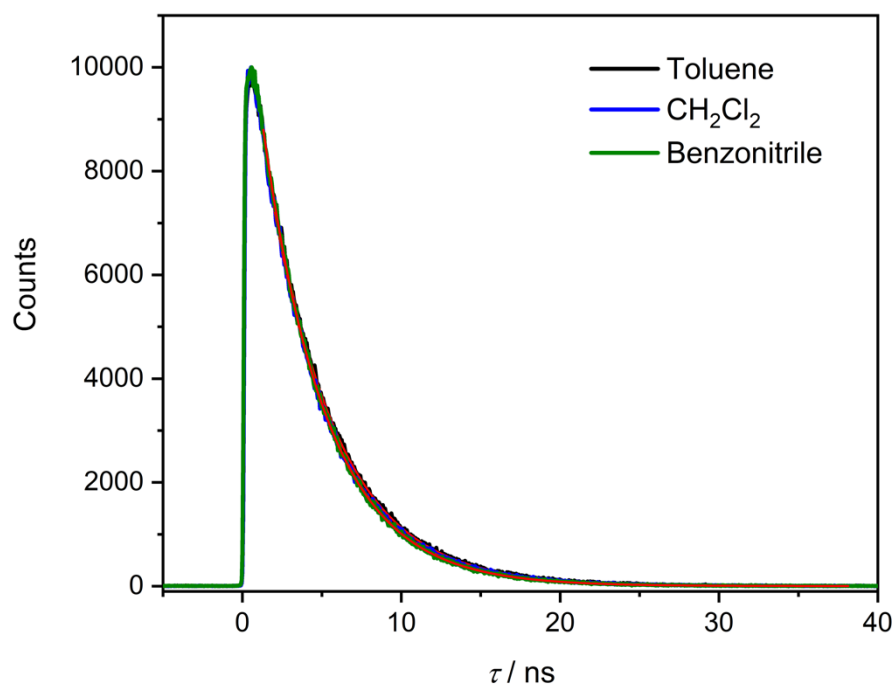


Figure S67. TCSPC spectra of degassed samples ($c \sim 0.1\text{--}0.2 \mu\text{M}$) of **1c**. Toluene (black, fit: red), CH_2Cl_2 (blue, fit: red) and benzonitrile (green, fit: red).

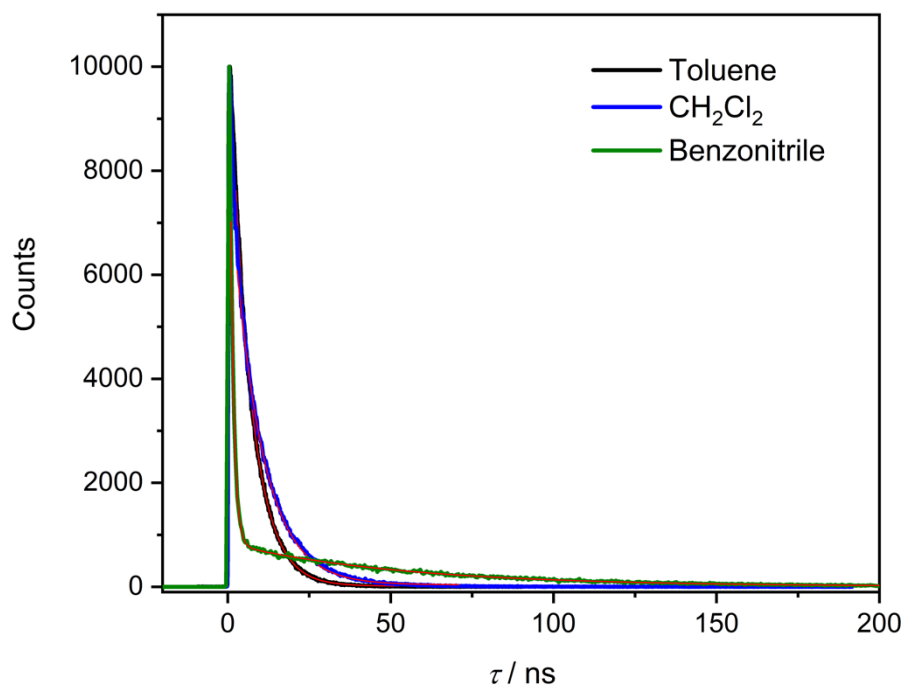


Table S7. Photoluminescence quantum yields (ϕ_{em})^a of samples of **1c** and **3c** in CH₂Cl₂, toluene and benzonitrile.

ϕ_{em} (1c)						
Entry	Toluene		CH ₂ Cl ₂		Benzonitrile	
	523nm	488nm	523nm	488nm	523nm	488nm
a	0.81	0.82	0.72	0.74	0.37	0.39
b	0.79	0.78	0.78	0.80	0.41	0.42
c	0.81	0.81	0.72	0.74	0.40	0.42
Avg. \pm CI ^b	0.83 \pm 0.016		0.75 \pm 0.034		0.40 \pm 0.019	

^aAll samples were degassed with Ar for 15 min prior to measurement. ^bAn average value of quantum yield obtained by averaging the six independent measurements at two excitation wavelengths. CI is the confidence interval at 95% confidence level.

ϕ_{em} (3c)						
Entry	Toluene		CH ₂ Cl ₂		Benzonitrile	
	523nm	488nm	523nm	488nm	523nm	488nm
a	0.89	0.88	0.88	0.90	0.85	0.83
b	0.90	0.90	0.86	0.86	0.87	0.88
c	0.87	0.87	0.88	0.88	0.86	0.87
Avg. \pm CI	0.89 \pm 0.014		0.88 \pm 0.016		0.86 \pm 0.019	

^aAll samples were degassed with Ar for 15 min prior to measurement. ^bAn average value of quantum yield obtained by averaging the six independent measurements at two excitation wavelengths. CI is the confidence interval at 95% confidence level.

Table S8. Results of time-correlated single photon counting experiments of samples ($c \sim 0.3 - 0.7 \mu\text{M}$) of **1c** and **3c** in toluene, CH_2Cl_2 , and benzonitrile.

		τ^a / ns		
		Toluene	CH_2Cl_2	Benzonitrile
1c			3.00 ± 0.32^b ; $[9.4 \pm 0.93]^d$	1.10 ± 0.02^b ; $[19.2 \pm 1.01]^d$ $(1.04 \pm 0.031)^e$
		6.27 ± 0.025	10.15 ± 0.08^c ; $[90.6 \pm 0.93]^d$	55.9 ± 1.12^c ; $[80.8 \pm 1.01]^d$ $(10.7 \pm 0.3)^e$
3c		4.27 ± 0.016	4.12 ± 0.01	3.98 ± 0.04 ; $(3.59 \pm 0.014)^e$

^aAll samples were bubbled with Ar 3 mins prior to the measurement unless stated otherwise; three independent measurements were performed and the displayed error is the standard deviation of the mean. ^bLifetime of the prompt fluorescence signal. ^cLifetime of the delayed fluorescence signal. ^dThe numbers in brackets are the relative amplitudes A associated with individual time components in the biexponential fit. ^eThe numbers in parentheses are lifetimes determined for samples bubbled with pure O_2 for 3 mins before the measurement.

Table S9. TD-DFT electronic transition energies and oscillator strengths^a and other excited state properties,^b and triplet energies.^c

	Toluene	CH ₂ Cl ₂	Benzonitrile	$\mu_{0\rightarrow 1}^d / \text{a.u.}$	$J_{\text{Coul}}^e / \text{cm}^{-1}$
S ₁ , 1c ^f	2.5877, (0.0272)	2.5904, (0.0268)	2.5746, (0.0280)	–	165 (toluene), 178 (CH ₂ Cl ₂),
S ₂ , 1c ^g	2.6491, (3.0263)	2.6567, (2.9916)	2.6349, (3.0864)	–	162 (benzonitrile)
S ₁ , PDicy ^h	2.6086, (1.1010)	2.6149, (1.0929)	2.5963, (1.1182)	4.13	–
T ₁ , PDicy ^{c,h}	1.2186, (1.1275)	1.2186, (1.1275)	1.2186, (1.1275)	–	–

^aEnergies in eV and corresponding oscillator strengths (in parentheses). ^bCalculated at the TD-CAM-B3LYP/6-31G(d)/PCM level of theory on gas phase B3LYP/6-31G(d) geometries. ^cEnergy (SMD, at 0K) in eV. Calculated at the ROB3LYP/6-31+G(2d,p) level of theory including unscaled ZPVE correction. UB3LYP result in parentheses. ^dTransition dipole moment (in atomic units; dichloromethane) of the electronic transition between the ground and the first excited state. ^eEstimate of the through-space Coulomb coupling (dichloromethane) calculated as 1/3 of the difference between the electronic transition energies of the S₁ and S₂ states. ^fThe lowest-energy doubly degenerate singlet excited state in the D₃ symmetry of cage **1c**. ^gThe lowest-energy non-degenerate singlet excited state in the D₃ symmetry of cage **1c**. ^h2,9-Dicyclohexylanthra[2,1,9-*def*:6,5,10-*d'e'f'*]diisoquinoline-1,3,8,10(2*H*,9*H*)-tetraone (Dicyclohexyl-PDI).

Table S10. Solvation Gibbs free energies^a of different states of dicyclohexyl-PDI (**PDicy**; see caption – *h* – of Table S9).

Species	$\Delta G_{\text{solv}}^\circ / \text{kcal mol}^{-1}$		
	Toluene	CH ₂ Cl ₂	Benzonitrile
S ₀ ^b	–24.3	–26.5	–26.4
T ₁ ^c	–24.3	–26.6	–26.5
PDicy ^{•–}	–38.1	–48.6	–50.0
PDicy ^{•+}	–47.0	–62.0	–65.4
1c , ^d charge separated state	–109.4	–137.1	–141.8

^aCalculated at B3LYP/6-31G(d) level of theory using SMD solvation model. ^bThe ground state of **PDicy**. ^cThe triplet state of **PDicy**. ^dCalculated as the sum of the solvation Gibbs free energies of **PDicy** (S₀), **PDicy**^{•–}, and **PDicy**^{•+}

Section K. Transient Absorption Spectroscopy

Global Lifetime Analysis. The broadband transient absorption data were analysed using global lifetime analysis.²³ We assumed a sequential model. This corresponds to a single population that evolves as a series of n successive exponential steps into further species without any losses or back-reactions. The exponential decay was convolved with a Gaussian instrument response function (IRF) to account for the finite duration of the excitation pulse. This analysis yields Evolution-Associated Difference Spectra (EADS), which represent the spectral evolution.²³ The analysis is summarized in Figure S68 below.

Figure S68. Global lifetime analysis of the transient absorption data measured for **1c** in benzonitrile on the ns- μ s timescale upon excitation at 532 nm. Evolution-associated difference spectra (EADS) and respective time constants (left panel), the spectra at given time delays (middle panel), and time profiles at given wavenumbers (right panel) with the best-fit (black line).

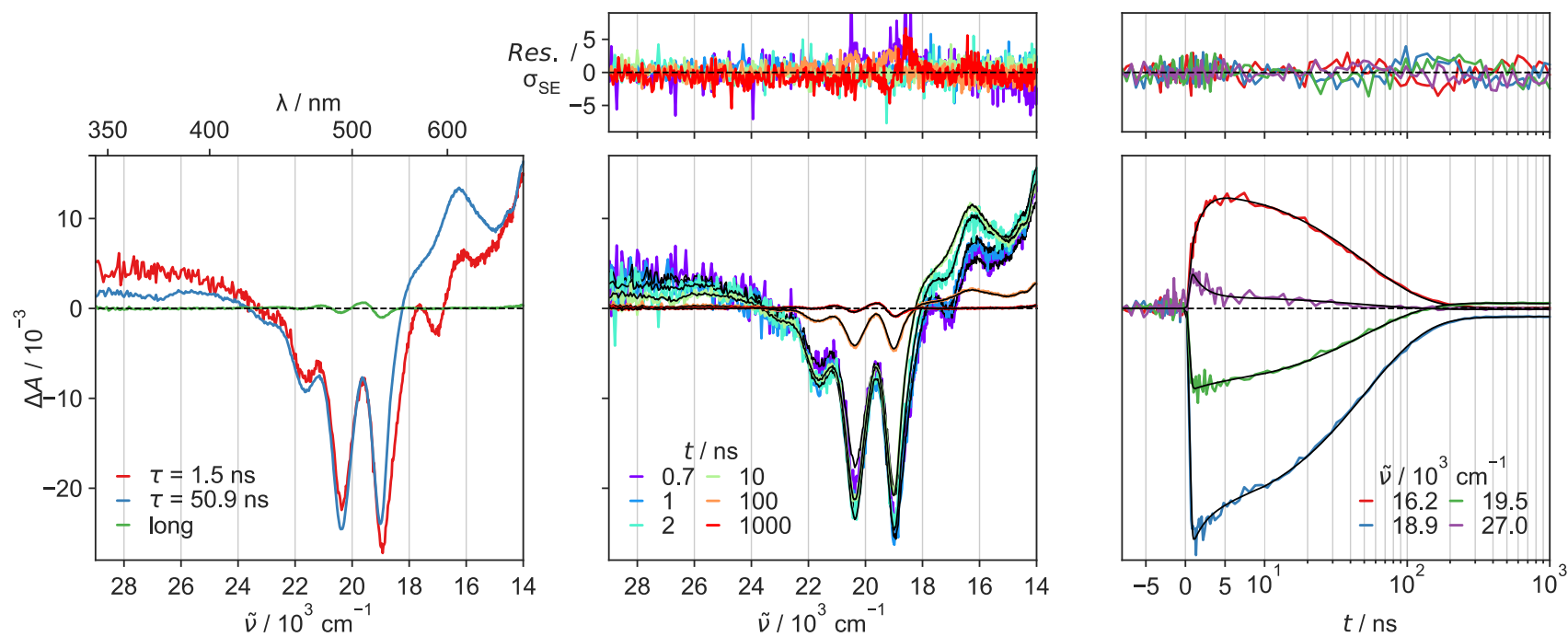
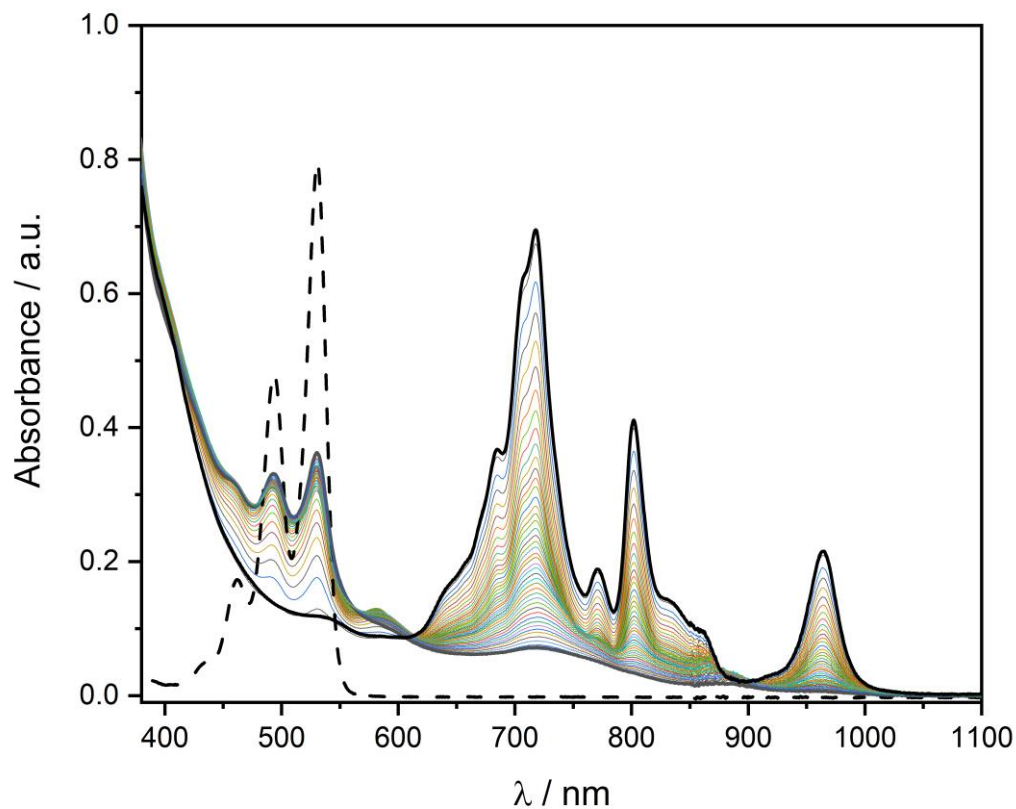
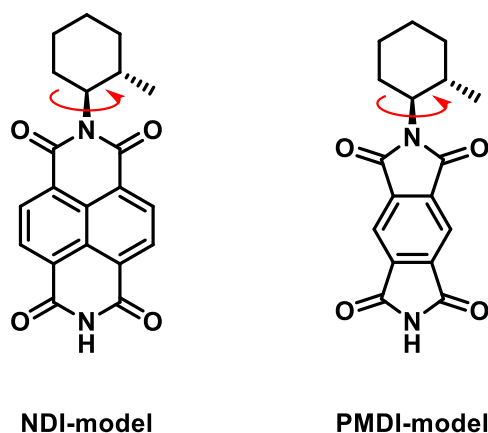


Figure S69. UV-Vis absorption spectra of degassed samples of **3c** (dashed line) in benzonitrile reduced (solid line) with excess cobaltocene. The spectrum of the generated **3c⁻** is highlighted in bold (black solid line). Slow diffusion of oxygen leads back to **3c** and formation of a small amount of an unknown species ($\lambda = 585$ nm), likely a product of **3c** and *in situ* generated superoxide species.



Section L. Computed Imidic C–N Bond Rotational Barriers



Scheme S2. Model compounds used for the calculation of the C–N bond rotational barrier (highlighted in red, ΔH of the reaction at 0K; see Table S11) using DFT calculations.

Table S11. DFT calculations of the imidic C–N bond rotational barrier^a, ΔH (0K), in model compounds according to Scheme S2.

Model	Energy ^a , ΔH (0K, in kcal mol ⁻¹)		
	B3LYP	BMK	M06-2X
NDI-model	30.4	31.3	30.8
PMDI-model	19.5	19.9	19.3

^aThe energy (in kcal mol⁻¹) calculated as the energy at 0K with the respective functional and 6-31+G(2d,p) basis set on gas phase B3LYP/6-31G(d) optimized geometries with unscaled zero-point vibrational energy correction.

Section M. Cartesian Coordinates

(R)-1a, B3LYP/6-31G(d), $E = -5268.84943199$ Hartree

C	0.713585	1.210997	5.036517
C	-0.713585	1.210997	-5.036517
C	-1.405547	0.012484	5.036517
C	1.405547	0.012484	-5.036517
C	-0.702423	-1.206620	5.031666
C	0.702423	-1.206620	-5.031666
C	0.691962	-1.223481	5.036517
C	-0.691962	-1.223481	-5.036517
C	1.396175	-0.005006	5.031666
C	-1.396175	-0.005006	-5.031666
C	0.693752	1.211626	-5.031666
C	-0.693752	1.211626	5.031666
C	-1.472086	2.473632	-5.122115
C	1.472086	2.473632	5.122115
N	-0.903714	3.592871	-5.341089
N	0.903714	3.592871	5.341089
N	2.659660	-2.579074	5.341089
N	-2.659660	-2.579074	-5.341089
N	-3.563374	-1.013796	5.341089
N	3.563374	-1.013796	-5.341089
N	-0.751738	5.847104	-3.471374
N	0.751738	5.847104	3.471374
N	4.687871	-3.574576	3.471374
N	-4.687871	-3.574576	-3.471374
N	5.439609	-2.272527	-3.471374
N	-5.439609	-2.272527	3.471374
C	-4.676836	-3.897972	-4.928069
C	4.676836	-3.897972	4.928069
C	-1.743381	4.768050	-5.535365
C	1.743381	4.768050	5.535365
C	-1.037324	5.999245	-4.928069
C	1.037324	5.999245	4.928069
C	-1.766582	7.320091	-5.231728
C	1.766582	7.320091	5.231728
C	-1.934261	7.506125	-6.746835
C	1.934261	7.506125	6.746835
C	-2.655568	6.304280	-7.370669
C	2.655568	6.304280	7.370669
C	-1.922114	4.994237	-7.055326
C	1.922114	4.994237	7.055326
C	-1.823206	5.760761	-2.570705
C	1.823206	5.760761	2.570705
C	-1.497144	5.734592	-1.118114
C	1.497144	5.734592	1.118114
C	-0.148944	5.738812	-0.694333
C	0.148944	5.738812	0.694333
C	0.906302	5.757335	-1.634269
C	-0.906302	5.757335	1.634269
C	0.608659	5.836220	-3.090392
C	-0.608659	5.836220	3.090392
C	-2.517415	5.727187	-0.179500
C	2.517415	5.727187	0.179500
C	-2.221960	5.746181	1.197073
C	2.221960	5.746181	-1.197073
O	2.984222	5.729387	2.958151
O	-2.984222	5.729387	-2.958151
O	1.505757	5.916131	-3.915322

O	-1.505757	5.916131	3.915322
O	3.469684	-5.449105	2.958151
O	-3.469684	-5.449105	-2.958151
O	5.876399	-1.654041	3.915322
O	-5.876399	-1.654041	-3.915322
O	6.453906	-0.280282	-2.958151
O	-6.453906	-0.280282	2.958151
O	4.370641	-4.262090	-3.915322
O	-4.370641	-4.262090	3.915322
C	-5.533365	-5.428182	-6.746835
C	5.533365	-5.428182	6.746835
C	-4.131883	-5.451929	-7.370669
C	4.131883	-5.451929	7.370669
C	-3.364079	-4.161718	-7.055326
C	3.364079	-4.161718	7.055326
C	-2.878271	0.038048	5.122115
C	2.878271	0.038048	-5.122115
C	-5.000943	-0.874213	5.535365
C	5.000943	-0.874213	-5.535365
C	-6.787451	-0.852351	7.370669
C	6.787451	-0.852351	-7.370669
C	-5.714160	-2.101273	4.928069
C	5.714160	-2.101273	-4.928069
C	4.895485	-2.998396	0.694333
C	-4.895485	-2.998396	-0.694333
C	5.439149	-2.093787	1.634269
C	-5.439149	-2.093787	-1.634269
C	5.044429	-2.740416	-0.694333
C	-5.044429	-2.740416	0.694333
C	5.714874	-1.570732	-1.118114
C	-5.714874	-1.570732	1.118114
C	7.467626	-2.077943	-6.746835
C	-7.467626	-2.077943	6.746835
C	5.286193	-0.832519	-7.055326
C	-5.286193	-0.832519	7.055326
C	7.222676	-2.130140	-5.231728
C	-7.222676	-2.130140	5.231728
C	-5.900569	-1.301438	2.570705
C	5.900569	-1.301438	-2.570705
C	-4.532847	-3.663548	1.634269
C	4.532847	-3.663548	-1.634269
C	-4.749985	-3.445224	3.090392
C	4.749985	-3.445224	-3.090392
C	-6.087319	-0.948817	-1.197073
C	6.087319	-0.948817	1.197073
C	-4.217730	-4.163860	-1.118114
C	4.217730	-4.163860	1.118114
C	-3.865359	-4.797364	1.197073
C	3.865359	-4.797364	-1.197073
C	-6.218597	-0.683449	0.179500
C	6.218597	-0.683449	-0.179500
C	-3.701182	-5.043738	-0.179500
C	3.701182	-5.043738	0.179500
C	-4.077363	-4.459323	-2.570705
C	4.077363	-4.459323	2.570705
C	-5.358644	-2.390996	-3.090392
C	5.358644	-2.390996	3.090392
C	-3.257562	-3.893837	-5.535365
C	3.257562	-3.893837	5.535365
C	5.456093	-5.189951	5.231728
C	-5.456093	-5.189951	-5.231728
C	-1.406185	-2.511680	-5.122115

C	1.406185	-2.511680	5.122115
H	-7.257235	0.062214	6.981568
H	7.257235	0.062214	-6.981568
H	3.574739	-6.316057	6.981568
H	-3.574739	-6.316057	-6.981568
H	3.682496	6.253843	6.981568
H	-3.682496	6.253843	-6.981568
H	-7.073789	-2.991099	7.216208
H	7.073789	-2.991099	-7.216208
H	6.127262	-4.630531	7.216208
H	-6.127262	-4.630531	-7.216208
H	0.946527	7.621630	7.216208
H	-0.946527	7.621630	-7.216208
H	-8.546089	-2.062070	6.946165
H	8.546089	-2.062070	-6.946165
H	6.058850	-6.370095	6.946165
H	-6.058850	-6.370095	-6.946165
H	2.487239	8.432166	6.946165
H	-2.487239	8.432166	-6.946165
H	-7.651708	-3.046312	4.807076
H	7.651708	-3.046312	-4.807076
H	6.464038	-5.103417	4.807076
H	-6.464038	-5.103417	-4.807076
H	1.187670	8.149730	4.807076
H	-1.187670	8.149730	-4.807076
H	-7.717526	-1.282223	4.748705
H	7.717526	-1.282223	-4.748705
H	4.969201	-6.042462	4.748705
H	-4.969201	-6.042462	-4.748705
H	2.748325	7.324685	4.748705
H	-2.748325	7.324685	-4.748705
H	-5.251813	-2.980632	5.378546
H	5.251813	-2.980632	-5.378546
H	-5.207210	-3.057888	5.378546
H	5.207210	-3.057888	-5.378546
H	0.044603	6.038520	5.378546
H	-0.044603	6.038520	-5.378546
H	-6.727119	0.209059	0.527805
H	6.727119	0.209059	-0.527805
H	3.182509	-5.930386	0.527805
H	-3.182509	-5.930386	-0.527805
H	3.544610	5.721327	0.527805
H	-3.544610	5.721327	-0.527805
H	-3.483770	-5.493471	1.936157
H	3.483770	-5.493471	-1.936157
H	-3.015600	5.763769	1.936157
H	3.015600	5.763769	-1.936157
H	-6.499370	-0.270298	-1.936157
H	6.499370	-0.270298	1.936157
H	6.935884	-0.843724	-8.457647
H	-6.935884	-0.843724	8.457647
H	4.198629	-5.584790	8.457647
H	-4.198629	-5.584790	-8.457647
H	2.737255	6.428514	8.457647
H	-2.737255	6.428514	-8.457647
H	4.813349	0.065358	-7.471250
H	-4.813349	0.065358	7.471250
H	-2.463276	4.135804	-7.471250
H	2.463276	4.135804	7.471250
H	4.791262	-1.694359	-7.523626
H	-4.791262	-1.694359	7.523626
H	-0.928273	4.996534	-7.523626

H	0.928273	4.996534	7.523626
H	3.862989	-3.302175	7.523626
H	-3.862989	-3.302175	-7.523626
H	2.350073	-4.201162	7.471250
H	-2.350073	-4.201162	-7.471250
H	-2.652853	-4.689193	-5.078316
H	2.652853	-4.689193	5.078316
H	5.387387	0.047159	-5.078316
H	-5.387387	0.047159	5.078316
H	2.482186	-0.035006	5.054250
H	-2.482186	-0.035006	-5.054250
H	-1.210777	2.167139	5.054250
H	1.210777	2.167139	-5.054250
H	-2.734534	4.642034	-5.078316
H	2.734534	4.642034	5.078316
H	-2.566397	2.378837	-5.026342
H	2.566397	2.378837	5.026342
H	3.343332	1.033146	-5.026342
H	-3.343332	1.033146	5.026342
H	1.271409	-2.132133	-5.054250
H	-1.271409	-2.132133	5.054250
H	0.776935	-3.411984	5.026342
H	-0.776935	-3.411984	-5.026342

(R)-1b, B3LYP/6-31G(d), $E = -4807.88775887$ Hartree

N	2.792535	-2.435264	5.236192
N	5.339146	-2.458452	-3.336427
N	0.712733	3.636038	5.236192
N	0.540491	5.853062	3.336427
N	-3.505268	-1.200774	5.236192
N	-5.339146	-2.458452	3.336427
N	4.798655	-3.394610	3.336427
N	-0.540491	5.853062	-3.336427
N	-2.792535	-2.435264	-5.236192
N	-0.712733	3.636038	-5.236192
N	3.505268	-1.200774	-5.236192
N	-4.798655	-3.394610	-3.336427
O	-6.410630	-0.517407	2.596975
O	3.653403	-5.293065	2.596975
O	2.757227	5.810472	2.596975
O	-1.794563	5.871728	3.335109
O	-4.187784	-4.490001	3.335109
O	5.982347	-1.381726	3.335109
O	1.794563	5.871728	-3.335109
O	-3.653403	-5.293065	-2.596975
O	6.410630	-0.517407	-2.596975
O	-5.982347	-1.381726	-3.335109
O	4.187784	-4.490001	-3.335109
O	-2.757227	5.810472	-2.596975
C	3.592803	-3.988880	6.935687
C	3.457694	-3.718068	5.420457
C	4.861943	-3.656381	4.781787
C	5.698462	-4.914475	5.079195
C	5.807305	-5.162435	6.589959
C	4.417727	-5.247471	7.234344
C	1.538609	-2.432643	5.008339
C	0.756901	-1.184348	4.925760
C	1.394392	0.070142	4.920726
C	0.647225	1.247669	4.925760
C	-0.757941	1.172508	4.920726
C	-1.404126	-0.063321	4.925760

C	-0.636451	-1.242650	4.920726
C	1.337426	2.548796	5.008339
C	1.491095	4.853485	5.420457
C	0.735547	6.038756	4.781787
C	1.406829	7.392251	5.079195
C	1.567148	7.610491	6.589959
C	2.335579	6.449600	7.234344
C	1.658070	5.105899	6.935687
C	-0.736097	5.815012	2.745163
C	-0.505052	5.731834	1.269533
C	-2.876035	-0.116153	5.008339
C	-4.948789	-1.135416	5.420457
C	-5.597490	-2.382375	4.781787
C	-7.105291	-2.477775	5.079195
C	-7.374452	-2.448056	6.589959
C	-6.753307	-1.202129	7.234344
C	-5.250873	-1.117019	6.935687
C	-5.799003	-1.545614	2.377989
C	4.238042	-4.249277	2.377989
C	1.560961	5.794891	2.377989
C	0.876239	5.728021	1.048176
C	1.429934	5.723327	-0.229095
C	5.403996	-2.270027	2.745163
C	5.216440	-2.428529	1.269533
C	-4.667899	-3.544984	2.745163
C	-4.711387	-3.303305	1.269533
C	4.522493	-3.622856	1.048176
C	4.241579	-4.100023	-0.229095
C	-5.398731	-2.105166	1.048176
C	-5.671513	-1.623304	-0.229095
C	0.505052	5.731834	-1.269533
C	0.736097	5.815012	-2.745163
C	-1.560961	5.794891	-2.377989
C	-0.876239	5.728021	-1.048176
C	-1.429934	5.723327	0.229095
C	-0.735547	6.038756	-4.781787
C	-1.491095	4.853485	-5.420457
C	-1.658070	5.105899	-6.935687
C	-2.335579	6.449600	-7.234344
C	-1.567148	7.610491	-6.589959
C	-1.406829	7.392251	-5.079195
C	-1.337426	2.548796	-5.008339
C	-0.647225	1.247669	-4.925760
C	0.757941	1.172508	-4.920726
C	1.404126	-0.063321	-4.925760
C	0.636451	-1.242650	-4.920726
C	-0.756901	-1.184348	-4.925760
C	-1.394392	0.070142	-4.920726
C	-1.538609	-2.432643	-5.008339
C	-3.457694	-3.718068	-5.420457
C	-4.861943	-3.656381	-4.781787
C	-5.698462	-4.914475	-5.079195
C	-5.807305	-5.162435	-6.589959
C	-4.417727	-5.247471	-7.234344
C	-3.592803	-3.988880	-6.935687
C	-4.238042	-4.249277	-2.377989
C	2.876035	-0.116153	-5.008339
C	4.948789	-1.135416	-5.420457
C	5.597490	-2.382375	-4.781787
C	7.105291	-2.477775	-5.079195
C	7.374452	-2.448056	-6.589959
C	6.753307	-1.202129	-7.234344

C	5.250873	-1.117019	-6.935687
C	5.799003	-1.545614	-2.377989
C	-5.403996	-2.270027	-2.745163
C	-5.216440	-2.428529	-1.269533
C	4.667899	-3.544984	-2.745163
C	4.711387	-3.303305	-1.269533
C	-4.522493	-3.622856	-1.048176
C	-4.241579	-4.100023	0.229095
C	5.398731	-2.105166	-1.048176
C	5.671513	-1.623304	0.229095
H	-7.256239	-0.303648	6.849349
H	7.256239	-0.303648	-6.849349
H	3.891086	-6.132264	6.849349
H	-3.891086	-6.132264	-6.849349
H	3.365153	6.435911	6.849349
H	-3.365153	6.435911	-6.849349
H	-6.951086	-3.349388	7.056461
H	6.951086	-3.349388	-7.056461
H	6.376198	-4.345123	7.056461
H	-6.376198	-4.345123	-7.056461
H	0.574887	7.694511	7.056461
H	-0.574887	7.694511	-7.056461
H	-8.455280	-2.478165	6.773235
H	8.455280	-2.478165	-6.773235
H	6.373794	-6.083405	6.773235
H	-6.373794	-6.083405	-6.773235
H	2.081486	8.561570	6.773235
H	-2.081486	8.561570	-6.773235
H	-7.495750	-3.402266	4.636558
H	7.495750	-3.402266	-4.636558
H	6.694324	-4.790377	4.636558
H	-6.694324	-4.790377	-4.636558
H	0.801426	8.192643	4.636558
H	-0.801426	8.192643	-4.636558
H	-7.622448	-1.642113	4.593578
H	7.622448	-1.642113	-4.593578
H	5.233336	-5.780177	4.593578
H	-5.233336	-5.780177	-4.593578
H	2.389112	7.422290	4.593578
H	-2.389112	7.422290	-4.593578
H	-5.087368	-3.260989	5.190151
H	5.087368	-3.260989	-5.190151
H	-5.367784	-2.775296	5.190151
H	5.367784	-2.775296	-5.190151
H	-0.280415	6.036285	5.190151
H	0.280415	6.036285	-5.190151
H	6.913819	-1.211446	-8.319416
H	-6.913819	-1.211446	8.319416
H	4.506053	-5.381820	8.319416
H	-4.506053	-5.381820	-8.319416
H	2.407766	6.593266	8.319416
H	-2.407766	6.593266	-8.319416
H	4.820045	-0.203978	-7.363752
H	-4.820045	-0.203978	7.363752
H	-2.233373	4.276270	-7.363752
H	2.233373	4.276270	7.363752
H	4.724771	-1.961301	-7.401988
H	-4.724771	-1.961301	7.401988
H	-0.663849	5.072422	-7.401988
H	0.663849	5.072422	7.401988
H	4.060922	-3.111122	7.401988
H	-4.060922	-3.111122	-7.401988

H	2.586672	-4.072293	7.363752
H	-2.586672	-4.072293	-7.363752
H	-2.889985	-4.542477	-4.961077
H	2.889985	-4.542477	4.961077
H	5.378893	-0.231562	-4.961077
H	-5.378893	-0.231562	4.961077
H	2.480367	0.099306	4.940354
H	-2.480367	0.099306	-4.940354
H	-1.326185	2.098407	4.940354
H	1.326185	2.098407	-4.940354
H	-2.488908	4.774039	-4.961077
H	2.488908	4.774039	4.961077
H	-2.433894	2.513461	-4.900239
H	2.433894	2.513461	4.900239
H	3.393668	0.851083	-4.900239
H	-3.393668	0.851083	4.900239
H	1.154181	-2.197714	-4.940354
H	-1.154181	-2.197714	4.940354
H	0.959774	-3.364544	4.900239
H	-0.959774	-3.364544	-4.900239
H	-6.218797	-0.702058	-0.400432
H	3.717398	-5.034607	-0.400432
H	2.501399	5.736665	-0.400432
H	6.218797	-0.702058	0.400432
H	-2.501399	5.736665	0.400432
H	-3.717398	-5.034607	0.400432

(R)-1c, B3LYP/6-31G(d), $E = -6419.41121681$ Hartree

C	4.775450	3.345757	5.174499
C	4.569444	3.449270	3.708010
C	5.053305	2.452447	2.829631
C	5.688433	1.308876	3.366694
C	5.871859	1.149661	4.831764
N	5.428887	2.191782	5.655589
C	3.930657	4.563637	3.191392
C	3.767394	4.710420	1.809434
C	4.247126	3.762214	0.903437
C	4.912520	2.603927	1.415917
C	6.166990	0.328834	2.514071
C	6.051978	0.477317	1.127421
C	5.453152	1.599751	0.551701
C	4.112001	3.922692	-0.551701
C	5.381736	1.797012	-0.903437
O	6.410418	0.151014	5.297312
C	5.699727	2.133594	7.120242
C	4.988394	0.956906	7.822662
C	5.275169	1.035107	9.340215
C	6.777220	1.072695	9.650949
C	7.461025	2.243098	8.932182
C	7.209084	2.181559	7.418637
N	3.549888	1.075456	7.622752
C	2.878665	0.009702	7.428948
C	1.405773	0.011111	7.341712
C	0.682069	1.218168	7.337024
C	-0.712509	1.211879	7.341712
C	-1.395999	-0.018395	7.337024
C	-0.693264	-1.222991	7.341712
C	0.713930	-1.199773	7.337024
C	-1.430931	-2.497848	7.428948
N	-0.843572	-3.612021	7.622752

C	-1.665492	-4.798529	7.822662
C	-1.002117	-6.002905	7.120242
C	-1.715256	-7.334029	7.418637
C	-1.787932	-7.582986	8.932182
C	-2.459629	-6.405592	9.650949
C	-1.741156	-5.085984	9.340215
N	-0.816304	-5.797445	5.655589
C	0.509785	-5.808540	5.174499
C	0.702433	-5.681890	3.708010
C	-0.402771	-5.602514	2.829631
C	-1.710697	-5.580765	3.366694
C	-1.940294	-5.660009	4.831764
C	1.986897	-5.685867	3.191392
C	2.195646	-5.617869	1.809434
C	1.134610	-5.559226	0.903437
C	-0.201193	-5.556330	1.415917
C	-2.798716	-5.505187	2.514071
C	-2.612620	-5.479825	1.127421
C	-1.341151	-5.522443	0.551701
C	1.341151	-5.522443	-0.551701
C	-1.134610	-5.559226	-0.903437
O	1.462515	-5.943295	5.929621
O	-3.074427	-5.627092	5.297312
C	-1.447734	2.488146	7.428948
N	-2.706316	2.536565	7.622752
C	-3.322902	3.841623	7.822662
C	-4.697610	3.869311	7.120242
C	-5.493828	5.152470	7.418637
C	-5.673092	5.339888	8.932182
C	-4.317591	5.332897	9.650949
C	-3.534013	4.050877	9.340215
N	-4.612582	3.605663	5.655589
C	-3.931565	4.510348	4.831764
C	-3.977736	4.271889	3.366694
C	-4.650534	3.150067	2.829631
C	-5.271878	2.232620	3.708010
C	-5.285236	2.462783	5.174499
C	-4.711327	2.952403	1.415917
C	-4.112001	3.922692	0.551701
C	-3.439358	5.002508	1.127421
C	-3.368274	5.176353	2.514071
C	-5.381736	1.797012	0.903437
C	-5.963040	0.907449	1.809434
C	-5.917554	1.122231	3.191392
O	-3.335991	5.476078	5.297312
O	-5.878302	1.705072	5.929621
C	-5.453152	1.599751	-0.551701
C	-4.247126	3.762214	-0.903437
O	4.415787	4.238222	5.929621
H	-6.485902	0.028538	1.451129
H	3.267666	5.602687	1.451129
H	3.218236	-5.631225	1.451129
H	-2.958333	5.742564	0.498705
H	6.452372	-0.309290	0.498705
H	-3.494039	-5.433273	0.498705
H	3.569482	5.321957	3.877667
H	2.824209	-5.752241	3.877667
H	-2.849244	6.027096	2.942332
H	6.644240	-0.546030	2.942332
H	-3.794996	-5.481065	2.942332
H	-5.257911	3.014056	7.500812
H	5.239205	3.046457	7.500812

H	0.018707	-6.060513	7.500812
H	-4.973335	6.018183	6.997574
H	7.698567	1.297943	6.997574
H	-2.725232	-7.316126	6.997574
H	-6.471074	5.084505	6.924511
H	7.638847	3.061862	6.924511
H	-1.167774	-8.146367	6.924511
H	-6.207295	6.277803	9.127827
H	8.540384	2.236774	9.127827
H	-2.333089	-8.514577	9.127827
H	-6.300951	4.530514	9.332096
H	7.074016	3.191526	9.332096
H	-0.773065	-7.722040	9.332096
H	-3.732332	6.207529	9.333088
H	7.242044	0.128530	9.333088
H	-3.509712	-6.336059	9.333088
H	-4.458243	5.426082	10.735071
H	6.928247	1.147910	10.735071
H	-2.470004	-6.573993	10.735071
H	-2.551215	4.068472	9.826631
H	4.799007	0.175181	9.826631
H	-2.247792	-4.243653	9.826631
H	-4.067043	3.177048	9.739358
H	4.784926	1.933638	9.739358
H	-0.717883	-5.110686	9.739358
H	-2.691994	4.654573	7.437928
H	5.376975	0.004049	7.437928
H	-2.684981	-4.658621	7.437928
H	-2.528214	-2.417933	7.357598
H	-0.829885	3.398464	7.357598
H	3.358099	-0.980531	7.357598
H	1.246701	-2.146532	7.359620
H	-2.482302	-0.006409	7.359620
H	1.235600	2.152941	7.359620
H	-6.393691	0.430284	3.877667
C	5.963040	0.907449	-1.809434
C	5.917554	1.122231	-3.191392
C	5.271878	2.232620	-3.708010
C	4.650534	3.150067	-2.829631
C	4.711327	2.952403	-1.415917
H	6.485902	0.028538	-1.451129
H	6.393691	0.430284	-3.877667
C	5.285236	2.462783	-5.174499
C	3.977736	4.271889	-3.366694
C	-2.195646	-5.617869	-1.809434
C	-1.986897	-5.685867	-3.191392
C	-0.702433	-5.681890	-3.708010
C	0.402771	-5.602514	-2.829631
C	0.201193	-5.556330	-1.415917
H	-3.218236	-5.631225	-1.451129
H	-2.824209	-5.752241	-3.877667
C	-0.509785	-5.808540	-5.174499
C	1.710697	-5.580765	-3.366694
C	-3.767394	4.710420	-1.809434
C	-3.930657	4.563637	-3.191392
C	-4.569444	3.449270	-3.708010
C	-5.053305	2.452447	-2.829631
C	-4.912520	2.603927	-1.415917
H	-3.267666	5.602687	-1.451129
H	-3.569482	5.321957	-3.877667
C	-4.775450	3.345757	-5.174499
C	-5.688433	1.308876	-3.366694

C	3.368274	5.176353	-2.514071
C	3.931565	4.510348	-4.831764
H	2.849244	6.027096	-2.942332
C	3.439358	5.002508	-1.127421
H	2.958333	5.742564	-0.498705
C	2.798716	-5.505187	-2.514071
C	1.940294	-5.660009	-4.831764
H	3.794996	-5.481065	-2.942332
C	2.612620	-5.479825	-1.127421
H	3.494039	-5.433273	-0.498705
C	-6.166990	0.328834	-2.514071
C	-5.871859	1.149661	-4.831764
H	-6.644240	-0.546030	-2.942332
C	-6.051978	0.477317	-1.127421
H	-6.452372	-0.309290	-0.498705
N	4.612582	3.605663	-5.655589
O	5.878302	1.705072	-5.929621
C	4.697610	3.869311	-7.120242
O	3.335991	5.476078	-5.297312
N	0.816304	-5.797445	-5.655589
O	-1.462515	-5.943295	-5.929621
C	1.002117	-6.002905	-7.120242
N	-5.428887	2.191782	-5.655589
O	-4.415787	4.238222	-5.929621
C	-5.699727	2.133594	-7.120242
O	3.074427	-5.627092	-5.297312
O	-6.410418	0.151014	-5.297312
C	1.715256	-7.334029	-7.418637
H	-0.018707	-6.060513	-7.500812
C	1.787932	-7.582986	-8.932182
H	2.725232	-7.316126	-6.997574
H	1.167774	-8.146367	-6.924511
C	2.459629	-6.405592	-9.650949
H	2.333089	-8.514577	-9.127827
H	0.773065	-7.722040	-9.332096
C	1.741156	-5.085984	-9.340215
H	3.509712	-6.336059	-9.333088
H	2.470004	-6.573993	-10.735071
C	1.665492	-4.798529	-7.822662
H	2.247792	-4.243653	-9.826631
H	0.717883	-5.110686	-9.739358
H	2.684981	-4.658621	-7.437928
N	0.843572	-3.612021	-7.622752
C	5.493828	5.152470	-7.418637
H	5.257911	3.014056	-7.500812
C	5.673092	5.339888	-8.932182
H	4.973335	6.018183	-6.997574
H	6.471074	5.084505	-6.924511
C	4.317591	5.332897	-9.650949
H	6.207295	6.277803	-9.127827
H	6.300951	4.530514	-9.332096
C	3.534013	4.050877	-9.340215
H	3.732332	6.207529	-9.333088
H	4.458243	5.426082	-10.735071
C	3.322902	3.841623	-7.822662
H	2.551215	4.068472	-9.826631
H	4.067043	3.177048	-9.739358
H	2.691994	4.654573	-7.437928
N	2.706316	2.536565	-7.622752
C	-7.209084	2.181559	-7.418637
H	-5.239205	3.046457	-7.500812
C	-7.461025	2.243098	-8.932182

H	-7.698567	1.297943	-6.997574
H	-7.638847	3.061862	-6.924511
C	-6.777220	1.072695	-9.650949
H	-8.540384	2.236774	-9.127827
H	-7.074016	3.191526	-9.332096
C	-5.275169	1.035107	-9.340215
H	-7.242044	0.128530	-9.333088
H	-6.928247	1.147910	-10.735071
C	-4.988394	0.956906	-7.822662
H	-4.799007	0.175181	-9.826631
H	-4.784926	1.933638	-9.739358
H	-5.376975	0.004049	-7.437928
N	-3.549888	1.075456	-7.622752
C	-2.878665	0.009702	-7.428948
C	1.447734	2.488146	-7.428948
C	1.430931	-2.497848	-7.428948
C	0.693264	-1.222991	-7.341712
H	2.528214	-2.417933	-7.357598
C	0.712509	1.211879	-7.341712
H	0.829885	3.398464	-7.357598
C	-1.405773	0.011111	-7.341712
H	-3.358099	-0.980531	-7.357598
C	-0.713930	-1.199773	-7.337024
H	-1.246701	-2.146532	-7.359620
C	-0.682069	1.218168	-7.337024
H	-1.235600	2.152941	-7.359620
C	1.395999	-0.018395	-7.337024
H	2.482302	-0.006409	-7.359620

Dicyclohexyl-PMDI, B3LYP/6-31G(d), $E = -1263.30164475$ Hartree

C	5.474911	0.137616	-1.274212
C	4.836003	-0.443785	-0.000153
C	5.474739	0.137070	1.274246
C	6.995760	-0.086578	1.267590
C	7.646304	0.488244	0.000237
C	6.995928	-0.086060	-1.267438
N	3.372530	-0.278875	-0.000214
C	2.685588	0.944054	-0.000043
C	1.228256	0.598726	-0.000019
C	1.110514	-0.795160	-0.000082
C	2.489533	-1.373732	-0.000143
C	-0.121659	-1.443117	-0.000077
C	-1.228282	-0.598632	-0.000026
C	-1.110541	0.795258	0.000049
C	0.121636	1.443211	0.000070
C	-2.489571	1.373832	0.000106
N	-3.372549	0.278987	0.000148
C	-2.685616	-0.943953	-0.000001
O	3.183609	2.052917	0.000041
O	2.811052	-2.544439	-0.000195
O	-3.183686	-2.052793	-0.000136
C	-4.836038	0.443801	0.000088
C	-5.474731	-0.137194	-1.274249
C	-6.995780	0.086306	-1.267517
C	-7.646209	-0.488514	-0.000104
C	-6.995861	0.085946	1.267517
C	-5.474817	-0.137550	1.274221
O	-2.811067	2.544549	0.000247
H	-5.021862	0.331410	2.156524
H	-5.256454	-1.210550	1.325986
H	0.212946	2.524487	0.000107

H	-0.212971	-2.524393	-0.000146
H	-4.977499	1.530439	0.000227
H	-7.437765	-0.366430	2.163680
H	-7.205756	1.164148	1.326332
H	-7.535956	-1.582554	-0.000255
H	-8.723505	-0.280964	-0.000110
H	-7.437666	-0.365783	-2.163836
H	-7.205634	1.164535	-1.326035
H	-5.256372	-1.210179	-1.326338
H	-5.021778	0.332034	-2.156411
H	4.977379	-1.530437	-0.000378
H	5.256489	1.210078	1.326367
H	5.021689	-0.332142	2.156365
H	7.437642	0.365427	2.163954
H	7.205509	-1.164827	1.326061
H	7.536183	1.582296	0.000451
H	8.723575	0.280566	0.000267
H	7.437945	0.366300	-2.163557
H	7.205672	-1.164288	-1.326313
H	5.256688	1.210646	-1.325913
H	5.021975	-0.331211	-2.156595

Dicyclohexyl-NDI, B3LYP/6-31G(d), $E = -1416.95545389$ Hartree

C	-5.655386	-0.372230	1.278029
C	-5.050912	0.235399	0.000063
C	-5.655423	-0.371932	-1.278039
C	-7.184415	-0.202259	-1.267938
C	-7.811272	-0.802226	-0.000038
C	-7.184384	-0.202577	1.268001
N	-3.556120	0.202000	0.000028
C	-2.895378	1.449405	0.000040
C	-1.407478	1.435006	0.000025
C	-0.710126	0.205965	-0.000020
C	-1.407888	-1.023059	-0.000039
C	-2.897307	-1.038291	-0.000076
C	0.710126	0.205965	-0.000022
C	1.407889	-1.023059	-0.000051
C	0.704071	-2.217469	-0.000062
C	-0.704070	-2.217469	-0.000062
C	1.407478	1.435006	-0.000007
C	2.895378	1.449406	-0.000005
N	3.556120	0.202001	-0.000056
C	2.897308	-1.038291	-0.000030
C	-0.703980	2.629862	0.000044
C	0.703979	2.629862	0.000030
C	5.050912	0.235400	-0.000031
C	5.655445	-0.372041	-1.278059
C	7.184442	-0.202386	-1.267935
C	7.811271	-0.802228	0.000041
C	7.184358	-0.202452	1.268004
C	5.655364	-0.372119	1.278010
H	5.223984	0.123813	2.156830
O	3.516654	-2.093376	0.000047
O	3.516801	2.502385	0.000056
O	-3.516801	2.502385	0.000061
O	-3.516653	-2.093376	-0.000075
H	-5.224081	0.124121	-2.156804
H	-5.400995	-1.434069	-1.340554
H	-7.434508	0.867483	-1.324198
H	-7.611524	-0.669693	-2.163786
H	-8.896172	-0.637720	0.000003

H	-7.657377	-1.891018	-0.000183
H	-7.434483	0.867145	1.324544
H	-7.611454	-0.670259	2.163739
H	-5.224012	0.123600	2.156908
H	-5.400951	-1.434379	1.340284
H	-1.260037	3.561085	0.000082
H	-1.260325	-3.148637	-0.000081
H	1.260037	3.561085	0.000041
H	1.260326	-3.148636	-0.000077
H	5.278289	1.302697	0.000009
H	5.401016	-1.434181	-1.340482
H	5.224110	0.123918	-2.156884
H	7.611553	-0.669932	-2.163724
H	7.434543	0.867345	-1.324304
H	7.657374	-1.891020	0.000014
H	8.896172	-0.637723	0.000074
H	7.611424	-0.670023	2.163801
H	7.434451	0.867280	1.324439
H	5.400926	-1.434263	1.340360
H	-5.278290	1.302696	0.000188

Dicyclohexyl-PDI, B3LYP/6-31G(d), $E = -1800.47620420$ Hartree

C	-1.425757	-7.712292	1.277642
C	1.425757	7.712292	1.277642
C	-1.425757	-7.712292	-1.277642
C	1.425757	7.712292	-1.277642
C	-1.425757	-9.250588	-1.267929
C	-1.425757	-9.250588	1.267929
C	1.425757	9.250588	1.267929
C	1.425757	9.250588	-1.267929
N	-0.626784	-5.689696	0.000000
N	0.626784	5.689696	0.000000
C	-1.163236	0.866828	0.000000
C	1.163236	-0.866828	0.000000
C	0.155594	1.422091	0.000000
C	-0.155594	-1.422091	0.000000
C	1.323178	0.594778	0.000000
C	-1.323178	-0.594778	0.000000
C	-2.253620	1.739354	0.000000
C	2.253620	-1.739354	0.000000
C	-2.090580	3.128920	0.000000
C	2.090580	-3.128920	0.000000
C	-0.823348	3.686659	0.000000
C	0.823348	-3.686659	0.000000
C	0.311076	2.842545	0.000000
C	-0.311076	-2.842545	0.000000
C	1.601197	3.421572	0.000000
C	-1.601197	-3.421572	0.000000
C	1.782752	4.896047	0.000000
C	-1.782752	-4.896047	0.000000
C	-0.680985	5.163628	0.000000
C	0.680985	-5.163628	0.000000
C	2.717580	2.603001	0.000000
C	-2.717580	-2.603001	0.000000
C	-2.576338	-1.210935	0.000000
C	2.576338	1.210935	0.000000
C	0.755342	7.177327	0.000000
C	-0.755342	-7.177327	0.000000
C	2.091068	9.807693	0.000000
C	-2.091068	-9.807693	0.000000
O	-1.662939	5.895366	0.000000

O	1.662939	-5.895366	0.000000
O	2.902005	5.395128	0.000000
O	-2.902005	-5.395128	0.000000
H	-2.950881	3.789460	0.000000
H	2.950881	-3.789460	0.000000
H	-3.478987	-0.611526	0.000000
H	3.478987	0.611526	0.000000
H	-3.700227	-3.062242	0.000000
H	3.700227	3.062242	0.000000
H	3.264492	-1.349283	0.000000
H	-3.264492	1.349283	0.000000
H	0.281187	-7.519076	0.000000
H	-0.281187	7.519076	0.000000
H	-2.453241	-7.341730	-1.339408
H	-2.453241	-7.341730	1.339408
H	2.453241	7.341730	-1.339408
H	2.453241	7.341730	1.339408
H	-0.390081	-9.617231	-1.323995
H	-0.390081	-9.617231	1.323995
H	0.390081	9.617231	-1.323995
H	0.390081	9.617231	1.323995
H	-3.156190	-9.534253	0.000000
H	3.156190	9.534253	0.000000
H	2.047516	10.904228	0.000000
H	-2.047516	-10.904228	0.000000
H	0.885554	7.338046	2.156582
H	0.885554	7.338046	-2.156582
H	-0.885554	-7.338046	-2.156582
H	-0.885554	-7.338046	2.156582
H	-1.937429	-9.623936	2.163765
H	-1.937429	-9.623936	-2.163765
H	1.937429	9.623936	2.163765
H	1.937429	9.623936	-2.163765

Section N. References

- (1) Sheldrick, G. M. Crystal Structure Refinement with *SHELXL*. *Acta Crystallogr. Sect. C* **2015**, *71*, 3–8.
- (2) Dolomanov, O. V.; Bourhis, L. J.; Gildea, R. J.; Howard, J. A. K.; Puschmann, H. OLEX2: A Complete Structure Solution, Refinement and Analysis Program. *J. Appl. Crystallogr.* **2009**, *42*, 339–341.
- (3) Gaussian 09, Revision D.01, Frisch, M. J.; Trucks, G. W.; Schlegel, H. B.; Scuseria, G. E.; Robb, M. A.; Cheeseman, J. R.; Scalmani, G.; Barone, V.; Mennucci, B.; Petersson, G. A.; Nakatsuji, H.; Caricato, M.; Li, X.; Hratchian, H. P.; Izmaylov, A. F.; Bloino, J.; Zheng, G.; Sonnenberg, J. L.; Hada, M.; Ehara, M.; Toyota, K.; Fukuda, R.; Hasegawa, J.; Ishida, M.; Nakajima, T.; Honda, Y.; Kitao, O.; Nakai, H.; Vreven, T.; Montgomery, J. A. Jr.; Peralta, J. E.; Ogliaro, F.; Bearpark, M.; Heyd, J. J.; Brothers, E.; Kudin, K. N.; Staroverov, V. N.; Kobayashi, R.; Normand, J.; Raghavachari, K.; Rendell, A.; Burant, J. C.; Iyengar, S. S.; Tomasi, J.; Cossi, M.; Rega, N.; Millam, J. M.; Klene, M.; Knox, J. E.; Cross, J. B.; Bakken, V.; Adamo, C.; Jaramillo, J.; Gomperts, R.; Stratmann, R. E.; Yazyev, O.; Austin, A. J.; Cammi, R.; Pomelli, C.; Ochterski, J. W.; Martin, R. L.; Morokuma, K.; Zakrzewski, V. G.; Voth, G. A.; Salvador, P.; Dannenberg, J. J.; Dapprich, S.; Daniels, A. D.; Farkas, Ö.; Foresman, J. B.; Ortiz, J. V.; Cioslowski, J.; Fox, D. J. Gaussian, Inc., Wallingford CT, **2009**.
- (4) Marenich, A. V.; Cramer, C. J.; Truhlar, D. G. Universal Solvation Model Based on Solute Electron Density and on a Continuum Model of the Solvent Defined by the Bulk Dielectric Constant and Atomic Surface Tensions. *J. Phys. Chem. B* **2009**, *113*, 6378–6396.
- (5) Lang, B. Photometrics of ultrafast and fast broadband electronic transient absorption spectroscopy: State of the art. *Rev. Sci. Instrum.* **2018**, *89*, 093112.
- (6) Banerji, N.; Duvanel, G.; Perez-Velasco, A.; Maity, S.; Sakai, N.; Matile S., Vauthey, E. Excited-State Dynamics of Hybrid Multichromophoric Systems:

- Toward an Excitation Wavelength Control of the Charge Separation Pathways. *J. Phys. Chem. A*, **2009**, *113*, 8202–8212.
- (7) Lang, B.; Mosquera-Vázquez, S.; Lovy, D.; Sherin, P.; Markovic, V.; Vauthey, E. Broadband ultraviolet-visible transient absorption spectroscopy in the nanosecond to microsecond time domain with sub-nanosecond time resolution. *Rev. Sci. Instrum.*, **2013**, *84*, 073107.
- (8) Tokunaga, E.; Terasaki, A.; Kobayashi, T. Femtosecond continuum interferometer for transient phase and transmission spectroscopy. *J. Opt. Soc. Am. B*, **1996**, *13*, 496–513.
- (9) Galsbøl, F.; Steenbøl, P.; Sørensen, B. S. The Preparation, Separation, and Characterization of the le_3 - and ob_3 -Isomers of Tris(trans-1,2-cyclohexanediamine)rhodium(III) Complexes. *Acta Chem. Scand.* **1972**, *26*, 3605–3611.
- (10) Yu, L.; Li, P. New Simple Primary Amine-Thiourea Organocatalysts and Their Application in Asymmetric Conjugate Addition. *Tetrahedron Lett.* **2014**, *55*, 3697–3700.
- (11) Nalluri, S. K. M.; Liu, Z.; Wu, Y.; Hermann, K. R.; Samanta, A.; Kim, D. J.; Krzyaniak, M. D.; Wasielewski, M. R.; Stoddart, J. F. Chiral Redox-Active Isosceles Triangles. *J. Am. Chem. Soc.* **2016**, *138*, 5968–5977.
- (12) Šolomek, T.; Powers-Riggs, N. E.; Wu, Y. L.; Young, R. M.; Krzyaniak, M. D.; Horwitz, N. E.; Wasielewski, M. R. Electron Hopping and Charge Separation within a Naphthalene-1,4:5,8-Bis(Dicarboximide) Chiral Covalent Organic Cage. *J. Am. Chem. Soc.* **2017**, *139*, 3348–3351.
- (13) Kaik, M.; Gawroński, J. Unprecedented Selectivity in the Formation of Large-Ring Oligoimines from Conformationally Bistable Chiral Diamines. *Org. Lett.* **2006**, *8*, 2921–2924.
- (14) Wolfram Research, Inc., *Mathematica*.

- (15) Jiang, S.; Bacsa, J.; Wu, X.; Jones, J. T. A.; Dawson, R.; Trewin, A.; Adams, D. J.; Cooper, A. I. Selective Gas Sorption in a [2+3] “propeller” Cage Crystal. *Chem. Commun.* **2011**, *47*, 8919–8921.
- (16) Jin, Y.; Voss, B. A.; Jin, A.; Long, H.; Noble, R. D.; Zhang, W. Highly CO₂-Selective Organic Molecular Cages: What Determines the CO₂ Selectivity. *J. Am. Chem. Soc.* **2011**, *133*, 6650–6658.
- (17) Jin, Y.; Voss, B. A.; Noble, R. D.; Zhang, W. A Shape-Persistent Organic Molecular Cage with High Selectivity for the Adsorption of CO₂ over N₂. *Angew. Chem. Int. Ed.* **2010**, *49*, 6348–6351.
- (18) Tozawa, T.; Jones, J. T. A.; Swamy, S. I.; Jiang, S.; Adams, D. J.; Shakespeare, S.; Clowes, R.; Bradshaw, D.; Hasell, T.; Chong, S. Y.; Tang, C.; Thompson, S.; Parker, J.; Trewin, A.; Bacsa, J.; Slawin, A. M. Z.; Steiner, A.; Cooper, A. I. Porous Organic Cages. *Nat. Mater.* **2009**, *8*, 973–978.
- (19) Beaudoin, D.; Rominger, F.; Mastalerz, M. Chiral Self-Sorting of [2+3] Salicylimine Cage Compounds. *Angew. Chem. Int. Ed.* **2017**, *56*, 1244–1248.
- (20) Hu, X. Y.; Zhang, W. S.; Rominger, F.; Wacker, I.; Schröder, R. R.; Mastalerz, M. Transforming a Chemically Labile [2+3] Imine Cage into a Robust Carbamate Cage. *Chem. Commun.* **2017**, *53*, 8616–8619.
- (21) Schneider, M. W.; Oppel, I. M.; Mastalerz, M. Exo-Functionalized Shape-Persistent [2+3] Cage Compounds: Influence of Molecular Rigidity on Formation and Permanent Porosity. *Chem. Eur. J.* **2012**, *18*, 4156–4160.
- (22) Reiss, P. S.; Little, M. A.; Santolini, V.; Chong, S. Y.; Hasell, T.; Jelfs, K. E.; Briggs, M. E.; Cooper, A. I. Periphery-Functionalized Porous Organic Cages. *Chem. Eur. J.* **2016**, *22*, 16547–16553.
- (23) Beckwith, J. S.; Rumble, C. A.; Vauthey, E. Data analysis in transient electronic spectroscopy – an experimentalist's view. *Int. Rev. Phys. Chem.*, **2020**, *39*, 135–216.